Masters Theses   Graduate School

12-2004

Effects of Pressure and Equivalence Ratio on Minimum Ignition Energies of Methane-Air Mixtures and Effect of Pressure on Breakdown Threshold Energies of Methane and Air

Sameer Vidyadhar Bondre
University of Tennessee, Knoxville

To the Graduate Council:

I am submitting herewith a thesis written by Sameer Vidyadhar Bondre entitled "Effects of Pressure and Equivalence Ratio on Minimum Ignition Energies of Methane-Air Mixtures and Effect of Pressure on Breakdown Threshold Energies of Methane and Air." I have examined the final electronic copy of this thesis for form and content and recommend that it be accepted in partial fulfillment of the requirements for the degree of Master of Science, with a major in Mechanical Engineering.

<div align="right">Ke Nguyen, Major Professor</div>

We have read this thesis and recommend its acceptance:

Jeffery Hodgson, David Irick

<div align="right">Accepted for the Council:</div>
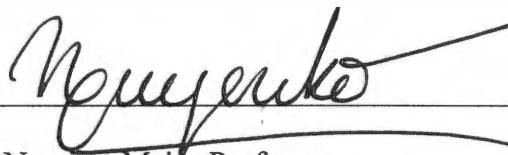
<div align="right">Carolyn R. Hodges</div>

<div align="right">Vice Provost and Dean of the Graduate School</div>

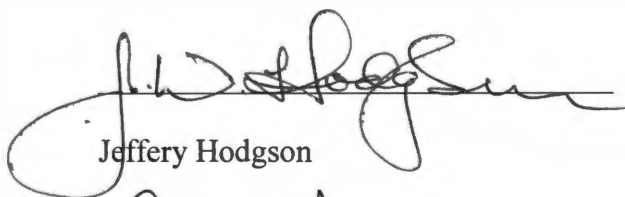(Original signatures are on file with official student records.)

To the Graduate Council:

I am submitting herewith a thesis written by Sameer Vidyadhar Bondre entitled "Effects of Pressure and Equivalence Ratio on Minimum Ignition Energies of Methane-Air Mixtures and Effect of Pressure on Breakdown Threshold Energies of Methane and Air." I have examined the final paper copy of this thesis for form and content and recommend that it be accepted in partial fulfillment of the requirements for the degree of Master of Science, with a major in Mechanical Engineering.
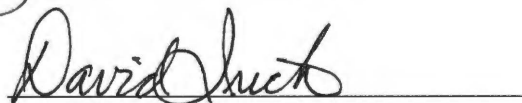
Ke Nguyen, Major Professor

We have read this thesis
and recommend its acceptance:

Jeffery Hodgson

David Irick

Accepted for the council:

Vice Chancellor and
Dean of Graduate Studies

EFFECTS OF PRESSURE AND EQUIVALENCE RATIO ON MINIMUM IGNITION ENERGIES OF METHANE-AIR MIXTURES AND EFFECT OF PRESSURE ON BREAKDOWN THRESHOLD ENERGIES OF METHANE AND AIR

A Thesis
Presented for the Master of Science
Degree
The University of Tennessee, Knoxville

Sameer Vidyadhar Bondre
December 2004

ABSTRACT

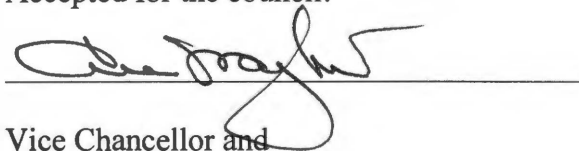An experimental investigation is conducted to determine the effect of pressure on breakdown threshold energies of methane and air. In addition the effect of pressure and equivalence ratios on minimum ignition energies of methane-air mixtures are also investigated. The pressures for the breakdown threshold energy experiments are varied from 0.02 to 1.17 MPa, and pressures and equivalence ratios for minimum ignition energy experiments are varied from 0.1 to 1.04 MPa and 0.6 to 1.2, respectively. The gas breakdown and the ignition of the methane-air mixture is achieved using a laser-induced spark from a 5.5 ns pulse Q-switched Nd:YAG laser at a wavelength of 1.064 μm. Since ignition is preceded by generation of a spark, thus determining the breakdown threshold energies can provide the insight on the generation of spark required for ignition. It is suggested that the gas that has lower breakdown threshold energy would provide the spark for ignition, and the minimum ignition energy would be close to the breakdown threshold energy of that gas. The breakdown threshold energies measured for methane at 0.02 MPa and 1.17 MPa are 23.23 and 1.9 mJ and for air at 0.02 MPa and 1.17 MPa are 28.84 and 2.74 mJ, respectively. The breakdown threshold energies of methane and air are found to be of the same order with breakdown threshold energies of air being a few millijoules higher than those of methane. It is observed that breakdown threshold energies of methane and air is always much larger than the minimum ignition energies of methane-air mixtures, and hence there is no correlation between breakdown threshold energy and minimum ignition energy. The mixture during the minimum ignition energy experiments ignited before the spark was generated. The temperature and pressure in the focused region were extremely high, which ignited the mixture directly or created a

rapidly expanding shockwave strong enough to ignite the mixture. The Results indicate that at a given equivalence ratio the minimum ignition energy decreases with increasing pressure. Furthermore at a given pressure minimum ignition energy is found to be lowest at stoichiometric and increases as the mixture deviates from stoichiometric. Similar to the breakdown threshold energy, the minimum ignition energy of methane-air mixture is found to be dependent on pressure.

Contents

List of Tables

List of Figures

xiii

CHAPTER 1

INTRODUCTION

Using laser energy as a source for ignition in natural gas engines has recently attracted considerable interest due to some distinct proposed advantages from both practical and fundamental standpoints. Using lasers for ignition eliminates the spark plugs, which are one of the main causes for heat losses. Laser beams can be focused down to any desired point in the combustion region such that complete combustion can be achieved. It is non-intrusive and offers a possibility of multi-point ignition, which would again assist in complete combustion. Igniting mixtures at different locations simultaneously will reduce the burning time, which is very important in fuel-lean combustion applications. Also lasers can deliver high-energy pulses rapidly, which is essential for continuous ignition. In addition selective chemistry is possible as the laser is a monochromatic light source. It can eliminate problems like wall effects, heat loss through electrodes, partial burn and can avoid misfire.

Ronney [1] proposed many advantages of using a laser as source of ignition. Using very lean combustion mixture in reciprocating engines or gas turbines will provide higher thermal efficiencies η and lower emissions of undesirable combustion products like NO_x. However, burning mixtures that are too lean may lead to misfire or flame blowout conditions, which limits the performance of the devices. An optical ignition source that provides multiple ignition sites could provide efficient combustion of lean mixtures in these devices. Using this type of multiple sites for ignition the total energy absorption percentage of the laser energy can be increased, which will make the use of

1

laser energy for ignition more economical. Also the ability of lasers to ignite mixture in regions that are away from the combustor wall will reduce formation of soot on the solid surface of the wall.

Another possible means of exploiting the benefits of lasers would be to modify the combustion chamber to obtain lower turbulence levels. All commercial combustion devices employ turbulence to accelerate mixing and burning, however this turbulence also increases heat losses to walls and pressure drops. Thus if the need for turbulence can be reduced by employing multipoint laser ignition then the combustion chamber can be redesigned to provide low turbulence levels, which ultimately lowers the heat losses.

One application can be in jet propulsion. There is always a problem in propulsion applications when burning mixtures at supercritical velocities. Normally using a flame holder into the flow solves this problem. This flame holder causes additional drag. A laser ignition source could eliminate the need for a flame holder.

Other advantages of laser ignition include the possibility of having very brief and rapidly repeating pulses of significant energy content. This would assist in complete combustion, which would lead to reduction in unburnt hydrocarbon emissions.

Ronney concluded that the primary benefits of laser ignition for practical combustion devices probably lie in the ability to choose the location(s) and timing of ignition events in ways that are not feasible with conventional ignition systems. These benefits may also facilitate the possibility of monitoring and controlling the burning process in real time. Since the laser ignition system may be able to reduce overall burning time, it would be possible to burn quickly and expand the product gases to low

temperatures. This would reduce the formation of NO_x and could shorten the length of the combustion section.

Unfortunately, the use of lasers for ignition presents some implications, which are not obvious. To achieve breakdown with practical-size lasers the pulse-width of the laser will be typically two orders of magnitude smaller than that of the spark plug, and the pulse energy of the laser will typically be one or two orders of magnitude smaller than that of the spark plug. Also lasers might produce a spark in a very small, nearly spherical volume in contrast to the elongated, cylindrical spark discharge. These differences relative to spark plugs might alter the properties of the plasma discharge, ion-electron recombination rate and plasma chemistry properties and subsequent time-space characteristics of temperature, intermediate reactions and products. There might be differences in minimum ignition energy, ignition delay time, magnitude of shock heating of surrounding mixture and the turbulent flame speed obtained from the laser and electric-spark ignition processes.

Very few studies have been done for studying laser ignition. The laser ignition studies have basically focused on the ignition process and flame propagation. Not much research has been done in determining the minimum ignition energies of different fuel-air mixtures at high pressures. For natural gas engines no data is available for minimum ignition energies at high pressures.

In this investigation the breakdown threshold energies of methane and air were determined using laser-induced spark ignition for pressures ranging from 0.02 MPa to 1.17 MPa. In addition, the minimum ignition energies of methane-air mixtures were determined for pressures ranging from 0.1 MPa to 1.04 MPa. In laser-induced spark

3

ignition, laser irradiance in the order of 10^{10} W/cm^2 was required to generate a spark at the end of the laser pulse. This spark was generated under the strong electric field of the laser beam, and two primary mechanisms were responsible for this optical breakdown: the electron cascade process and the multiphoton ionization process.

In multiphoton ionization process as discussed by Chen [2], the electron density increases constantly with the rate constant proportional to $(I_L)^m$, where I_L is the laser irradiance and m is the number of photons required in the multiphoton ionization process. As multiphoton ionization needs a certain number of photons to reach the ionization energy, it is dependent on the laser wavelength.

$$m/\lambda \; \alpha \; mh\upsilon > \epsilon_I$$

where, λ is the laser wavelength, $h\upsilon$ is the photon energy and ϵ_I ionization energy. For example, the photon energy for a 10.6 μm CO_2 laser is 0.1 eV and a 1.064 μm Nd-YAG laser is 1.0 eV and the ionization potential for O_2, H_2, CH_4 and N_2 is 12.071, 15.425 eV, 12.51 and 14.531 eV, respectively; the multiphoton ionization process will require the absorption of 120 to 140 CO_2 photons or 12 to 14 Nd-YAG photons to ionize these gases. The multiphoton ionization cross section was measured as 4 x 10^{-142} (W/cm^2)$^{-12}$ [3] under the above conditions. Using a typical nanosecond laser with output energy of tens to hundreds mJ/pulse, the electron growth through multiphoton ionization process is not quite sufficient to support the breakdown at atmospheric pressure, but it is possible to supply the required initial electrons for the impact ionization breakdown. For this type of non-resonant laser-induced breakdown the energy absorption of the initial plasma is very inconsistent, and is via electron-neutral inverse bremsstrahlung. When the electron density is sufficiently high, the absorption mechanism transfers to the electron-ion

4

inverse bremsstrahlung process. For the final ionization state, photon absorption by excited state species also contribute significantly. Once the plasma is created the incoming laser beam is absorbed nearly 100%, and the plasma temperature increases rapidly. Once the temperature and pressure increase greatly, the plasma starts expanding rapidly and drives a shock wave outward into the ambient gas to release the pressure. For a laser using a very short pulse (< 10 psec) and for gases at very low pressure (< 10 Torr) the multiphoton ionization process alone must provide the breakdown, since there is not sufficient time for electron-molecule collisions to occur and also the collision effects are negligible at this low pressure. The breakdown threshold energy will be much higher than the nanosecond laser-induced breakdown energy.

The electron cascade process is not a self-initiating process. For this process to occur there should always be initial electrons present in the region. The electrons then absorb more photons via the inverse bremsstrahlung process and increase their kinetic energy. When the electrons gain sufficient energy, they start colliding with other gas molecules and ionize them. This leads to a cascade of electrons and breakdown of the gas. This process can be described as

$$e^- + X \rightarrow 2e^- + X^+, e^- + X^+ \rightarrow 2e^- + X^{++}, \ldots$$
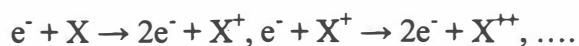
where, e^- is electron, X is gas molecule, X^+ is positive ion and X^{++} is double positive ion.

For laser pulses with long wavelengths this process usually predominates at high pressures since the gas molecules are close to each other and the chances of colliding increase. In combustion applications the generation of sparks for ignition is generally associated with this process.

The initial electrons required for the electron cascade process can be generated either by the multi-photon ionization process (if the laser irradiance is high enough), the thermionic emission in a larger particle, or through the electron-tunnel effect [4, 5]. Normally the laser beams are pulsed at Q-switch pulse duration of nanoseconds, and focused to a small volume for providing enough irradiance. There are some losses such as diffusion of electrons out of the focal volume, radiation, quenching of excited states due to collision, etc. Consequently focal volume, pressure, type of gas and the presence of impurities, such as aerosol particles or low ionization potential organic vapors assist in the generation of initial electrons.

For the process that consists of multiphoton absorptions in the presence of losses, the optical intensities need to be extremely high to induce breakdown in the gases. To achieve this high-energy laser sources with short pulse durations and tightly focused beams are needed so that the pulse-energy can be sufficiently concentrated in the space and time to produce breakdown. These conditions lead to difficulties in producing laser pulses of energy, which are smaller than the minimum ignition energies for highly reactive mixtures with low minimum ignition energies. This is one of the reason why there has not been much research done in determining minimum ignition energies at high pressures.

The objective of this investigation was to determine the effect of pressure breakdown threshold energies of methane and air using a laser-induced spark. In addition the effect of pressure and equivalence ratio on minimum ignition energies of methane-air mixtures was also investigated. This was done because in laser-induced spark ignition the formation of a spark precedes the ignition process. Hence it was important to have

6

knowledge of the condition at which the spark was produced. It was assumed that the gas that would breakdown first would provide the spark for the ignition of the mixture. Thus if at a given there was any correlation between the breakdown threshold energies of methane and air and minimum ignition energies of methane-air mixtures, then the minimum ignition energy of methane-air mixtures at that pressure would be close to the breakdown threshold energy of the gas that breaks down first at that pressure. Although large numbers of studies have been carried out on laser-induced breakdown in gases there is little data available for methane and air at high pressures. The results obtained in this investigation were then compared with the results obtained in previous studies at low pressures.

CHAPTER 2

LITERATURE SURVEY

For internal combustion engines, gas turbines and for explosion and fire hazard assessment knowledge of the ignition of premixed combustible gases is of great importance. It is important to have data for the minimum ignition energy of the mixture at the pressures at which it will be igniting in an engine. As a laser spark ignition proceeds first with the formation of spark, it is important to know at which conditions the spark is produced. To determine these conditions the breakdown threshold energies of the gases need to be determined for the same pressures. Determining the gas breakdown threshold also will help in the selection of optics windows and beam delivery system.

This chapter gives an overview of the available literature on studies of the breakdown threshold energies and minimum ignition energies of different gases. Section 2.1 presents previous studies of the breakdown threshold energies of different gases. Section 2.2 reviews studies on the minimum ignition energies of mixtures of different gases.

2.1 BREAKDOWN THRESHOLD ENERGIES OF DIFFERENT GASES

In the past few decades a lot of studies have been carried out for determining the breakdown threshold energies of a number of gases using different laser systems. Most of the investigations have been carried out using inert gases such as Argon, Neon, Xenon,

etc. In this section a brief description of the results obtained from these investigations is presented.

Dewhurst [6, 7] used laser-induced breakdown to measure the breakdown threshold of rare gases such as helium, argon, neon, krypton and xenon. A single picosecond pulse from a ruby laser with time durations of 18 ± 4 ps was used to achieve the breakdown. Breakdown threshold energies were measured for pressures below ~7000 Torr. Dewhurst expected that the breakdown threshold was caused by a pressure-independent process called multiphoton ionization. However, experimental results showed breakdown threshold to be caused by a pressure-dependent process.

Dewhurst used rare gases to produce results, which showed no evidence of a pressure-independent breakdown process at pulse duration of 7 ps. Breakdown threshold intensities never exceeded 10^{13} W/cm^2, which indicated that breakdowns were caused by cascade collision ionization and not multi-photon ionization.

Fig 2.1 shows the breakdown threshold measurements for the rare gases. This shows the dependence of the relative intensity of the breakdown threshold on pressure. For helium and argon the results are compared with those obtained by Krasyuk [8] results with 30-100 ps pulses, and an important difference is observed between the two results. No transition to pressure independent multiphoton ionization process was observed, but the breakdown threshold intensity behavior with pressure was similar to the previous results at 1.06 and 0.53 μm wavelengths. The breakdown threshold energy always varies with the pressure p as $I \propto p^{-m}$, where I is the laser irradiance, p is the gas pressure and m is obtained from the results shown in Fig 2.1. Moreover, within the pressure range used
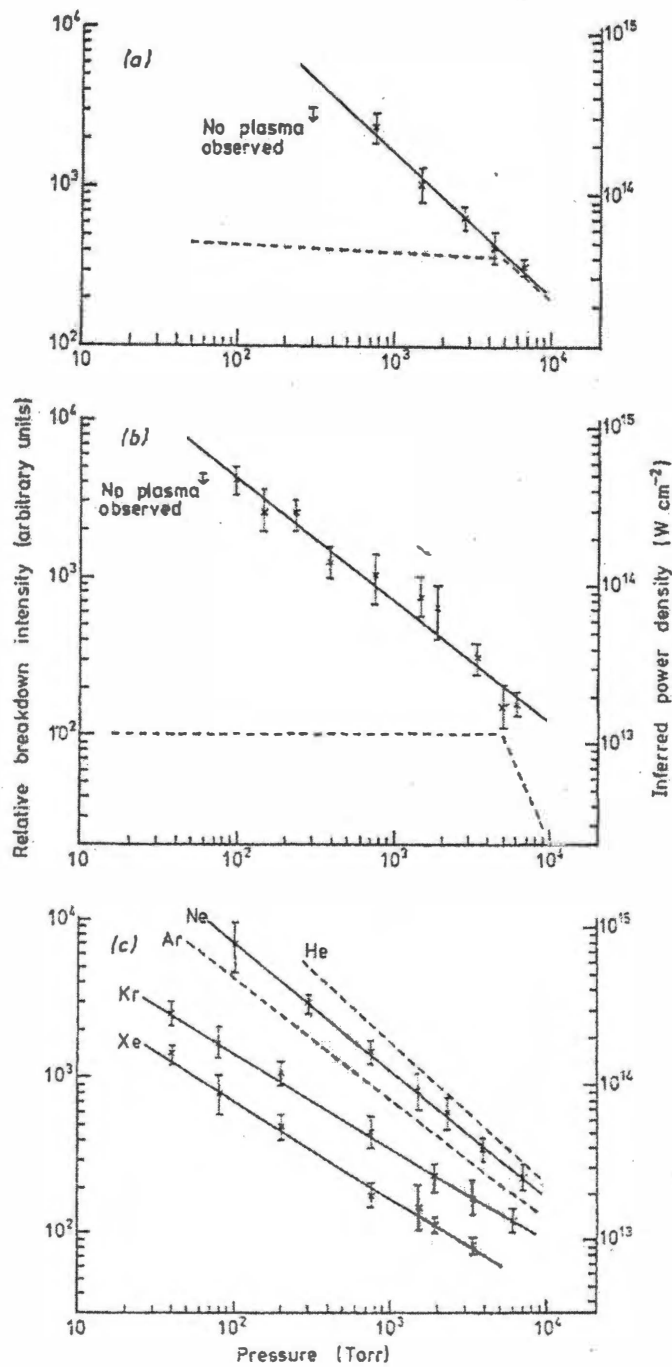
Figure 2.1 Breakdown thresholds in (a) helium; (b) argon; (c) neon, krypton and xenon, with the results for He and Ar summarized for comparison. The gradients of the full lines are: 0.90, 0.78, 0.81, 0.61, and 0.63, respectively from Dewhurst [6] and the dotted lines are those of Krasyuk [8].

there is no transition for other rare gases. The results also show that at any given pressure, the breakdown threshold is approximately proportional to the ionization potential of the gas used. Two things could be concluded: firstly, even if impurities create some free electrons they do not determine the breakdown threshold and secondly, there is no evidence of resonance effects, which could cause anomalously low breakdown thresholds in a particular gas.

It can be seen from the results that the breakdown threshold intensities are strongly pressure-dependent and become higher at low pressures than expected for the onset of multi-photon ionization, which is contrary to the theoretical prediction of Bunkin and Prokhorov [9]. Table 2.1 shows breakdown threshold intensities at 0.694 μm for rare gases such as He, Ar, Ne, Kr, and Xe predicted from theoretical multiphoton ionization probabilities and calculated from perturbation theory and a quantum mechanical treatment of the radiation field. These were derived without considering the effect on the transition probabilities of large radiation field, and also the results were not lowered to take into account the nature of radiation.

Experimental ionization probabilities could be used for predicting the onset of multiphoton ionization. Known probabilities taken from Voronov and Delone [10] and Voronov et al [11] were used to predict breakdown thresholds for Kr and Xe at laser irradiance of 1.1×10^{13} and 5.6×10^{12} W/cm^2, respectively. Thus, for pressures less than 8000 Torr, threshold intensities in both gases were expected to be pressure independent.

Unfortunately, both theoretical and experimental ionization probabilities discussed above do not directly relate to strong radiation fields. Keldysh [5] showed that the behavior of multiphoton ionization is related to a field parameter γ defined as

12

Table 2.1 Predicted breakdown thresholds at 0.6943 µm from theoretical multiphoton ionization probabilities. The laser pulse duration is taken as 18 ps from Bebb and Gold [12]

Gas	Predicted thresholds (W cm-2)	
	Bebb and Gold (1966)	Gold and Bebb (1965)
He	3.7×10^{13}	3.4×10^{14}
Ne	1.1×10^{13}	3.5×10^{13}
Ar	1.4×10^{12}	9.3×10^{13}
Kr	1.1×10^{12}	3.0×10^{13}
Xe	3.0×10^{12}	1.4×10^{13}

$$\gamma^2 = I_0(2m\omega^2/e^2E^2)$$

where I_0 is the ionization potential of the gas, e, m and ω are the electronic charge, mass and angular frequency of the radiation, respectively. Most determinations of the multiphoton ionization probabilities have been taken in the range $\gamma >> 1$.

The experimental results showed that there is no multi-photon ionization theory, which quantitatively explains breakdown threshold measurements in the regime $\gamma \leq 1$. Also for any give pressure, the breakdown threshold increased with increasing ionization potential, and no evidence of resonance effects was observed.

Williams et al. [13] used a Nd: YAG laser at a wavelength of 0.53 μm to measure breakdown thresholds of laboratory air with pulses varying from 30 to 140 ps for a variety of focal point sizes. The rms of laser-induced breakdown field E_B corresponding to the peak-on-axis irradiance, was found to increase as the pulse-width was decreased. The results were compared with the results obtained from earlier work done under similar conditions but using laser with a wavelength of 1.06 μm. For an equal pulse width and same focal point size, E_B was greater for 0.53 μm than at 1.06 μm. However, the increase was weaker than the dependence predicted by cascade theory.

Table 2.2 summarizes the breakdown thresholds for air at 0.53 μm. No air breakdown was observed for the 14 μm spot size for the highest output value available for the laser. Fig 2.2 shows more clearly the functional dependence of the breakdown electric field E_B, for air at 0.53 μm wavelength. This is done by plotting E_B versus the inverse pulse width on a log-log plot. The observed pulse width dependence of E_B at 0.53 μm is characteristic of a cascade ionization process in the high electric field limit.

Table 2.2 Laser induced breakdown data for air at 0.53 μm for spot size of 3.4 and 7.2 μm. The absolute accuracy of these data is estimated to be ± 20% in the breakdown field from Williams et al [13]

		Air breakdown $\lambda = 0.53\,\mu m$			
W_D (μm)	t_p (ps)	E_B (MV/m)	I_B (TW/cm^2)	P_B (MW)	ϵ_B (kJ/cm^2)
	20	~170	~72	~13.1	~1.5
3.4	33 ± 5	120 ± 6	38 ± 3	7.0 ± 0.7	1.3 ± 0.1
	80 ± 5	83 ± 7	18 ± 2	3.3 ± 0.4	1.5 ± 0.2
	100 ± 10	70 ± 5	13 ± 2	2.4 ± 0.3	1.4 ± 0.1
	140	65 ± 4	10.7 ± 2	1.9 ± 0.2	1.6 ± 0.2
	32 ± 3	129 ± 9	44 ± 5	35.8 ± 4	1.5 ± 0.2
7.2	89 ± 5	80 ± 7	17 ± 3	13.8 ± 1.4	1.6 ± 0.2
	110 ± 10	66 ± 4	11.5 ± 1.2	9.4 ± 1.0	1.4 ± 0.2
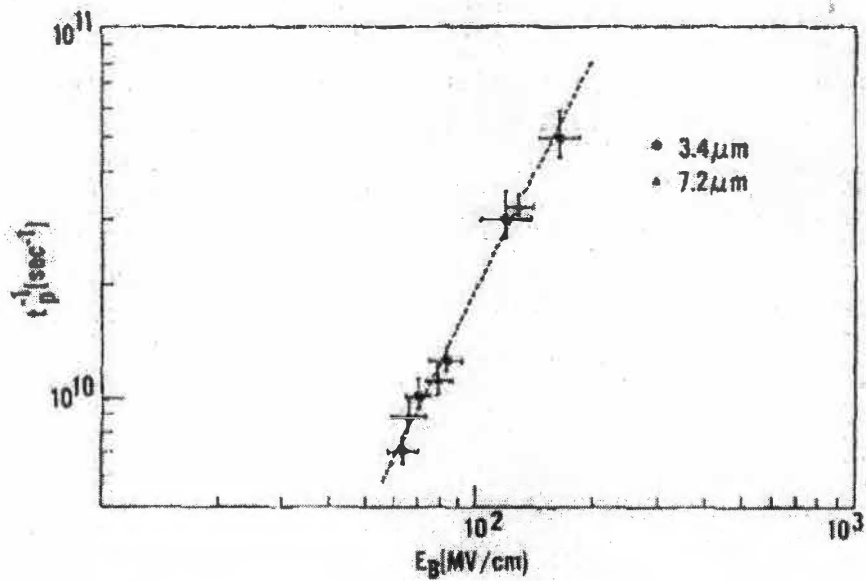
Figure 2.2 Pulse width dependence of E_B for air at 0.53 μm for spot size of 3.4 and 7.2 μm. The slope of the linear least square fit of the data is 0.48 ± 0.08 which is approximate inverse $(t_p)^{1/2}$ dependence. Owing to the lack of spot size dependence exhibited at this wavelength both sides of data were used in the linear least square fit from Williams et al [13]

This limit corresponds to a situation in which the increase in energy of the free electrons is simply proportional to the input irradiance and all the losses are negligible. The ionization rate is exponentially dependent on E for the lower field limit and the resulting pulse width dependence is relatively weak.

Williams et al. concluded that the breakdown irradiance threshold at 0.53 μm exhibited a $1/t^{1/2}$ dependence, which is stronger dependence than that seen at 1.06 μm under similar conditions. The thresholds at 0.53 μm are higher than those at 1.06 μm. A multi-photon-assisted cascade ionization process is suggested as the breakdown mechanism for air under the given conditions.

Rosen and Weyl [14] performed an experimental investigation of laser-induced breakdown for N_2, Ar, Ne and Xe using an Nd: YAG laser of 15 ns pulse at 0.53 and 0.35 μm wavelengths. In the pressure range of 0.2<p<15 atm the breakdown threshold intensity I^{th} was measured. In their investigation the threshold was defined as the appearance of a visible flash and/or greater than 5% absorption of beam energy.

Fig 2.3 shows the measured breakdown thresholds in argon at 0.53 and 0.35 μm. Also shown are experimental results of Buscher et al (1965) [15] who used a frequency-doubled Nd: YAG beam and a frequency doubled ruby beam. The variation with pressure was found to be $p^{-0.85}$. The focal power densities plotted represent the peak values. From the Fig 2.3 it can be seen that there is quite close agreement between the two sets of experiments, although it is expected that threshold intensities of Buscher et al to be approximately 35% lower as they used longer pulse duration. On the other hand, the thresholds measured in Rosen and Weyl's work using a frequency-tripled Nd: YAG beam ($\lambda = 35$ μm) appear to be about three to five times higher than those measured
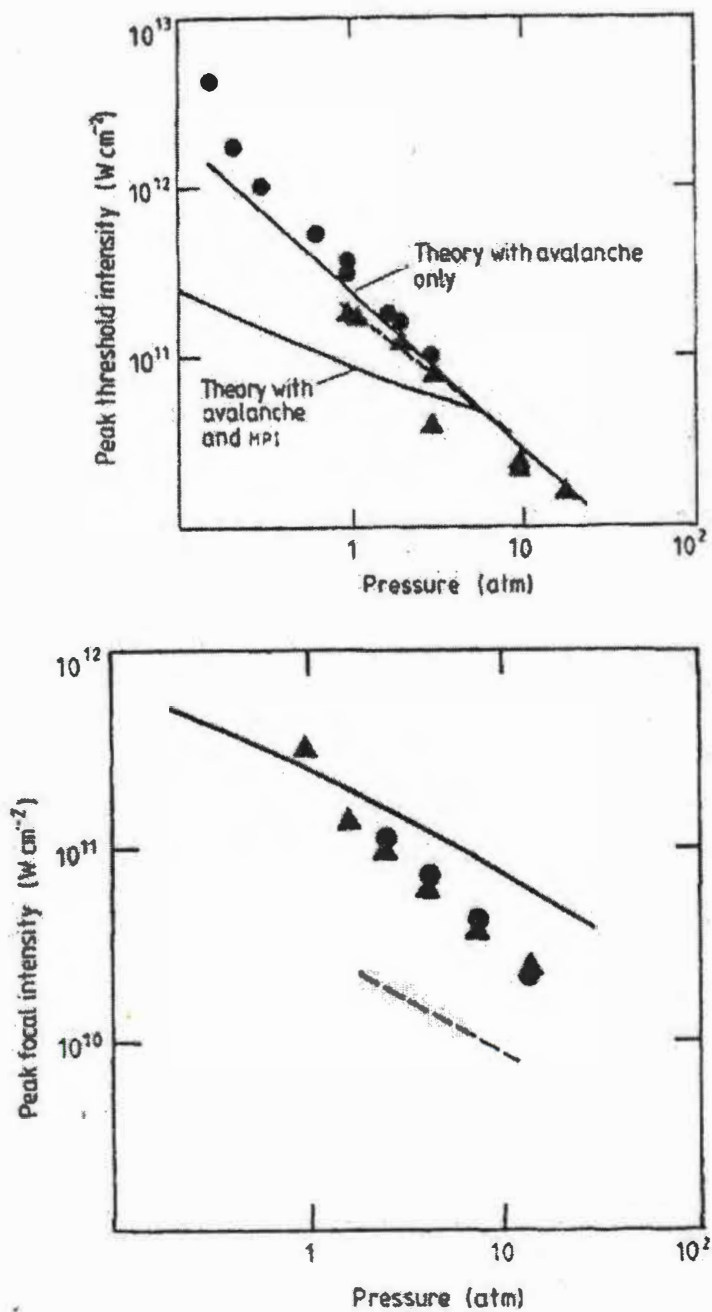
Figure 2.3 The breakdown threshold in argon at $\lambda = 0.53$ μm and $\lambda = 0.35$ μm from Rosen and Weyl [14] where the round spots represent Rosen and Weyl's results and the triangular spots represent Buscher.

18

using a frequency-doubled ruby ($\lambda = 0.53$ μm), with very similar pulse duration and focal spot size.

Breakdown thresholds measured for neon at 0.35 and 0.53 μm are shown in Fig 2.4. At 0.35 μm the breakdown thresholds are seen to be about 2 to 2.5 times higher than at 0.53 μm. Also the thresholds measured in their work are about a factor of 8 higher than the thresholds measured by Alcock et al [16] with a frequency-doubled ruby beam ($\lambda = 0.35$ μm) and a shorter pulse ($\tau_p = 8$ ns). The thresholds are much higher in neon than in argon because the ionization energy of neon is higher (21.6 eV) as compared to argon (15.8 eV).

Fig 2.5 shows the breakdown thresholds for xenon at 0.53 and 35 μm. The thresholds at 0.35 μm is about three times lower than that at 0.53 μm. The variation with pressure follows nearly a p^{-1} law at both wavelengths. Thresholds are again higher than those reported by Buscher et al, but the discrepancy is only a factor of 2 as compared to 3 to 5 for argon.

For nitrogen, the breakdown thresholds at 0.53 and 0.35 μm are shown in Fig 2.6. The dependency of pressure is much weaker, $I^{th} \alpha \, p^{-0.6}$, as compared to rare gases. The threshold of nitrogen is extremely high. It is higher than in neon, even though neon has an ionization potential of $\varepsilon_{Ne} = 21.6$ eV as compared to $\varepsilon_{N2} = 15.5$ eV for nitrogen. Argon and nitrogen have similar ionization energies; still the breakdown threshold of nitrogen is 10 times higher than argon at the same pressure and wavelength.

To summarize, the breakdown threshold intensity I^{th} in the pressure range $0.2 < p < 15$ atm was measured. At $p = 3$ atm I^{th} for 0.53 μm was found to be 1×10^{12}, 8×10^{10}, 5×10^{11} and 4×10^{10} and for 0.35 μm was found to be 5×10^{11}, 1×10^{11}, 1×10^{12}
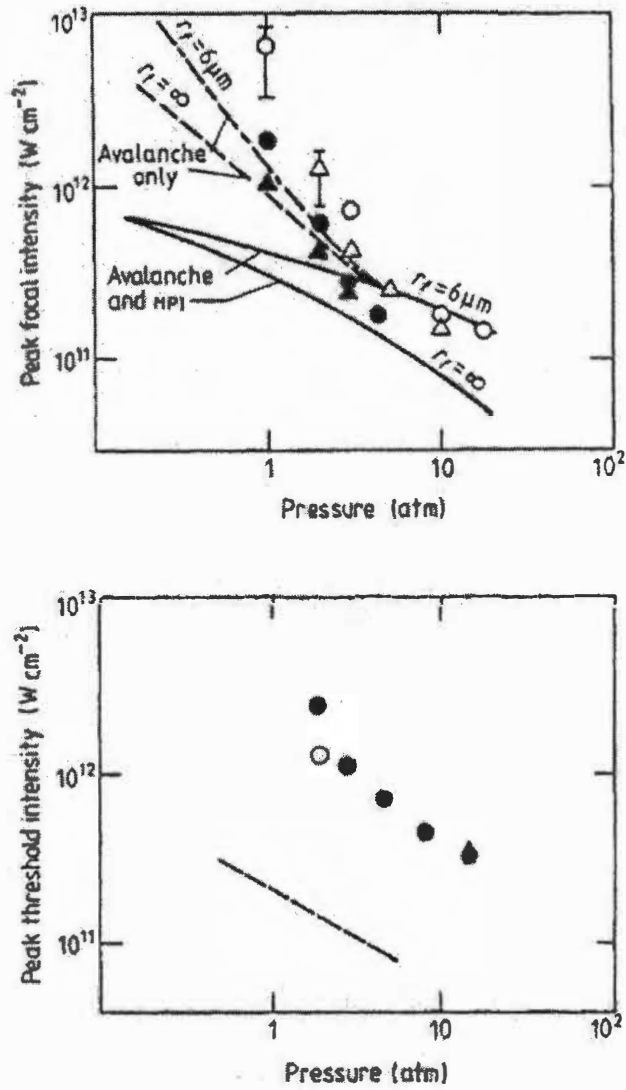
Figure 2.4 The breakdown threshold in neon at $\lambda = 0.53$ μm and $\lambda = 0.35$ μm from Rosen and Weyl [14]
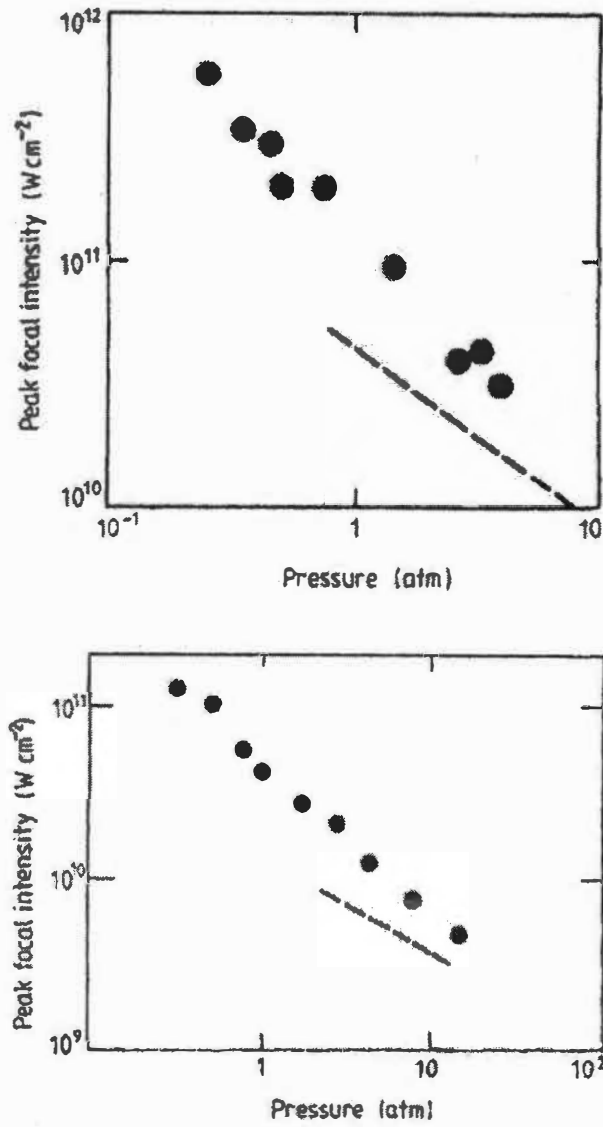
Figure 2.5 The measured breakdown threshold in xenon at $\lambda = 0.53$ μm and $\lambda = 0.35$ μm from Rosen and Weyl [14]
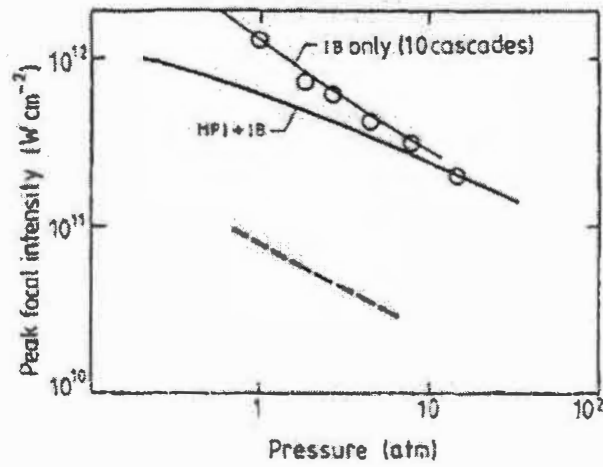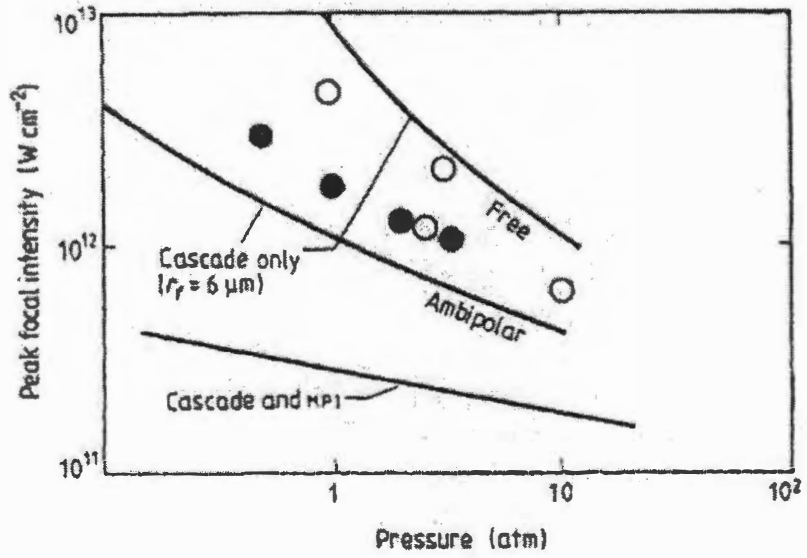
Figure 2.6 The measured breakdown threshold in nitrogen at $\lambda = 0.53$ μm and $\lambda = 0.35$ μm from Rosen and Weyl [14].

and 2×10^{10} W/cm^2 for N$_2$, Ar, Ne and Xe respectively. The p^{-1} scaling of Ith for Ne, Ar and Xe and $p^{-0.6}$ scaling for N$_2$ indicates that the threshold is associated at both wavelengths with avalanche breakdown rather than multi-photon ionization. Multi-photon ionization of gases provides the seed electrons and reduces diffusion losses out of the focal volume.

Turcu et al. [17] measured high thresholds for KrF laser breakdown at 0.248 μm wavelengths and a focal spot of 9 μm in several noble gases and air, at focused power densities up to 3×10^{13} W/cm^2. Fig 2.7 shows the laser irradiance (I) for breakdown threshold as a function of gas pressure p in the cell. The pressure dependence of helium was found to be $I \alpha p^{-1}$, which is good agreement for the inverse bremsstrahlung absorption process creating gas breakdown. Irradiance dependence on the power of the pressure was slightly different for various gases like -1.27 for neon, -1.36 for argon, -1.25 for krypton and -1.17 for air. This shows that even though the photon absorption process for these gases may be by inverse bremsstrahlung, electron diffusion out of small focal volume may also be significant.

The results obtained by Turcu et al. confirmed the high breakdown threshold reported previously ($I \leq 10^{11}$ W/cm^2) in the intensity range of overlap. To avoid the breakdown at an irradiance of $I \approx 10^{13}$ W/cm^2 the pressure in the X-ray source chamber was maintained at ≤ 530 mbar. It is further investigated by measuring at this intensity the laser energy transmitted through the breakdown region at a helium pressure of 1 atmosphere. It was seen that 86% of the laser energy was transmitted through the focal region. This small absorption and apparent distortion of the KrF laser beam was due to the low electron density of $\sim 10^{19}$ electrons/cm^3 produced in helium at atmospheric
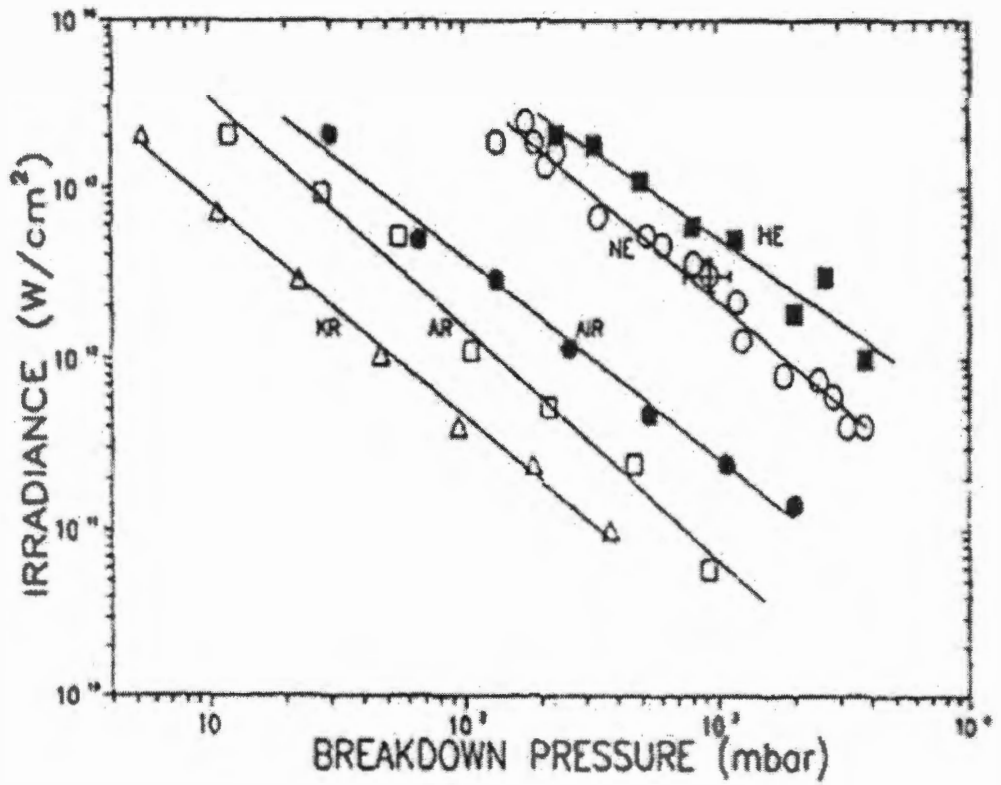
Fig 2.7 Breakdown threshold in gases for KrF excimer laser at 0.248 μm wavelength from Turcu et al. [17]

pressure, which is three orders of magnitude smaller than the critical density for absorption of KrF radiation at 0.248 μm ($\sim 10^{22}$ electrons/cm^3).

Turcu et al. concluded that the results from the investigation showed a good agreement with the inverse bremsstrahlung absorption model. The breakdown thresholds are high which, confirmed the trend established by previous measurements at low irradiances.

Phuoc [18] measured the breakdown threshold laser intensities of air, O_2, N_2, H_2 and CH_4 using a Q-switched Nd:YAG laser operating at 0.53 μm and 1.064 μm with a pulse of 5.5 ns. The breakdown threshold energies were measured for the pressure range of 150 to about 3040 Torr.

Fig 2.8 shows the breakdown threshold laser energies and laser intensities at 150 Torr and 3040 Torr and the values are shown in Table 2.3 for easy reference. It can be seen that laser intensity range from 10^{12} to 10^{14} W/cm^2 is sufficient to create a breakdown spark in the gases at pressures ranging from 150 Torr to about 3000 Torr. The breakdown thresholds for methane were found to be consistently lower than those for other gases. This can be attributed to the low ionization potential of methane (12.51 eV), which is lower than that of nitrogen (15.58 eV) and hydrogen (15.425 eV). Although oxygen has an ionization potential of 12.07 eV, which is the lowest ionization potential compared to the other gases investigated, the thresholds of oxygen were found to be in the range similar to those of nitrogen and hydrogen and was a factor higher than the thresholds of methane.

The data shows dependence of the threshold irradiance on pressure as $I_{thr} \alpha\ p^{-n}$, which is agreement with the inverse bremsstrahlung absorption process for creating

25
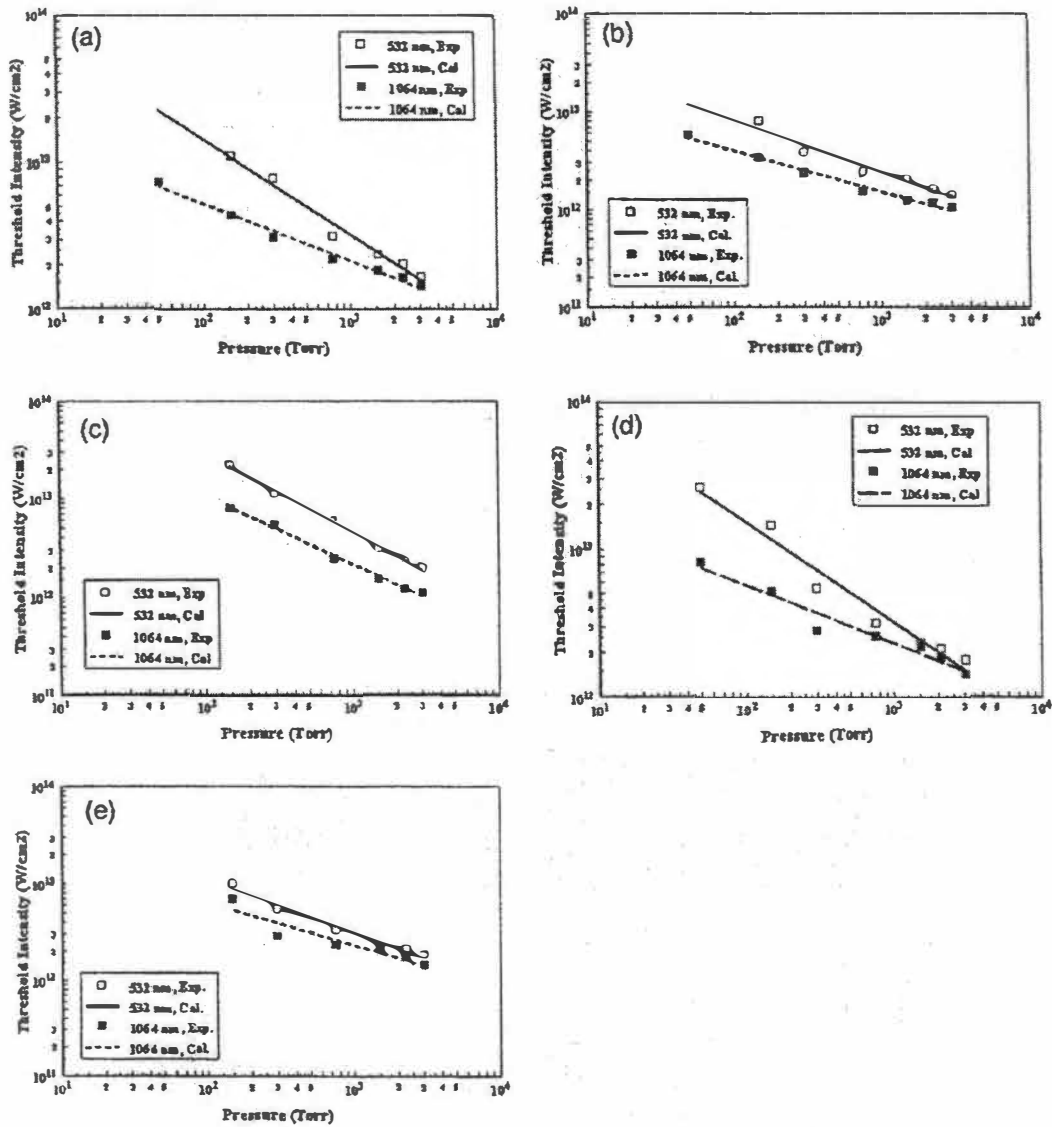
Fig 2.8 (a) Breakdown thresholds in air (b) Breakdown thresholds in CH_4 (c) Breakdown thresholds in H_2 (d) Breakdown thresholds in N_2 (e) Breakdown thresholds in O_2 from Phuoc [18].

Table 2.3 Breakdown threshold laser energy, E_{thr} (mJ), and laser intensity I_{thr} (W/cm^2), in gases from Phuoc [18]

Breakdown threshold laser energy, E_{thr} (mJ), and laser intensity, I_{thr} (W/cm^2), in gases (75 mm focal length)

Gas	Pressure	E_{thr} (mJ)		I_{thr} (W/cm^2)	
		532 nm	1064 nm	532 nm	1064 nm
Air	156	20.14	32.31	1.08×10^{13}	4.35×10^{12}
	3040	3.06	10.53	1.65×10^{12}	1.40×10^{12}
CH$_4$	150	14.97	25.09	8.05×10^{12}	3.37×10^{12}
	3040	2.67	7.83	1.44×10^{12}	1.05×10^{12}
H$_2$	150	42.00	60.00	2.26×10^{13}	8.07×10^{12}
	3040	3.76	8.29	2.03×10^{12}	1.12×10^{12}
N$_2$	150	26.37	38.13	1.42×10^{13}	5.13×10^{12}
	3040	3.34	10.74	1.80×10^{12}	1.45×10^{12}
O$_2$	150	18.88	51.60	1.02×10^{13}	6.94×10^{12}
	3040	3.45	10.50	1.85×10^{12}	1.41×10^{12}

breakdown. The degree by which the thresholds depend on the pressure was found to be strong at shorter wavelength than at the longer wavelength. At $\lambda = 0.53$ µm, the pressure dependence of threshold in hydrogen was strongest among the gases investigated with n = 0.78. Breakdown thresholds in other gases showed a weaker dependence with n = 0.67 for nitrogen, n = 0.65 for air, and n $\approx$ 0.55 for both methane and oxygen. At $\lambda = 1.064$ µm, the threshold in hydrogen still showed a strong pressure dependence with n = -0.69, while the pressure dependence of threshold in other gases became much weaker with n $\approx$ -0.4. This difference in the degree by which the threshold depend on the pressure might be due to the effect of the diffusion loss out of the focal volume which is more significant at $\lambda = 0.53$ µm than at $\lambda = 1.064$ µm.

The present data shows that the breakdown threshold laser intensity at 0.53 µm was higher than that at 1.064 µm. The effect of wavelength reported here was more profound at low pressure and it became less significant as the pressure increased. This indicates that multi-photon ionization process may play a more important role at 0.53 µm wavelength and low pressure than at 1.064 µm wavelength and high pressure.

Phuoc concluded that data shows p^{-n} pressure dependence, which is in good agreement with the electron cascade process for creating gas breakdown. For 1.064 µm laser beam, except for hydrogen, the pressure dependence was found to be similar for all gases with n $\approx$ 0.4. For 0.53 µm, the pressure dependence was much stronger showing the important effect of the diffusion loss.

2.2   MINIMUM IGNITION ENERGIES OF DIFFERENT GASES

Lewis and von Elbe [19] were among the first to determine the minimum ignition energy required to produce flame propagation. Many researchers have been comparing their results with the results reported by Lewis and von Elbe. They determined the minimum ignition energy of mixtures of methane, oxygen and nitrogen for pressures of 0.25, 0.33, 0.5 and 1 atm at room temperature using capacitance discharge electrical sparks. In some cases nitrogen was replaced by helium, argon or carbon dioxide.

Lewis and von Elbe measured the capacitances and gap voltage of condensed electric spark circuits to produce sparks, which were just powerful enough to ignite various explosive mixtures. These data of the capacitances and gap voltages were used to calculate the minimum ignition energies of the mixtures. They also varied various parameters such as inductance, electrode voltage and electrode distance to determine their effect on the minimum ignition energies.

Lewis and von Elbe carried a number of tests by replacing the circuit link with a helix of heavy wire to in order to vary the inductance and oscillatory frequency as shown in Fig 2.9. The results failed to show any change in the values in minimum ignition energies for the changes in the inductance and oscillating frequency. To determine the effect of voltage the breakdown voltage between the electrodes was increased considerably by applying much higher voltage. This was possible by either taking advantage of the breakdown time lag or by charging the condensers and connecting them with the electrode circuit by a fast-acting switch in place of a removable circuit link. As seen from the results in Table 2.4, the minimum ignition energy was found to be
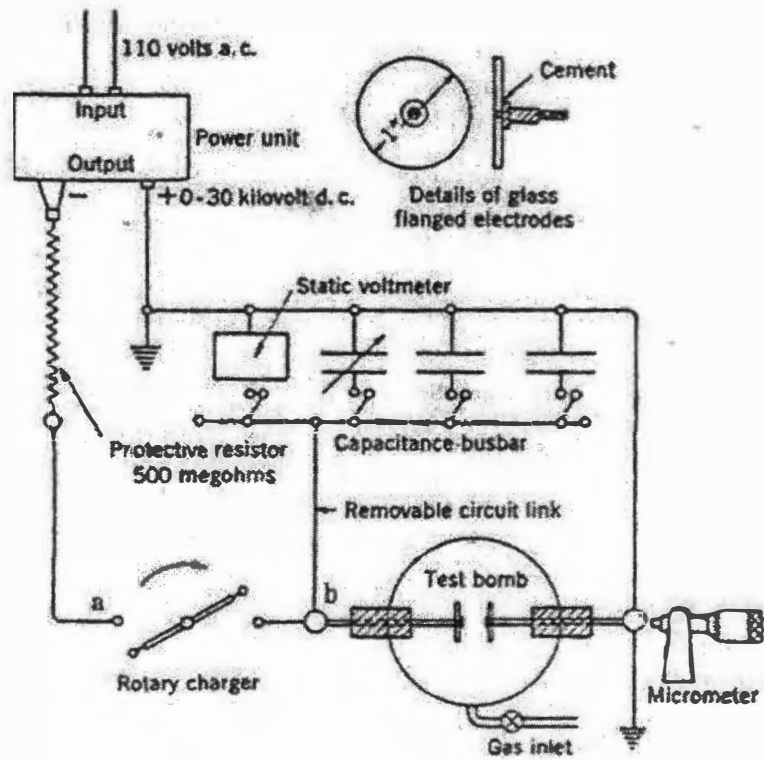
Figure 2.9 Schematic of the setup in which the circuit link was replaced with a helix of heavy wire employed by Lewis and von Elbe [19]

Table 2.4 Results showing the minimum spark ignition energy to be independent
of gap voltage from Lewis and von Elbe [19]

	Gap voltage* kilovolt	Minimum ignition energy, millijoule
8.7 percent natural gas** in air at 1 atmosphere	6.1	0.5
	9.9	0.5
0.5 atmosphere	8.6	1.7
	10.2	1.7
0.33 atmosphere	5.4	2.4
	7.5	2.4
0.25 atmosphere	4.5	4.0
	6.8	4.2
8.5 percent methane in air at 0.33 atmosphere	14.2	2.6
	20.0	2.6

* The distance between the electrodes was held constant for each
pair or runs

** Approximately 83 percent CH_4, and 17 percent C_2H_6

31

essentially independent of over voltage. This observation implies that as the gap voltage was increased the capacitance had to be decreased correspondingly. In general it appeared that in spark discharges the largest part of energy goes into production of atoms, free radicals, and thermal motion, while only a small fraction goes into production of ions.

Lewis and von Elbe determined the effect of electrode distance on the minimum ignition energy by comparing two systems, one with free electrode tips and other with glass-flanged tips. The results in Fig 2.10 show that above the critical distance of 0.08 inch the data obtained from the two systems coincides. Below this distance the minimum ignition energy increases abruptly with glass-flanged electrodes and gradually with point electrodes.

Above the critical distance the minimum ignition energy remains constant over a considerable range of the electrode distance as long as the pressure of the gas is not too low. These results are shown in Fig 2.11 for a stoichiometric mixture of methane and air at various pressures. It appears that if the quenching effect of the electrodes could be removed then the data for low pressures would also fall on a horizontal line. For many years these data were used as the baseline for the minimum ignition energy required to produce flame propagation. However these data did not agree with the computational predictions.

Frendi and Sibulkin [20] used two mathematical models for predicting the minimum ignition energy of a stoichiometric methane-air mixture at pressure of 1 atm and temperature of 298 K. The only difference between the two mathematical models was that in one the pressure variations were allowed and in the other the pressure was

32
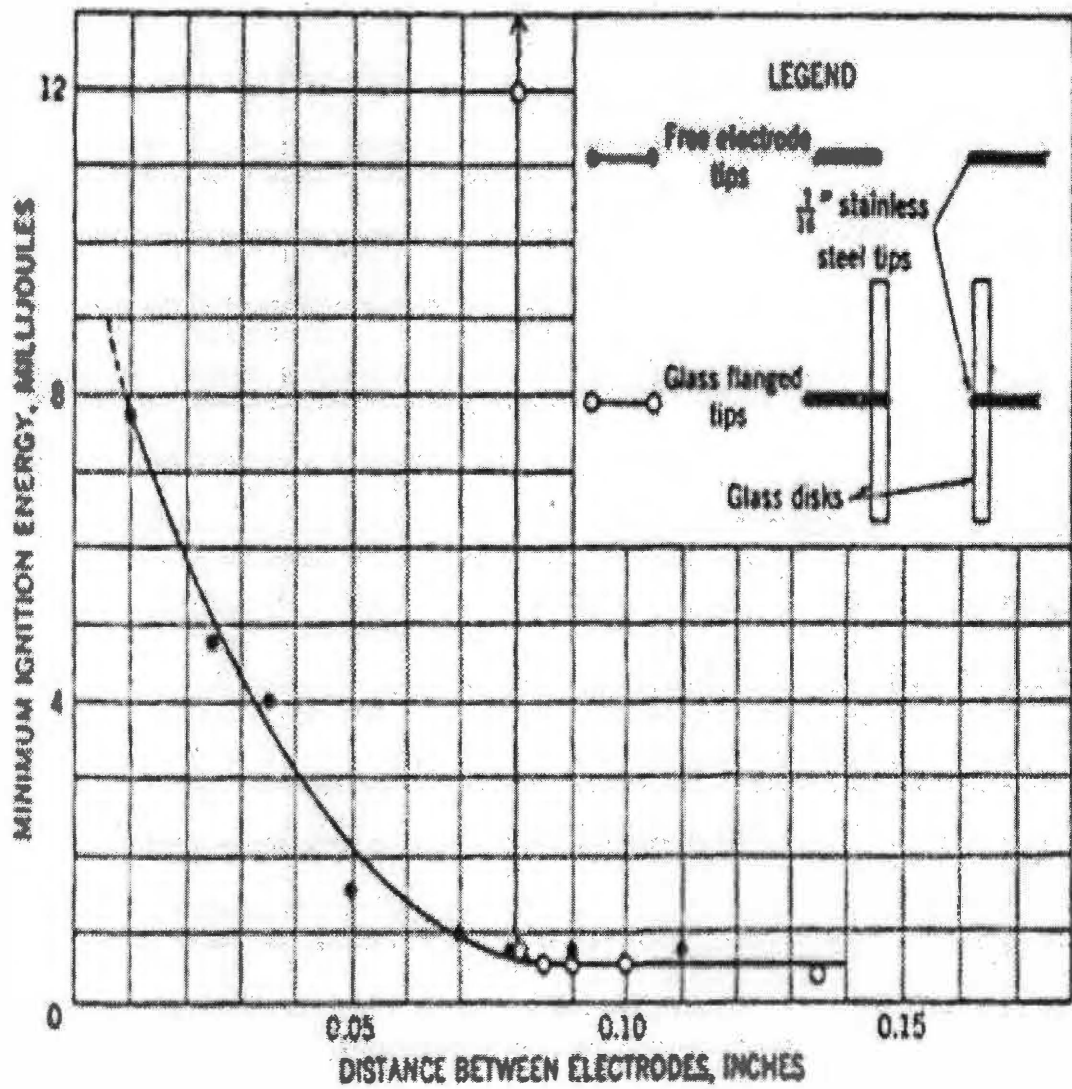
Figure 2.10 Minimum ignition energies for free and glass-flanged electrode tips as function of electrode distance. Stoichiometric mixture of natural gas and air at one atm from Lewis and von Elbe [19]
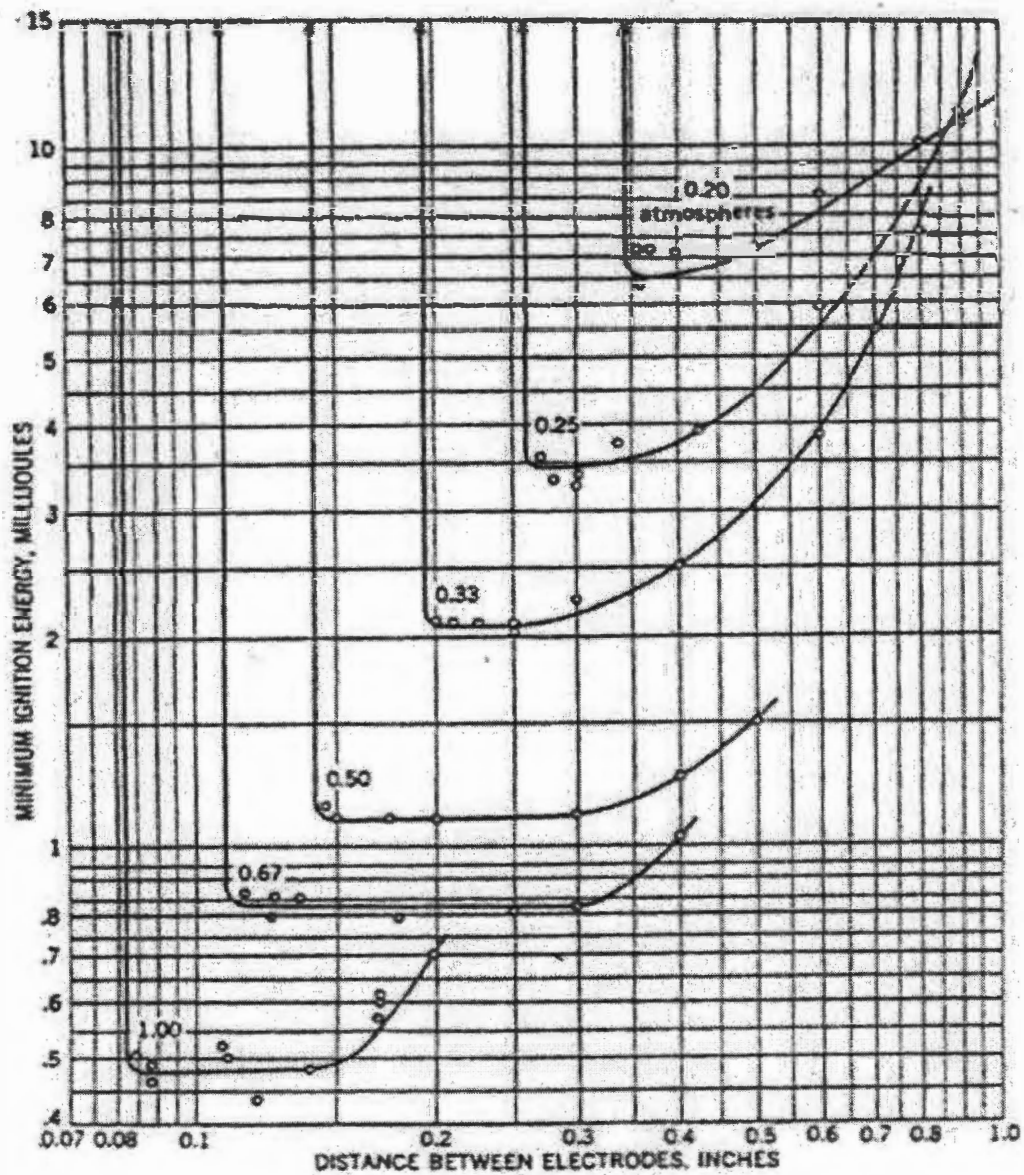
Figure 2.11 Minimum ignition energies for glass-flanged electrode tips as functions of electrode distance and pressure. Stiochiometric mixture of methane and air from Lewis and von Elbe [19]

assumed to be uniform. In their models they studied the effect of initial pressure wave generated by spark on the minimum ignition energy by comparing the results of both models. They also investigated the dependence of minimum ignition energy on the spark kernel radius (r_{ig}) and ignition time.

Fig 2.12 shows the comparison of the results from the constant pressure assumption with the variable pressure model. The kernel radius was fixed to 0.167 mm. The models predicted same minimum ignition energies for a long ignition times ($\tau_{ig} > 2\mu s$). However for short ignition times ($\tau_{ig} < 2\mu s$), the variable pressure model predicted higher minimum ignition energies. At short ignition times the minimum ignition energy remained constant.

The effect of changing the kernel radius on minimum ignition energy for different ignition times is shown in Fig 2.13. The minimum ignition energy for a kernel radius larger than 0.3 mm increases in proportion to the volume (r^3_{ig}) of the ignition kernel. For ignition kernel radius below $r_{ig} = 0.1$ mm, the minimum ignition energy reaches a constant value for ignition times of $\tau_{ig} = 2.75$ μs and 27.5 μs. For $\tau_{ig} = 100$ μs and 500 μs the curve approaches an asymptotic behavior.

Fig 2.14 shows the variation of the ignition energy density ($E"_{ig}$) with spark kernel radius for different ignition times. For $r_{ig} > 0.2$ mm, the ignition energy density is a constant for values of $\tau_{ig} \leq 100$ μs, and tends to be constant for larger ignition times. The ignition energy density increases rapidly at all ignition times for kernel radii smaller than 0.2 mm.

Fig 2.15 shows the variation of minimum ignition energy with ignition time fordifferent kernel radii. The regions where both the models predict the same values

35
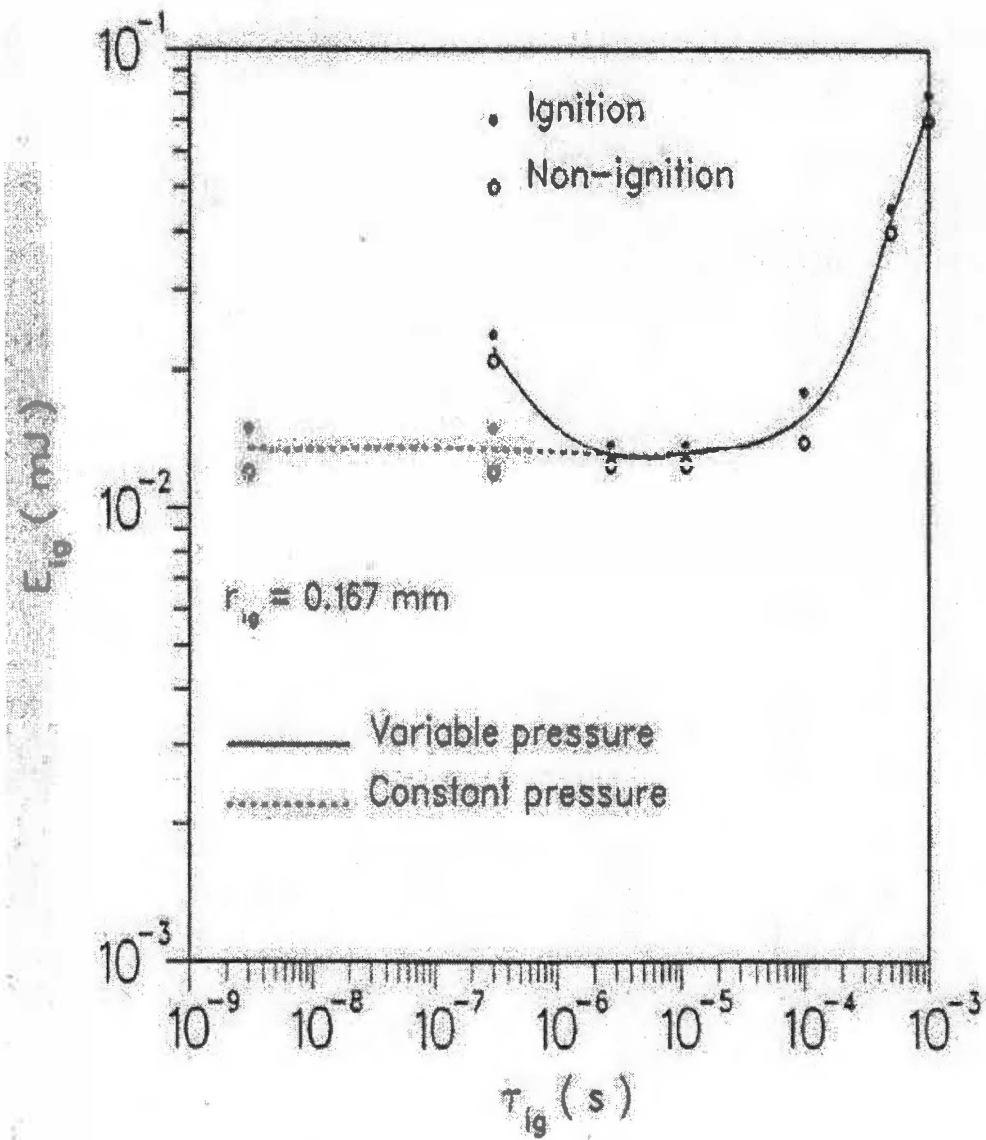
Figure 2.12 Comparison of minimum ignition energies obtained by the variable pressure and constant pressure models. Stoichiometric methane-air mixture, spherical geometry from Frendi and Sibulkin [20]
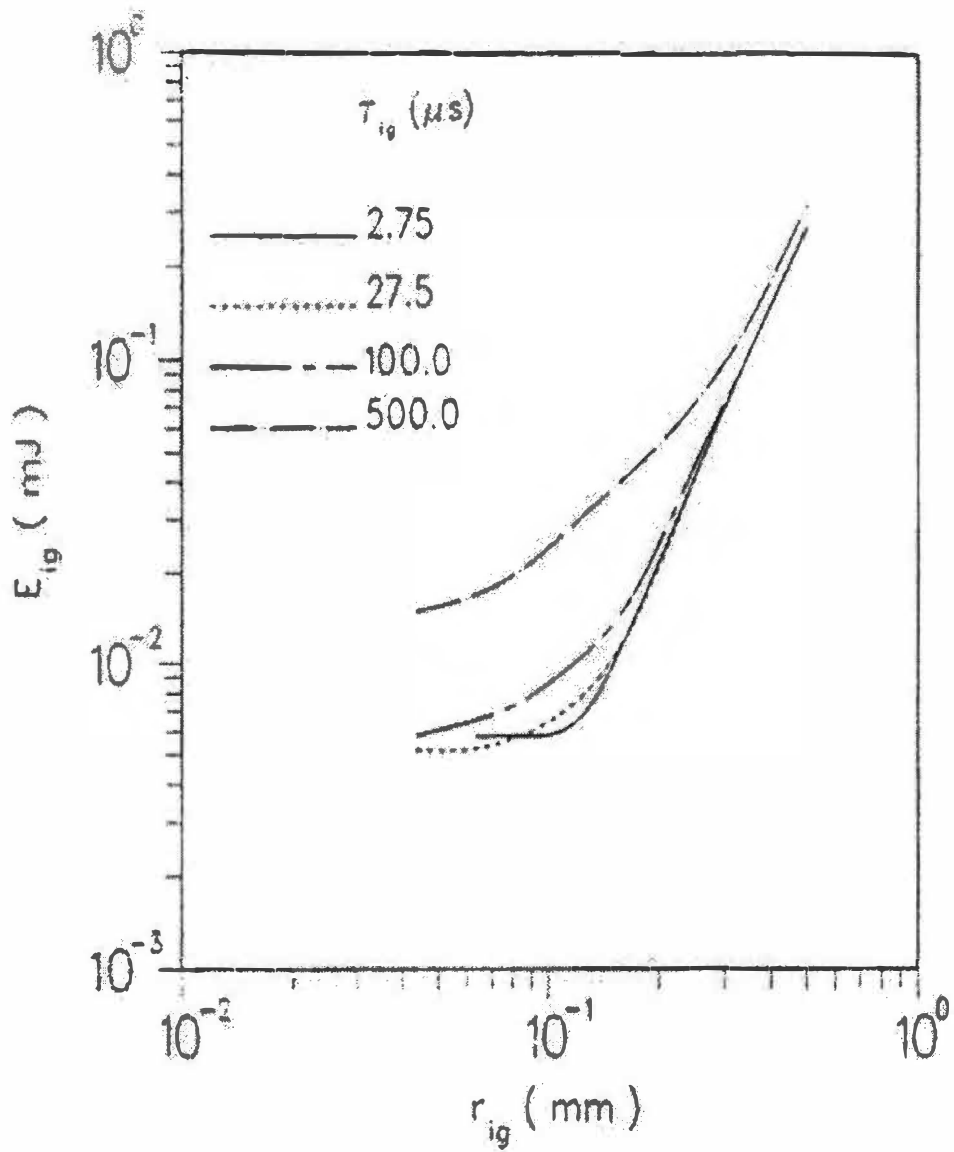
Figure 2.13 Variation of minimum ignition energy with kernel radius for different ignition times. Stoichiometric methane-air mixture, spherical geometry from Frendi and Sibulkin [20]

37
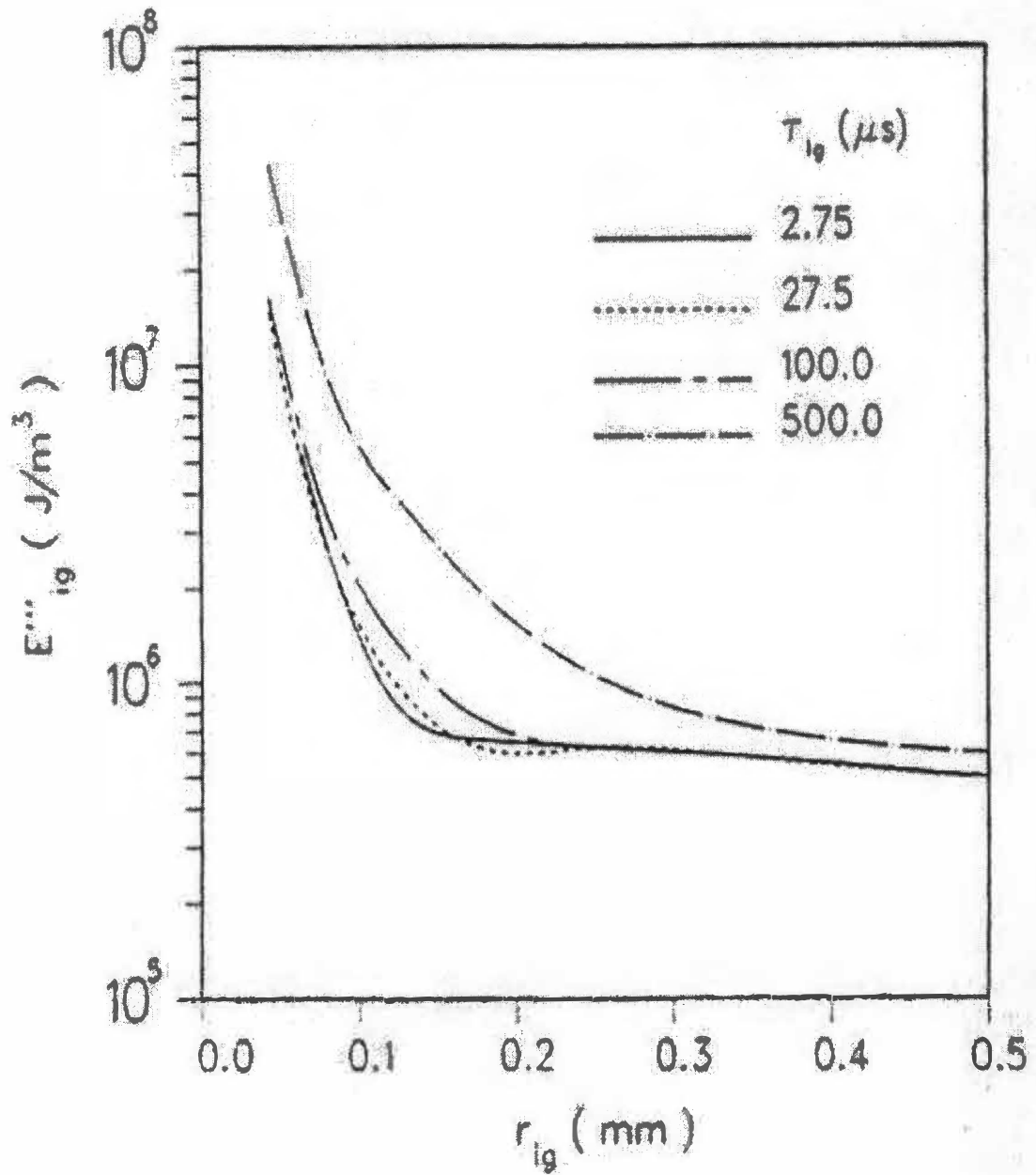
Figure 2.14 Variation of minimum ignition energy density with kernel radius for different ignition times. Stoichiometric methane-air mixture, spherical geometry from Frendi and Sibulkin [20]
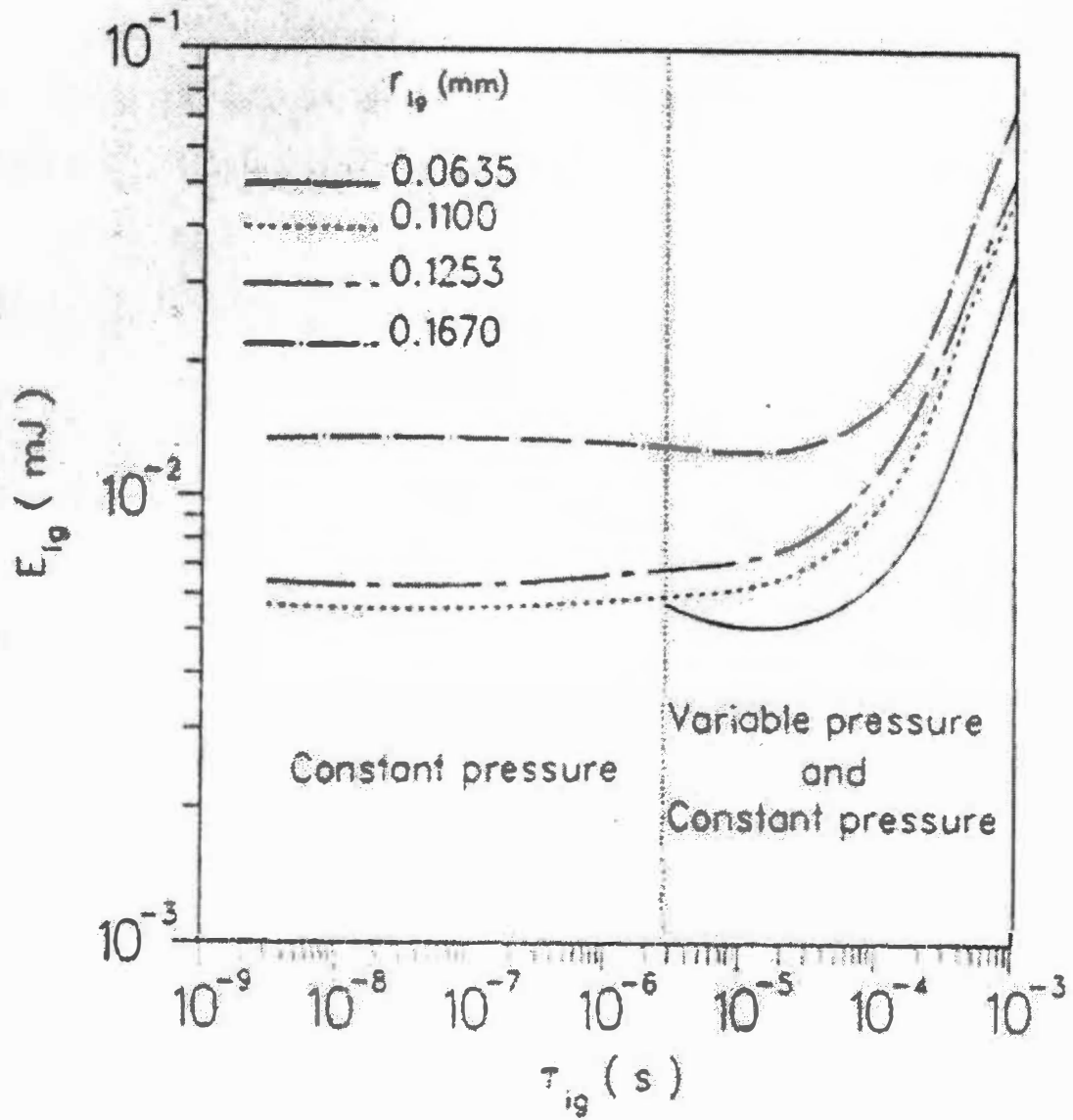
Figure 2.15 Variation of minimum ignition energy with ignition time for different kernel radii. Stoichiometric methane-air mixture, spherical geometry from Frendi and Sibulkin [20]

($\tau_{ig} > 2$ μs) and different values ($\tau_{ig} < 2$ μs) are separated by a dotted vertical line. For 2 μs $< \tau_{ig} < 100$ μs the minimum ignition energy is nearly constant, but for $\tau_{ig} > 100$ μs it increases in proportion with ignition time ($E_{ig} \propto \tau_{ig}$).

The variation of the ignition energy density with ignition time for different kernel radii is shown in Fig 2.16. The general trend of the curve in this figure is similar to that of the minimum ignition energy; the only difference being the ignition energy density is higher for smaller kernel radii.

Frendi and Sibulkin concluded that minimum ignition energy is strongly dependent on the kernel radius and ignition time, and minimum ignition energy of 0.005 mJ is found for an ignition kernel radius of 0.0635 mm and an ignition time of 27.5 μs. This value is about 70 times smaller than the values reported from capacitance discharge experiments. The values were close to the ones obtained experimentally when the kernel radius of 0.5 mm is used.

Sloane and Ronney [21] used a computational model to determine the minimum ignition energies for stoichiometric methane-air mixtures. A detailed chemical model which included thermodynamic, transport and chemical models, which were used to reproduce the burning velocities and heat release rates of steady planer flames, to properly simulate the dynamics of flame ignition. In addition to the detailed chemical model, calculations were also made using simplified models based on two different one-step kinetic expressions. Fig 2.17 shows the results of the heat release profiles and temperature profiles in a planar flame for two one-step models and the detailed model.

Fig 2.18 shows the minimum ignition energy as a function of radius of energy deposition region (r_0) for the detailed kinetics model. As r_0 decreases to about 0.03 cm
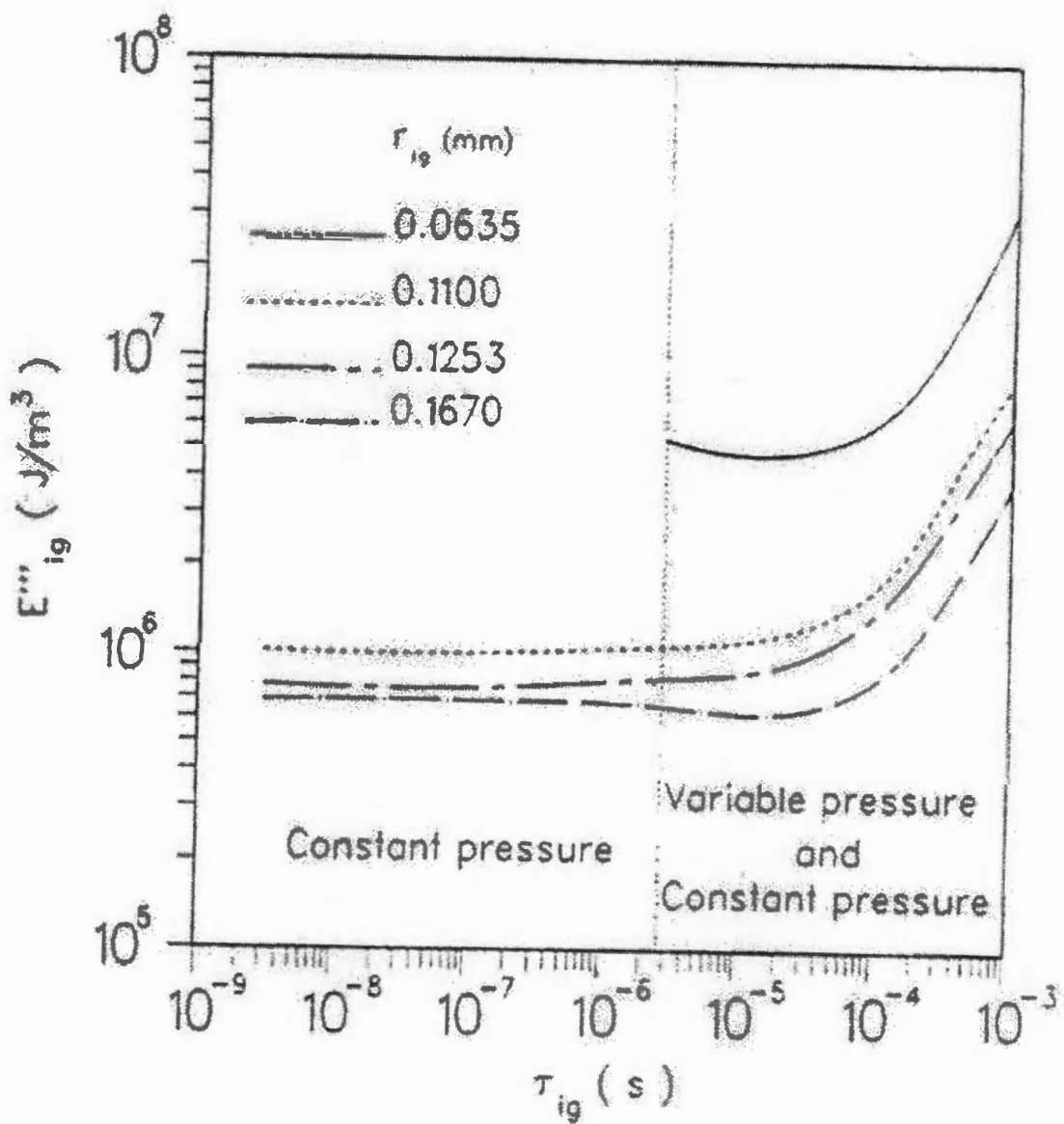
Figure 2.16 Variation of minimum ignition energy density with ignition time for different kernel radii. Stoichiometric methane-air mixture, spherical geometry from Frendi and Sibulkin [20]
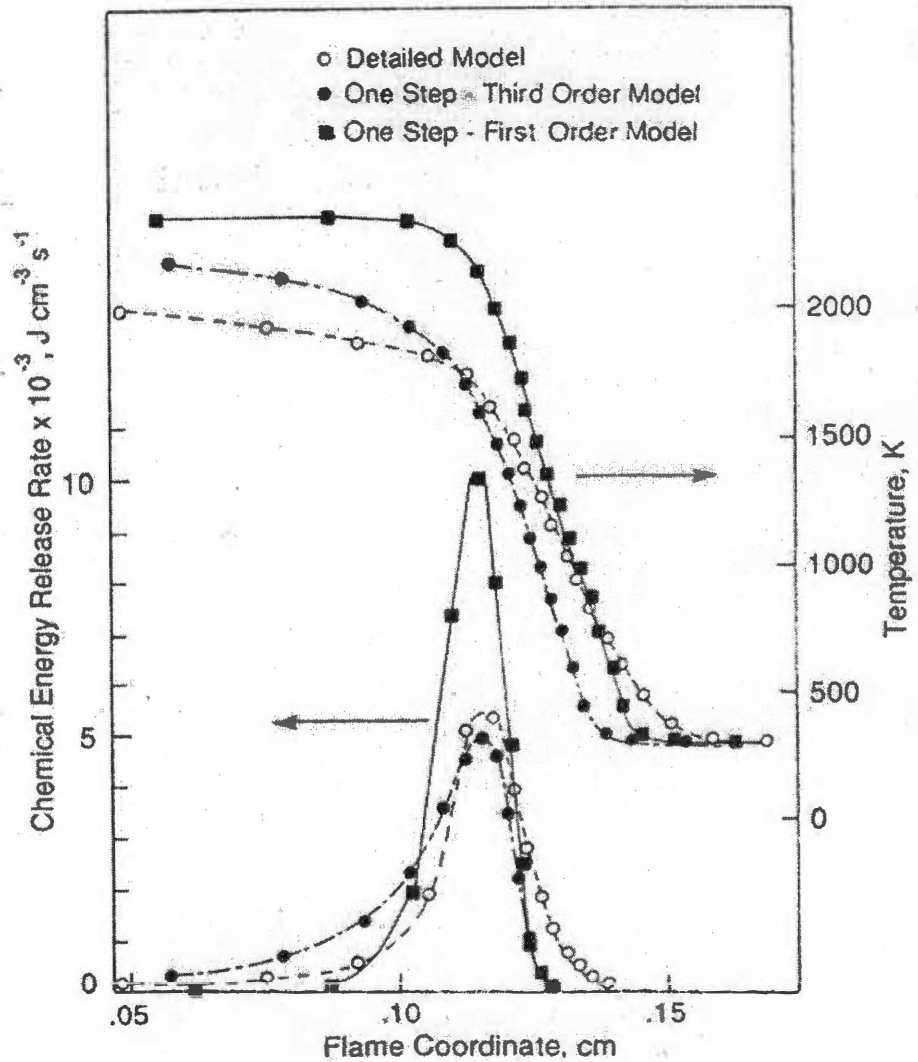
Figure 2.17 Spatial dependence of the chemical heat release rate in a planar stoichiometric methane-air flame for the detailed model, the one-step third-order model, and the one-step first-order model from Sloane and Ronney [21]

IGNITION PHENOMENA
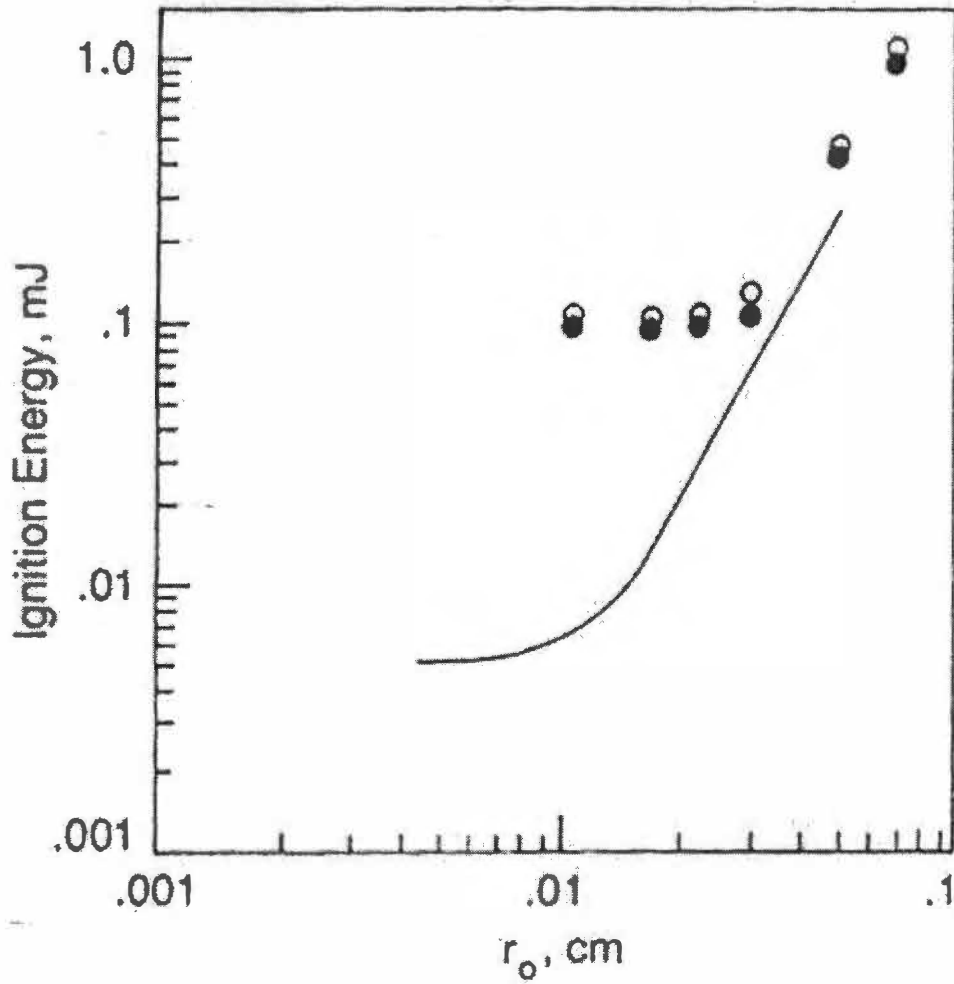
Figure 2.18 Minimum ignition energy as a function of the radius of the ignition energy deposition region for an energy deposition time of 27.5 μs determined using the detailed model. Results are shown with open and filled circles; the open circles indicate energies where ignition occurred, and the filled circles indicate energies where ignition did not occur. The solid line is a result of Frendi and Sibulkin (1990) for the same energy deposition time from Sloane and Ronney [21]

43

the minimum ignition energy decreases to about 0.1 mJ. The spark gap used in the experimental study is 0.2 cm, which is about 7 times the critical radius obtained in this computation. This longer length of energy deposition region in the experiments could be accounted for the much difference in the minimum ignition energy predicted by the model and measured by the experiments. Thus it seemed despite of the steps were taken in the experiments to minimize the effects of heat losses, their effects and the inefficiency of energy transfer from electrical circuit to gas could be the reasons for the differences between model and experimental results.

Sloane and Ronney computed minimum ignition energies using third-order kinetic model that was employed by Frendi and Sibulkin [20]. Fig. 2.19 shows the comparison of the results of Sloane and Ronney with those of Frendi and Sibulkin. It can be seen that Sloane and Ronney's results are 50% higher than those of Frendi and Sibulkin for small r_0 and are practically the same at large r_0, which suggests that the numerical schemes used are reasonably accurate.

The effects of r_0 on the minimum ignition energy were determined with first-order model and third-order models and are shown in Fig 2.20. At small r_0, the minimum ignition energies from first-order models are 30% higher than the results obtained from the third-order model. At large r_0 the predictions remain the same for both the models. Sloane and Ronney showed that the one step kinetic expression gives approximately the correct heat release profile in the reaction zone of the developed flame front where the fuel and oxygen concentrations are low relative to their initial values. But during the ignition process these concentrations are much higher and hence a moderate temperature

44
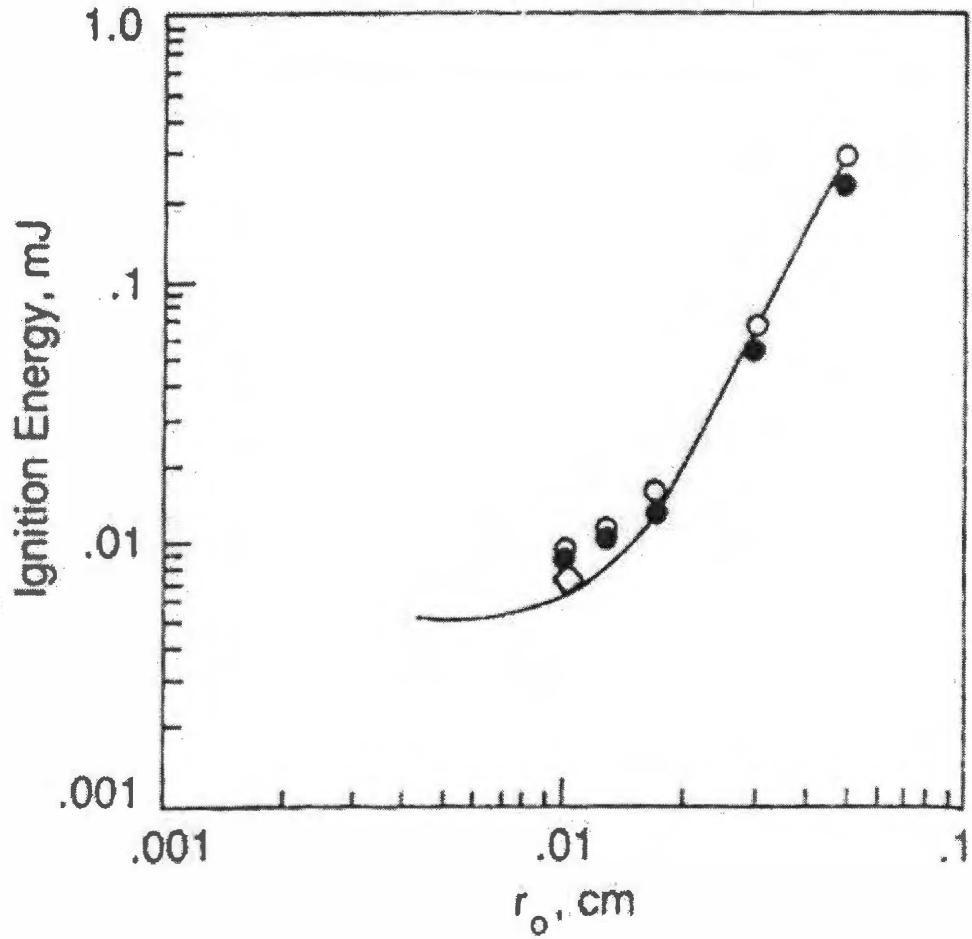
Figure 2.19 Minimum ignition energy as a function of the radius of the ignition energy deposition region for an energy deposition time of 27.5 μs determined using the third-order model. Symbols have the same meanings as in Fig 2.18. The diamond indicates the minimum ignition energy obtained with a 25% higher value of the one-step kinetics. The solid line shows the result of Frendi and Sibulkin (1990) from Sloane and Ronney [21]
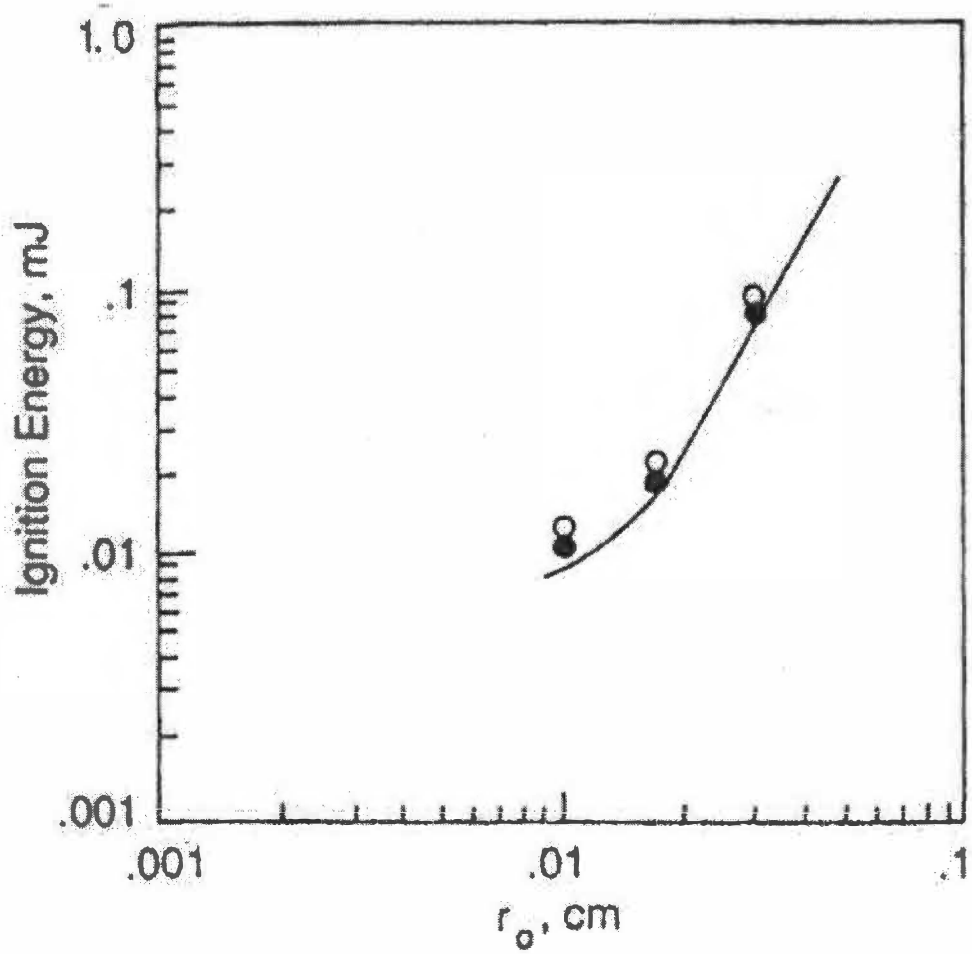
Figure 2.20 Minimum ignition energy as a function of the radius of the ignition energy deposition region for an energy deposition time of 27.5 μs determined using the first-order model. From Sloane and Ronney [21]

increase due to the ignition energy input is sufficient to cause significant heat release early in the calculation. This allows a successful ignition to occur at much lower ignition energy in the one-step model than in the detailed model.

Fig 2.21 and 2.22 illustrate this and show how minimum ignition energy can be so low for one-step kinetic model. Fig 2.21 shows temperature profiles as a function of time for one-step third order and detailed models for $r_0 = 0.017$ cm and ignition energy input, which is slightly greater than minimum ignition energy for the former model. Fig 2.22 shows the corresponding energy profiles at 20 µs in the detailed model. It shows that the chemical reactions are slightly endothermic overall because of initiation reactions, which dominate under these conditions. No such effect occurs in the one-step model as only exothermic reaction occurs and its own rate limitation delays this reaction and there is no time for radicals to be created. Consequently, in one-step model at 27.5 µs the energy input plus exothermic reaction drives the temperature to almost 3500 K, whereas in the detailed model the temperature is only about 2000 K. Thus quantitatively, the one-step kinetic model provides a good picture of variation of the minimum ignition energy with the size of the deposition region. However, even though the models are reasonably adequate in describing the flame speed for planer flame propagation, they are inadequate to quantitatively predict the minimum ignition energy.

Sloane and Ronney concluded that a chemical model capable of predicting minimum ignition energies must be able to model homogeneous initiation, early flame development, and the transition to a fully developed propagation flame. A satisfactory one-step expression that will accurately model all these stages in the ignition process over a range of compositions, pressures, etc. may be difficult to determine. However, a

47
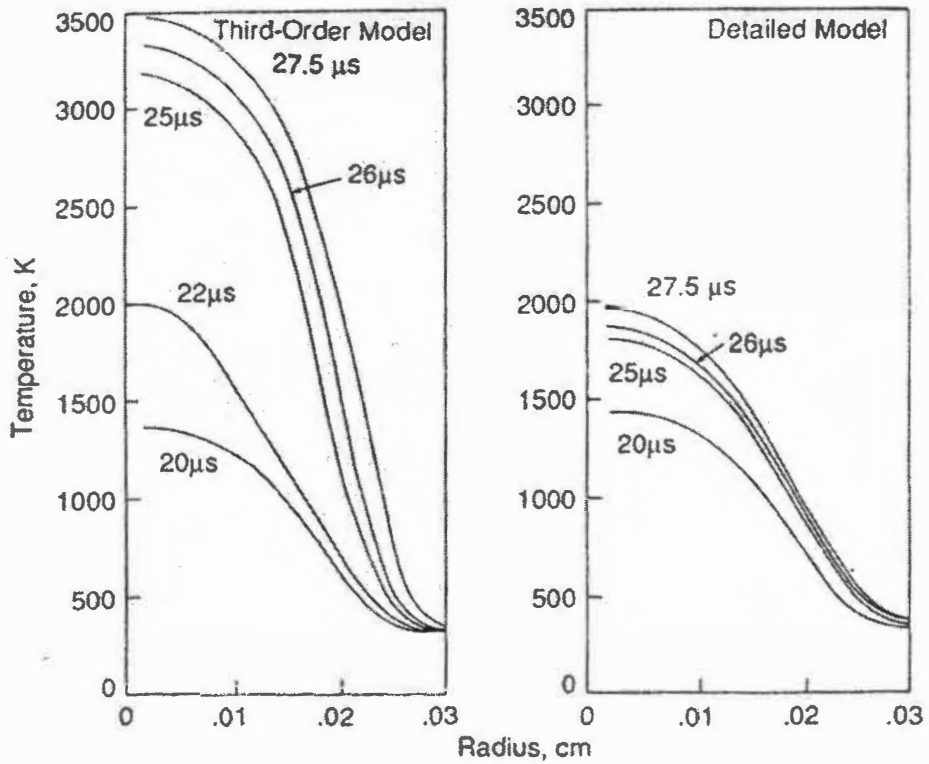
Figure 2.21 Temperatures as a function of time in the developing ignition kernel for the third-order model and for the detailed model. In both cases 0.0214 mJ of ignition energy were added with $r_0 = 0.017$ cm and $t_{ig} = 27.5$ μs from Sloane and Ronney [21]
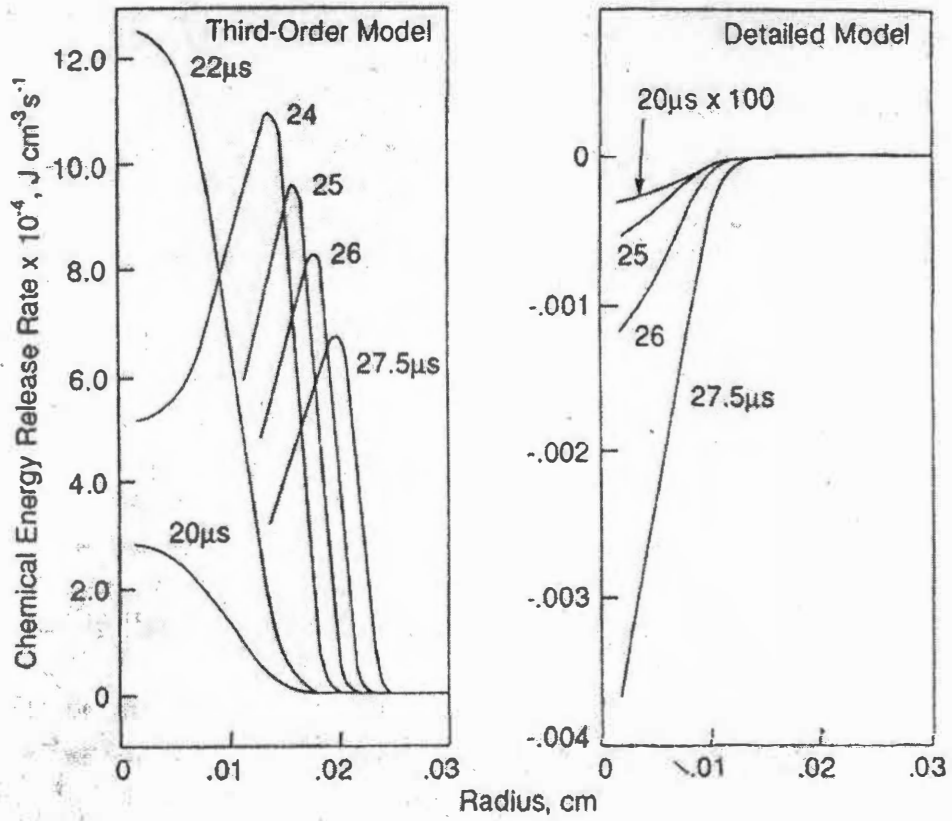
Figure 2.22 Chemical energy release rate as a function of time in the developing kernel for the same conditions as in Fig 2.21 from Sloane and Ronney [21]

simplified mechanism for ignition should be able to reproduce not only the steady planer burning velocity but also the homogeneous induction time at temperatures close to and above the adiabatic flame temperature.

Many investigations were done to determine different working conditions and properties of laser initiated ignition such as determination of ignition-delay times in laser initiated ignition [22, 23], investigation of laser-initiated detonation waves for supersonic combustion [24], laser-induced plasmas and applications [25], time-resolved imaging of flame kernels during a laser spark ignition [26], and laser spark ignition and extinction of a methane-air diffusion flame [27]. But these investigations did not include any studies on minimum ignition energies or breakdown threshold energies hence the description of their research has been limited up to this point only.

Kindon and Weinberg [28] were the first to use a laser beam to determine the minimum ignition energy of methane-air mixtures and to investigate up to what extent it depends on the species carrying the plasma energy. Kingdon and Weinberg used fine fibers or wires for igniting the mixtures. These fibers or wires were used as a target placed at the focal spot and they absorbed the laser energy and delivered it to the mixture.

Kingdon and Weinberg used a ruby laser with a dye cell Q-switch with a 40 ns pulse and a maximum power of 30J in the experiment. By using vanadyl phthalocyanine dye in nitrobenzene at twice the normal concentration and the laser being operated well above the threshold they improved the pulse reproducibility factor by 10. A photodiode was used to monitor pulses. A polaroid sheet was mounted in such a way that it could be rotated so that the beam energy could be attenuated in a controlled manner.

As Kingdon and Weinberg had to approach the ideal instantaneous point ignition as closely as possible the laser was passively Q-switched and the target size was decreased. This gave pulse duration of approximately 20 ns half-width at maximum and an initial target diameter of approximately 12 μm.

Fig 2.23 shows the minimum ignition energies for the mixtures containing between 6 and 8.6% CH$_4$ in air. It is seen that the plot (curve 5) does not differ greatly from those obtained in spark ignition experiments (curves 2, 3, 4). Curve 3 obtained from the circuit inductance experiments, which yields lowest ignition energy, was drawn so that it would be confirmed that no ignition occurs below it. Curves 2 and 4 represent 1% and 80% ignition probability. In spite of given conditions of large quenching distances, reduced pressure or ignition close to flammability limits, there is no evidence that laser ignition energies are appreciably smaller in consequence of the absence of losses due to massive electrodes.

In the next step the amount of material in the plasma and the target material was varied. The former was achieved simply by placing several fibers side by side in the focal spot and the latter was done by using different wire and quartz fibers and by coating with sodium chloride. In order to vary the quenching distance, which might affect the result, these measurements were carried out for very lean (6%) and near stoichiometric (8.6%) methane/air mixtures. The two ignition energies were close to 1.5 and 0.5 mJ in the two cases. No matter what variable was imposed, the minimum ignition energy in this particular system proved to be totally independent of plasma constitution both as regards different substances and different amounts of the same substance within the plasma. For 20 ns half widths initiation by focused laser beam an independent

51
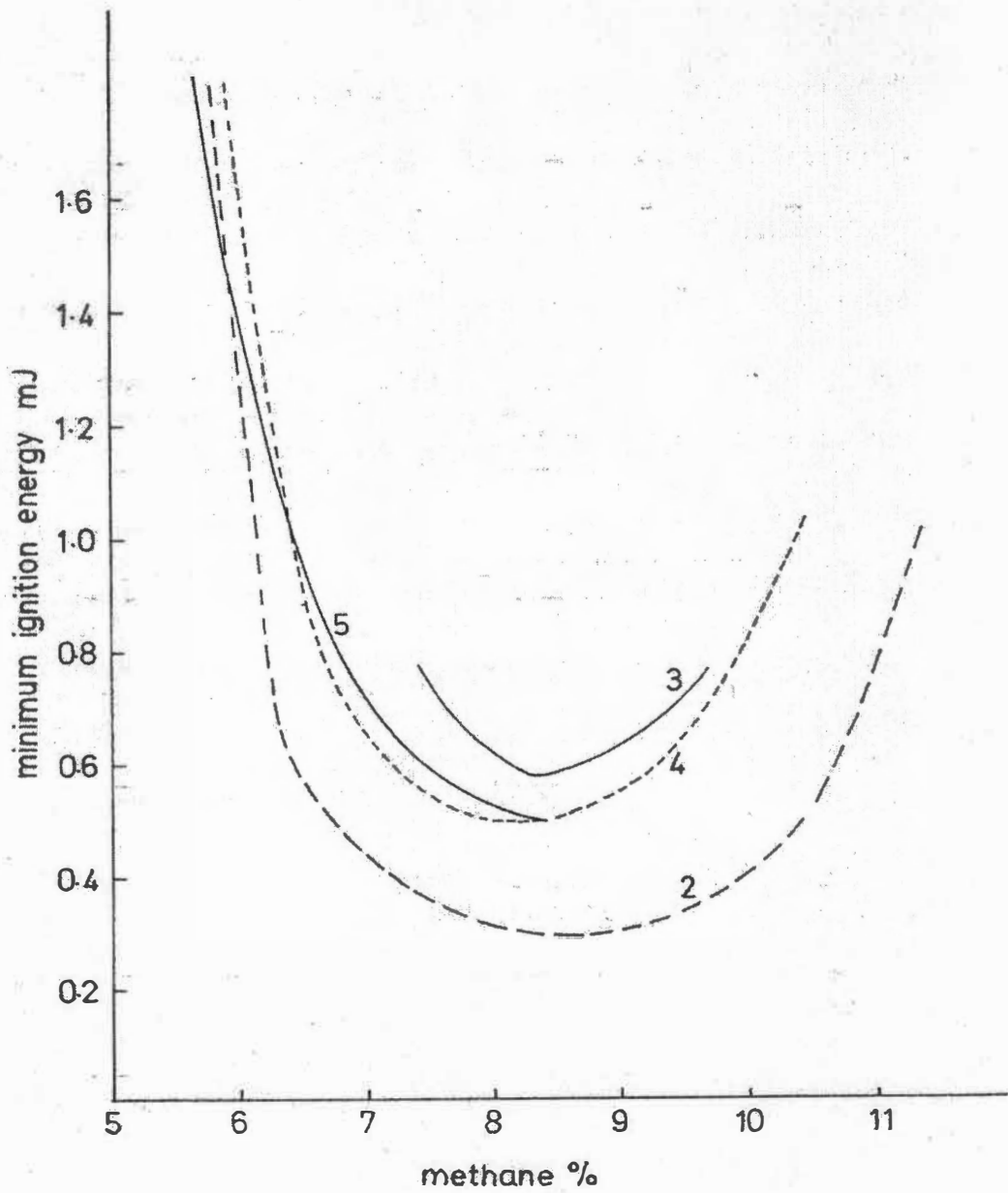
Figure 2.23 Comparison with spark ignition energies from Kingdon and Weinberg [28]

verification of the theory of point ignition is observed: the criterion is propagation-limited and the decisive stage is reached when the flame kernel grows to a critical radius. The propagation reaction wave attains the quenching distance before any of the plasma material reaches it.

To establish how the above conclusion would be affected by changes in the plasma dimensions, targets were placed in a slightly defocused area of the beam varying the extent of the plasma. Fig 2.24 shows results for two compositions. Although the dimensions of both sets of the results are well within the respective quenching distances (approximately 2 and 4 mm), it is much more appreciable fraction of it in the case of 8.6% mixture – for which a quite measurable increase is observed. But still every one of the results is once again independent of the target material or amount of it in the plasma.

Kingdon and Weinberg concluded that the minimum ignition energies are not affected plasma constitution and appear to be independent of plasma volume. The initial laser pulse is responsible for the expanding ignition front. The behavior of this front is independent of the constitution of the plasma, which is left behind. As long as the cloud is dense it absorbs energy for the duration of the incoming beam, which enables it to expand rapidly, eventually becoming turbulent and breaking through the front. This can result in suppression or promotion of propagation, depending on the constitution of plasma. Hence the leading edge of an extended pulse is responsible for ignition. The above conclusion completely vindicates the propagation-limited theory of point ignition and validates previous experimental spark-based measurements, showing them to be independent of plasma constitution and hence electrode materials as long as the discharge duration is short.

53
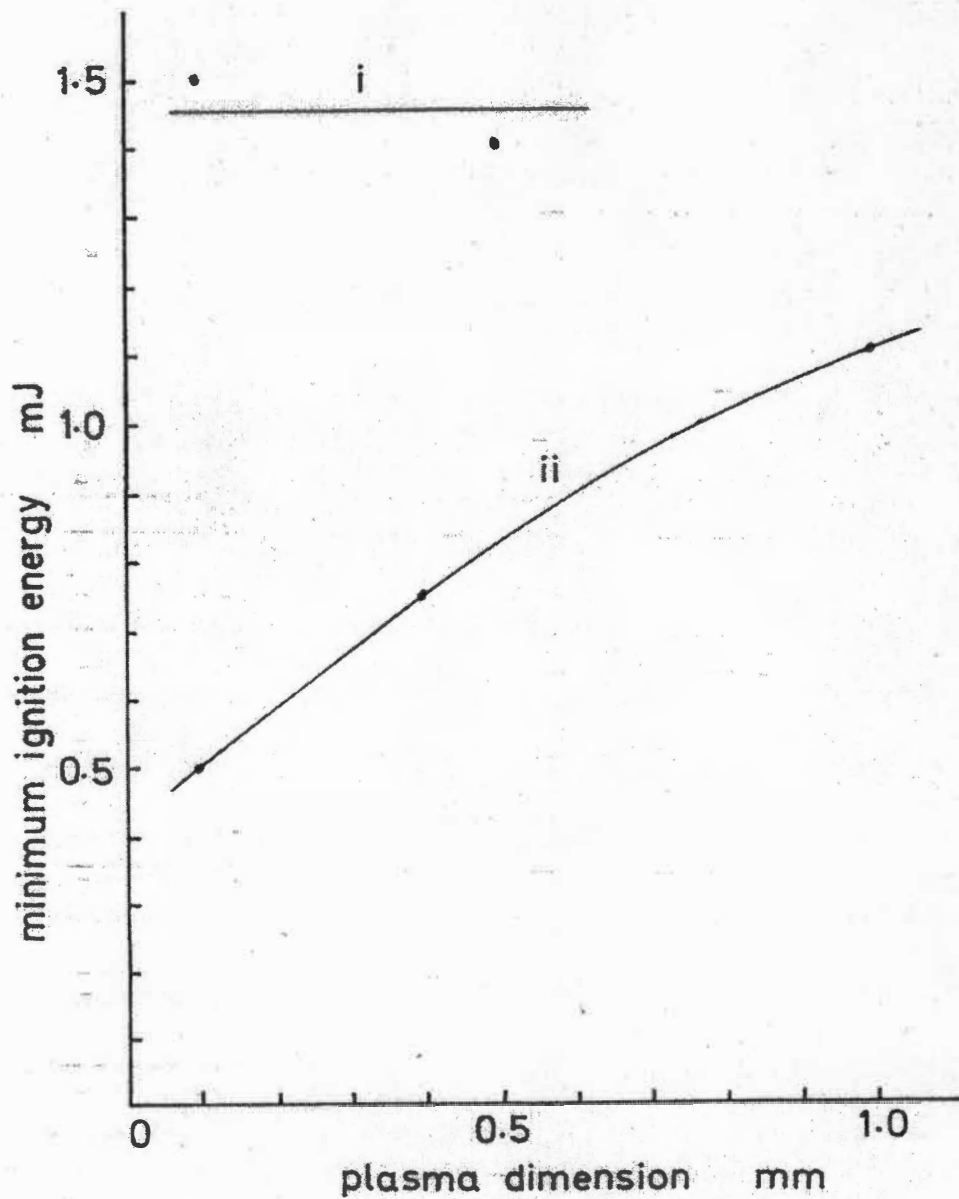
Figure 2.24 Effect of extent of plasma. (i) 6% CH_4, quenching distance 4 mm. (ii) 8.6% CH_4, quenching distance 2 mm from Kingdon and Weinberg [28]

Lim et al. [29] used laser ignition sources to determine minimum ignition energies of methane-air mixtures. The motivation that led to their investigation was that the data on minimum spark ignition energies of gases obtained experimentally and used extensively still did not agree with most detailed computational models available. The emphasis in this investigation was to have a better characterization of the ignition source and its effect on the minimum ignition energy.

A Q-switched nanosecond and a pulse mode-locked picosecond laser were used as an ignition source. The CH_4-air mixtures at a pressure of 1 atm and of varying stoichiometry were ignited and the minimum ignition energy was measured through repeated trials at varying laser spark energies. The laser spark kernel sizes were also measured by imaging the visible emission of these sparks. This was done to verify that the difference in minimum ignition energies obtained by picosecond and nanosecond sparks were due to the dependence of ignition energies on spark kernel size.

Fig 2.25 shows the minimum ignitions energies for methane-air mixtures for different stoichiometry at a pressure of 1atm using nanosecond and picosecond laser-induced sparks. The results obtained by Lim et al. are also compared to those obtained by electric and laser discharge measurements and calculations. As seen in the figure the minimum ignition energy curve for picosecond pulses lies at a higher energy than that of the nanosecond pulses. This difference however decreases towards the lean and rich flammability limits of the mixture. In addition the laser ignition results lie at higher energies than the electric discharge results. However, the difference decreases towards the flammability limits. The results from the experiment are bracketed by two model calculations; a simple gas model based on homogeneous heating of a minimum flame

55
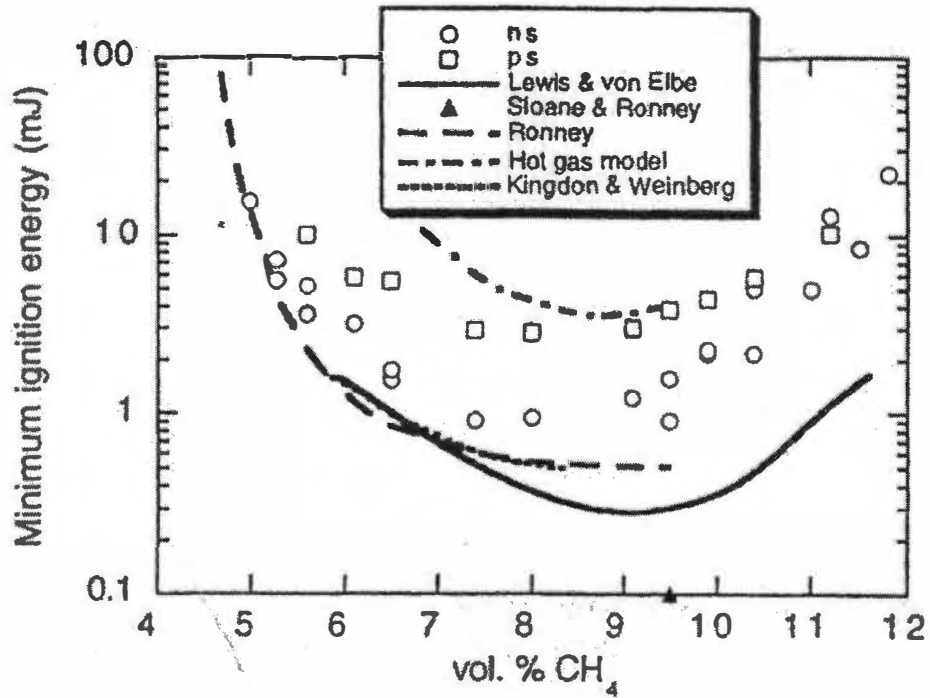
Figure 2.25 Measured and calculated minimum ignition energies of CH_4-air mixtures at 1 atm. For comparison, also shown are results from electric spark ignition experiments by Lewis and von Elbe [19] and Ronney [1], laser spark ignition experiments by Kingdon and Weinberg [28], a numerical computation by Sloane and Ronney [21] from Lim et al [29].

volume whose energy depends on the quenching distance for a mixture and a temperature specified through a chemical induction time as the upper limits and the detailed computation by Sloane and Ronney [21] as the lower limits.

Fig 2.26 displays contours plots of sample images for picosecond and nanosecond pulse laser-induced sparks of 5 mJ nominal energy. It is observed that the picosecond pulse sparks are nearly spherical while the nanosecond sparks are elongated along the direction of the laser beam. While capturing the images of the sparks it was observed that sparks generated from nanosecond laser pulses were much brighter than those generated by picosecond pulses for the same spark energy.

Fig 2.27 summarizes results for both laser sources and for range of spark energies in terms of the half width at half maximum (HWHM) of the sparks parallel and perpendicular to laser beam. It was observed that the width of sparks transverse to the laser was independent of the pulse energy for both laser sources. For picosecond sparks there is a slightly smaller traverse width (HWHM = 0.018 cm) compared to the nanosecond sparks (HWHM = 0.022 cm). The measurements showed the critical radius of deposition (r^*) for picosecond sparks was larger than the spark kernel size (r) which means according to the prediction by Sloane and Ronney [21] the minimum ignition energy should be independent of r, and for nanosecond sparks r was only slightly larger than r^*. Hence it is expected that the minimum ignition energy to be close to 0.1 mJ. However, the minimum ignition energy measurements do not support this conclusion. For the picosecond laser the minimum ignition energy is about 25 times larger than the value predicted and for nanosecond laser the value is about 10 times larger.
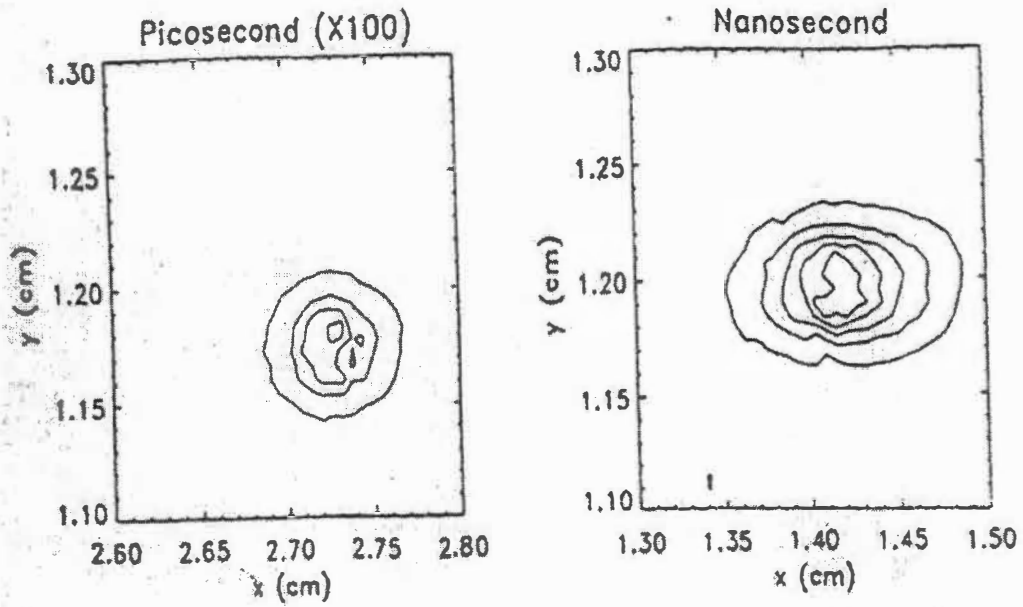
Figure 2.26 Contour plots with equal increments in intensity level of the spark emission intensity profile for nanosecond and picosecond laser breakdown. Spark energy is 5 mJ in both cases. For ps sparks the intensity scale has been multiplied by 100 from Lim et al [29]
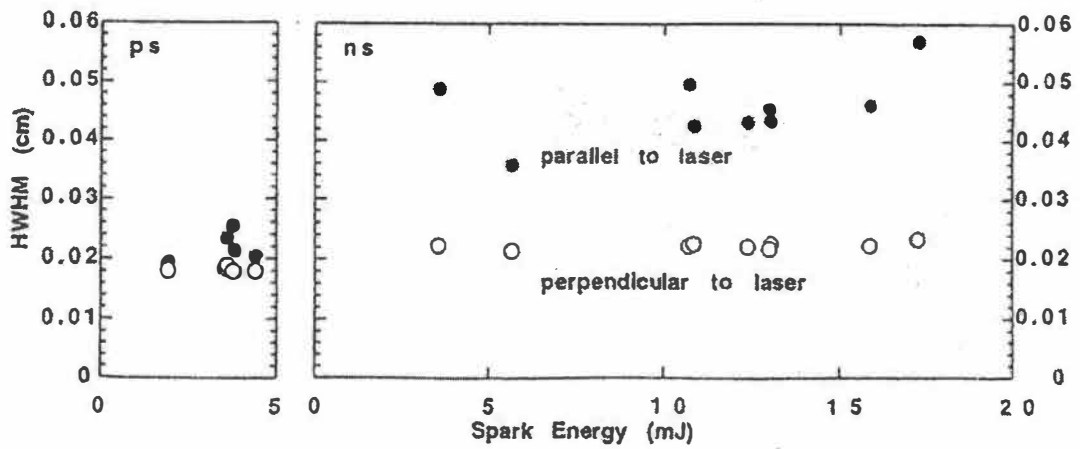
Fig 2.27 Compilation of spark width and length relative to the laser propagation direction as a function of spark energy for ns and ps laser sources from Lim et al [29]

Lim et al. concluded that the experiments showed the minimum ignition energy trends as expected and are quantitatively consistent with other measurements for very lean and rich methane-air mixtures. For near-stoichiometric mixtures the measured values are higher than expected. These results may be due to the size of the energy deposition region with some possible influence of gas dynamic shock losses.

Phuoc and White [30] experimentally investigated laser-induced spark ignition using a nanosecond pulse at 1064 nm from a Q-switched Nd-YAG laser. It was found that laser irradiance of the order of 10^{12} to 10^{13} W/cm^2 was enough to ignite a mixture having 6.5 to 17% methane by volume. The dependence of breakdown threshold laser energy E_{thr} on the gas pressure was also studied. Numerous test were performed and showed that mixtures having less than 6.5% or more than 17% methane by volume were not ignitable even with laser energy E_0 up to 200 mJ. Also no mixtures could be ignited for E_0 less than 35 mJ. An ignition was successful when the time-resolved pressure measurement, the time-resolved emission spectra of luminous OH radical were recorded, and the rapid water condensation was seen on the observation windows.

Fig 2.28 shows a comparison of measured and calculated breakdown threshold laser energies, E_{thr}, versus pressure of air and methane. The breakdown threshold was defined as the laser energy at which the gas breaks down on more than 50% of the shots. It can be seen that when the pressure is lower than 17 Torr, gas breakdown was not possible for the range of laser energies used. When the gas pressure increased from 17 to 1010 Torr, the threshold laser energy decreased drastically from 190 mJ to 15 mJ. Air had the breakdown threshold energies slightly higher than methane.
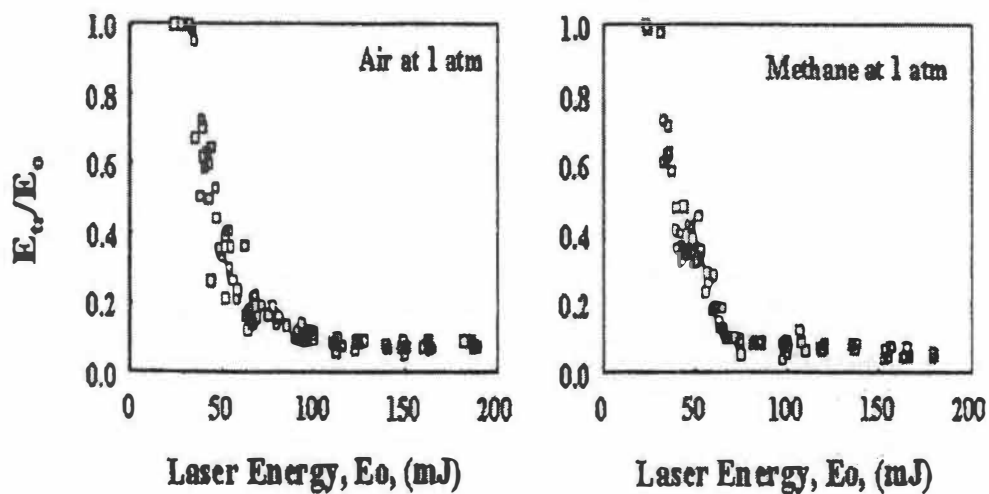
Figure 2.28 Dependence of the laser energy transmitted through the focal volume, Etr/Eo, and the absorption coefficients, Kv,air and Kv, CH$_4$ on the initial laser energy Eo from Phuoc and White [30]
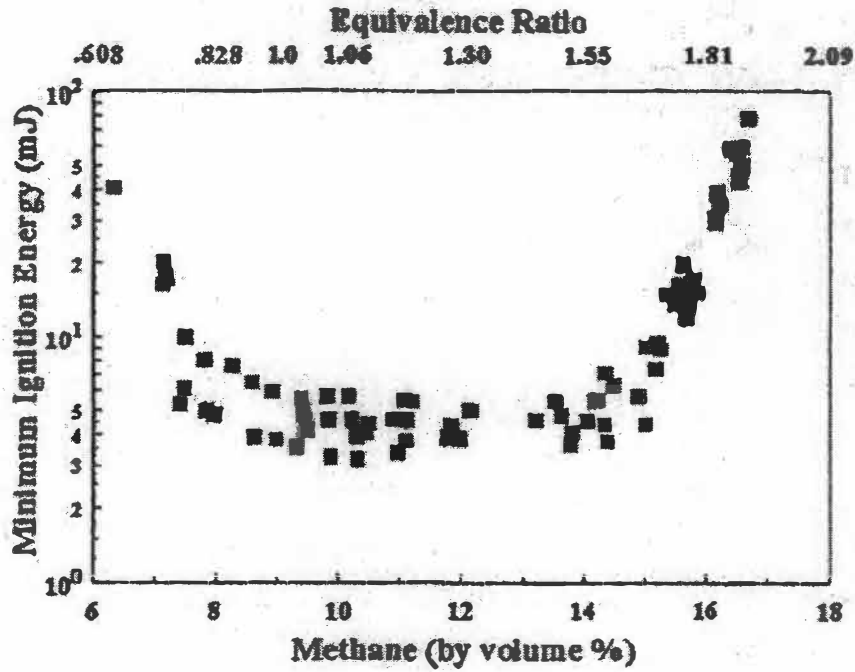
Fig 2.29 Measured minimum ignition energies of methane/air mixture at 1 atm as a function of methane volume fraction from Phuoc and Whie [30].

The minimum ignition energies of methane-air mixtures of different methane volume fractions were measured and are plotted in Fig 2.29. It is clear from the figure that the minimum ignition energies remained at their lowest values of about 3 to 4 mJ for mixtures having about 10% methane to 15% methane. There was a sharp increase in the value of minimum ignition energy to about 40 mJ for 6.5% methane and about 70 mJ for 17% methane. The minimum ignition energies reported here for stoichiometric methane-air mixture at 1 atm are similar to those reported by Lim et al. for a picosecond laser but are higher than those measured for nanosecond laser beam by a factor of 3. The present results are also about one order of magnitude higher than those reported by Lewis and von Elbe [19].

Such high minimum ignition energies can be due to several properties such as short pulse duration and small focal volume associated with the laser beam. Spark created by picosecond or nanosecond laser pulse has a different mechanism. This spark can ignite the mixture directly, or by force of a shock wave, or by the hot gas that remains after expansion. The rapid dissipation of energy and the small spark size increase the heat loss and limit the time the energy remains within the relevant dimension of flame kernel, and the spark kernel will decay rapidly to ambient condition without heating the surrounding gas to a temperature above ignition temperature. Hence one has to increase the energy source, which leads to higher minimum ignition energy.

Phuoc and White concluded that there is strong pressure dependence for the threshold laser energy, which is incompatible with the multi-photon ionization process, which predicts weak pressure dependence. However, it agrees with the electron cascade theory. The results of minimum ignition energy show an increase of ignition energy

63

towards lean and rich side of stoichiometric. The minimum ignition is about one order magnitude higher than that measured in the electric spark study. This might be due to the different ignition mechanisms between laser spark and electric spark ignition. Their results show that laser-induced spark ignition successfully ignites mixtures with 17% of methane by volume, which is richer than the upper flammability limit, but it fails to ignite mixture below 6.5% methane, which is lower than lower flammability limit. Thus one can infer that laser-induced spark ignition works poorly at fuel-lean conditions and favors the fuel-rich conditions.

Lee et al. [31] measured minimum ignition energies of fuel-air mixtures involving propane, dodecane, and jet-A fuel at a range of pressures and equivalence ratios. An Nd-YAG laser operating at 0.53 μm with a pulse duration of ~10 ns was used as an ignition source. The 8 mm diameter beam was focused down to a focal spot size of 0.2 mm.

Fig 2.30 shows minimum ignition energy measurements for propane-air mixture at pressures of 1, 0.5 and 0.33 atm as obtained by Lee et al. For comparison the plot also shows the laser ignition measurements of Lim et al. [29] and data by Lewis and von Elbe [19]. The data is quite close to Lim et al. This was due the similarities in the laser and optical systems used in the respective studies. Phuoc and White [30] reported a much higher ignition energy using an Nd-YAG laser but with a 75-mm focal length lens, while Lee et al. used 100-mm focal length lens. Apparently focal spot size which controls the energy density in laser sparks has an effect on the measurement of the ignition energy.

Ignition energy for a dodecane-air mixture is plotted as a function of equivalence ratio is shown in Fig 2.31. The minimum ignition energy occurs at a relatively large equivalence ratio of about 3.6-3.75. In comparison to propane, dodecane has higher
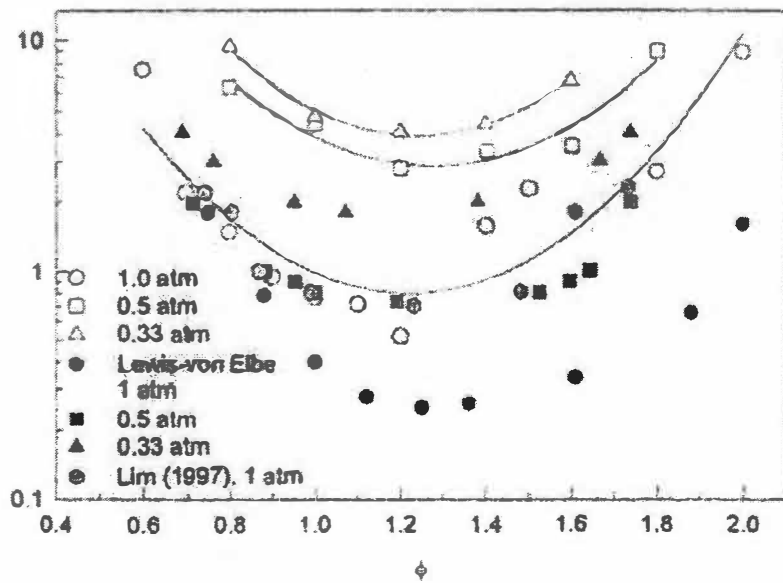
Figure 2.30 Minimum ignition energy of propane-air mixtures at various equivalence ratios and pressure from Lee et al. [31]
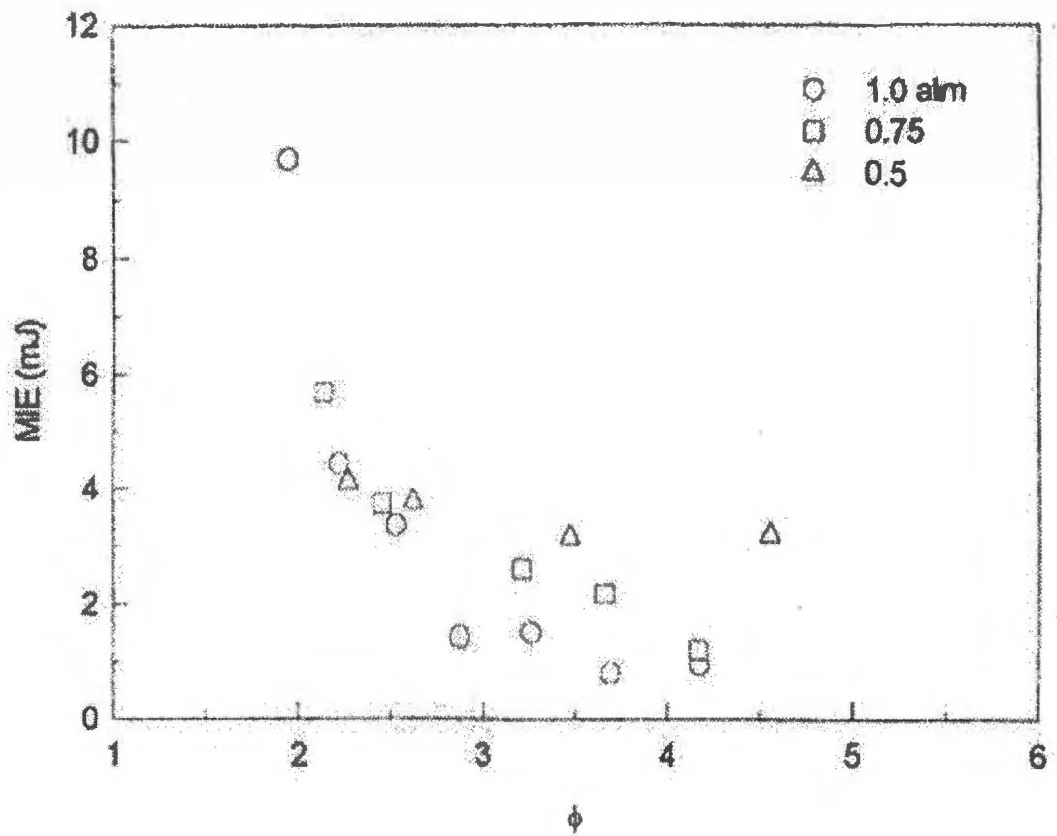
Fig 2.31 Minimum ignition energy for dodecane-air mixtures from Lee et al. [31]

minimum ignition energy of ~1 mJ at 1.0 atm using laser sparks. This minimum ignition energy steadily increases with decreasing pressure, where the required laser spark energy is up to 3 mJ at a pressure of 0.5 atm. The minimum ignition energy occurs far in the fuel-rich side in contrast to electrode ignition where the minimum ignition energy occurs close to the stoichiometric fuel-air ratio.

Lee et al. concluded that minimum ignition energies obtained by using laser sparks are consistently larger than corresponding data obtained using electrical sparks for propane-air mixtures at 1 atm and at lower pressures, perhaps due to the different electromagnetic and thermal conditions that exist within and near spark plasmas. The heavier hydrocarbons exhibit progressively larger optimum equivalence ratio corresponding to minimum ignition energy, away from the stoichiometric equivalence ratio.

CHAPTER 3

EXPERIMENTAL APPARATUS AND PROCEDURE

This chapter contains a detailed description of the experimental apparatus and procedure used in the determination of minimum ignition energy and breakdown threshold energies of methane and air. Section 3.1 gives the description of the experimental apparatus used in this investigation. Section 3.2 describes the experimental procedure and the test conditions for the experiments.

3.1 EXPERIMENTAL APPARATUS

In this investigation, using laser-induced breakdown, breakdown threshold energies of methane and air were determined for pressures ranging from 0.02 to 1.17 MPa. In addition minimum ignition energies of methane-air mixtures were determined for pressure varying from 0.1 to 1.04 MPa and equivalence ratio varying from 0.6 to 1.2. The sparks for the breakdown and ignition were produced from a Q-switched Nd-YAG laser having a 5.5 ns pulse at a wavelength of 1064 nm. Figure 3.1 and 3.2 show a schematic and a photograph of the equipment setup used in this experimental investigation, respectively.

The laser beam from the Nd-YAG laser passed through a beam splitter, which reflected approximately 3% of the laser beam on to the energy meter P2, which measured the reflected laser energy from the beam splitter. The transmitted laser beam from the beam splitter then passed through a plano convex lens L1 of a focal length of 100mm,
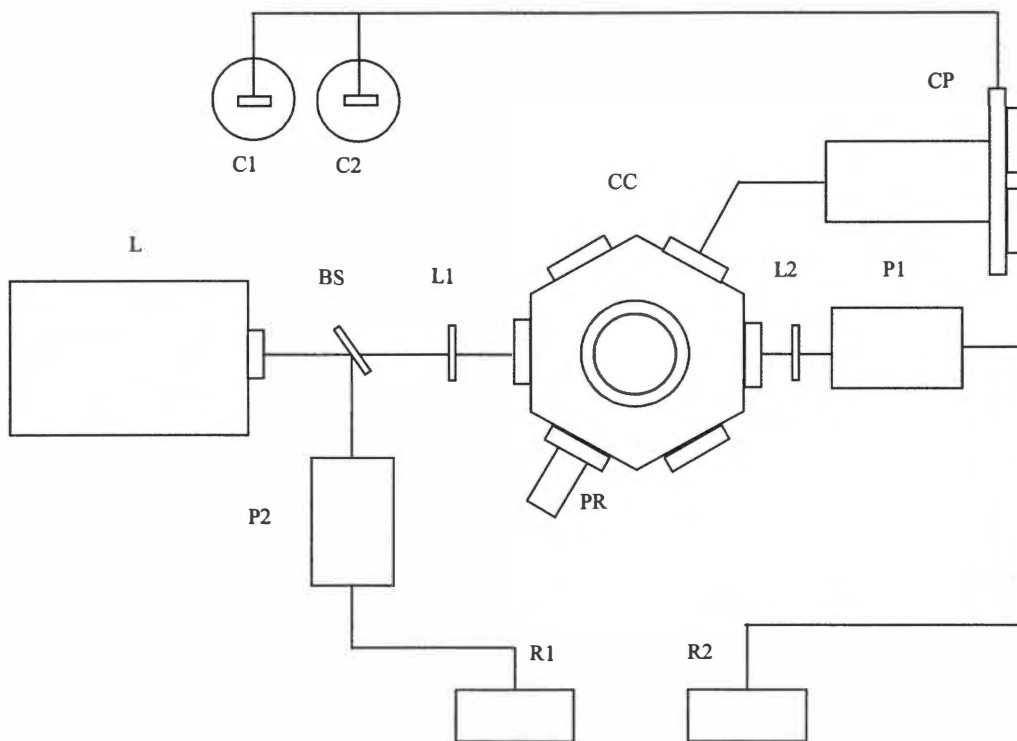
Figure 3.1 Sketch of the Experimental Apparatus: (L) Nd-YAG Laser; (BS) 3% Beam Splitter; (L1) and (L2) 100mm Focal Length Plano-Convex Lenses; (CC) Combustion Chamber; (P1) and (P2) Pyroelectric Energy Detectors; (PR) Pressure Relief Valve; (R1) and (R2) Energy Readouts; (CP) Control Panel; (C1) and (C2) Gas Cylinders.
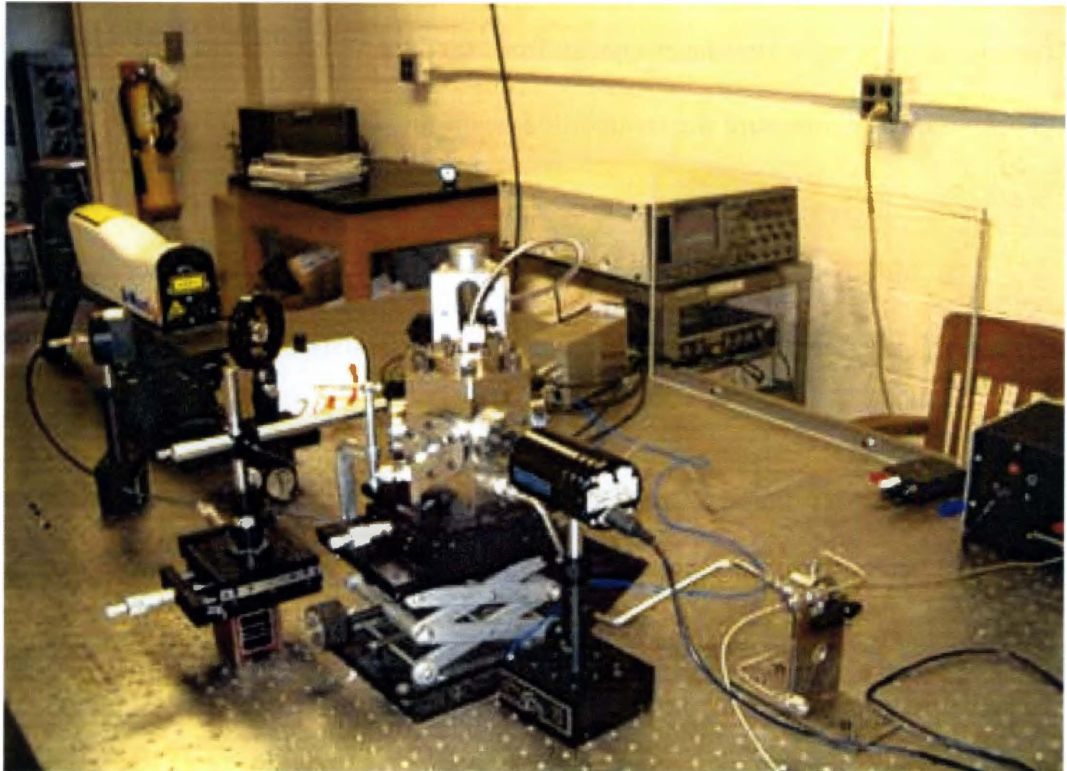
Figure 3.2 Photograph of the setup used in the experiment

L1, which focused the laser beam down to a spot at the center of the combustion chamber to create the spark for ignition. The beam was focused to an approximated size of 17 μm [18]. The laser beam coming out of the combustion chamber passed through lens L2, which collimated the laser beam on to the energy meter P1. The energy meter P1 measured the transmitted laser energy from the chamber. This arrangement allowed the energy meters to measure the transmitted beam through the chamber with and without the breakdown.

A high-pressure combustion chamber as shown in Figure 3.3 was used in the investigation for all experiments. This chamber consists of a main chamber body and a cap flange both machined from a 316 stainless steel. The chamber is a hexagonal body with 1" diameter windows drilled on each of its sides. The chamber is 12 cm tall with a 6.5 cm inner diameter and a minimum wall thickness of 2.4 cm. The internal volume of the chamber is approximately 0.4 liters. The chamber is designed to withstand a pressure of about 20 MPa.

The hexagonal cap flange is secured to the main chamber using six 3/8-16 Cr-alloy bolts. An O-ring is used to seal the gap between the flange and the main chamber. To observe the ignition and breakdown process and flame propagation in the chamber a 3.75 cm diameter fused silica window was fitted into the flange as an observation window. It was secured to the flange with another smaller cylindrical flange with six 10-32 Cr-alloy bolts. The fused silica window was sealed with the rubber gaskets to prevent gases from escaping from the top.

The main chamber body was equipped with six 2.5 cm windows held in place by cylindrical stainless steel flanges. Each stainless steel flange was secured using six 10-32
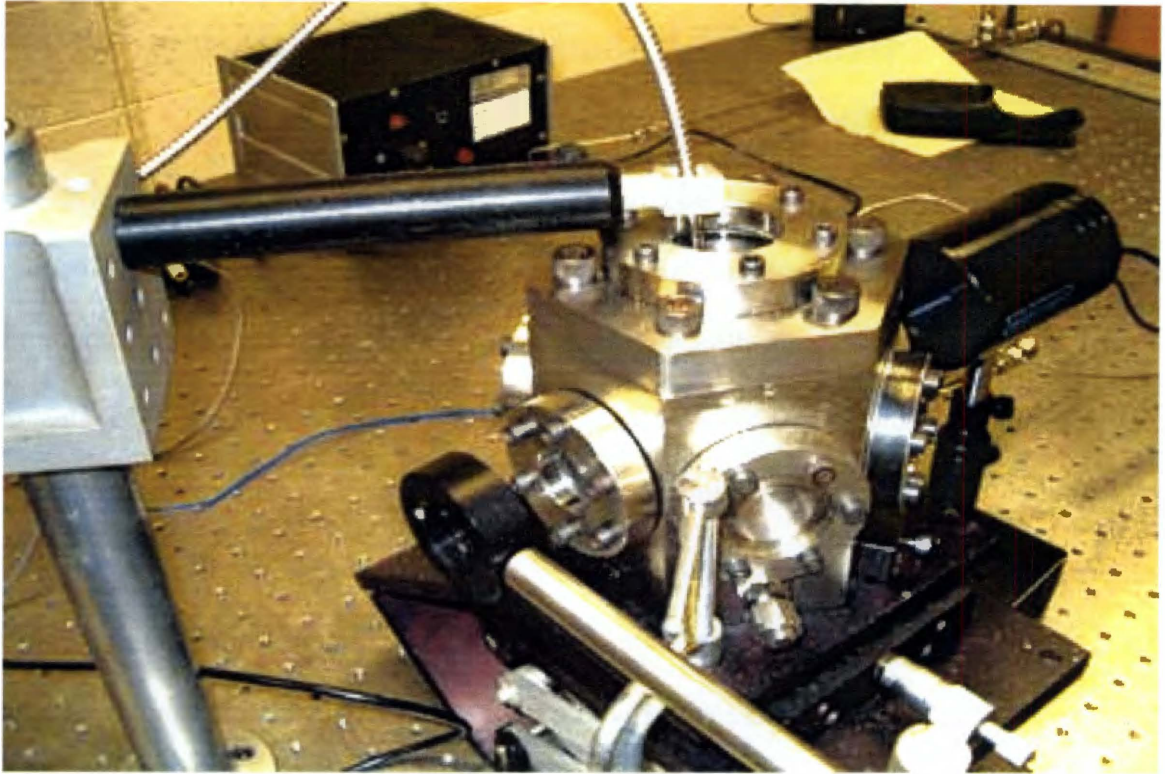
Figure 3.3 Photograph of the combustion chamber used in the experiment

Cr-alloy bolts. All the six windows were made of 1.25 cm thick fused silica. Two of these six windows were used for the beam entry and exit; one was used for installing a pressure transducer for measuring pressure inside the chamber during ignition; one was used for installing the fiber optic cable to trace the time curve for the combustion; one was used to install the relief valve and the remaining one was used as another observation window for observing the ignition and combustion process from the side.

Fig 3.4 and 3.5 show the schematic and the photograph of the control panel that was used for introducing methane and air into the combustion chamber. The pressure gauge P_F was used for controlling the quantity of methane. Toggle switch T_F, control valve K_F and needle valve N_F were used to introduce methane into the combustion chamber. To obtain a better resolution of the pressure inside the combustion chamber for methane the pressure gauge P_F had a range of 0 to 1000 mbar absolute. The pressure gauge P_F was used only till the pressure inside the combustion chamber was 0.35 MPa. Above this pressure the pressure gauge with a range of −30 Hg to 15 psi gauge was used. Similarly pressure gauge P_A, toggle switch T_A, control valve V_A and needle valve N_A were used to introducing air into the combustion chamber. The pressure gauge P_A had a range of -30 inches of Hg to 300 psi gauge.

3.2   DESCRIPTION OF EXPERIMENTAL CONDITIONS AND PROCEDURE

This section gives the brief outline and description of the experimental conditions and the procedure followed for carrying out experiments during this investigation. The experiments for determining breakdown threshold energies of methane and air were
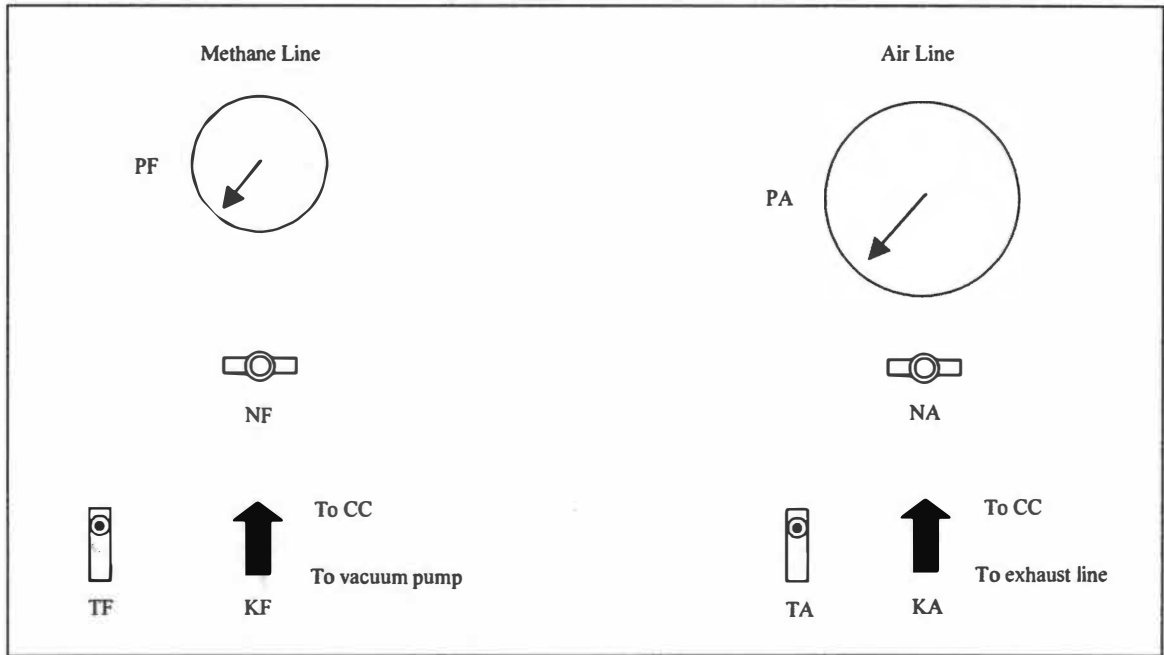
Figure 3.4 Sketch of the control panel used in during the experimentation: (CC) Combustion chamber; (PF) and (PA) Pressure gauges for methane and air; (NF) and (NA) Needle valves for methane and air; (KF) and (KA) Control valves for methane and air; (TF) and (TA) Toggle switch for methane and air.
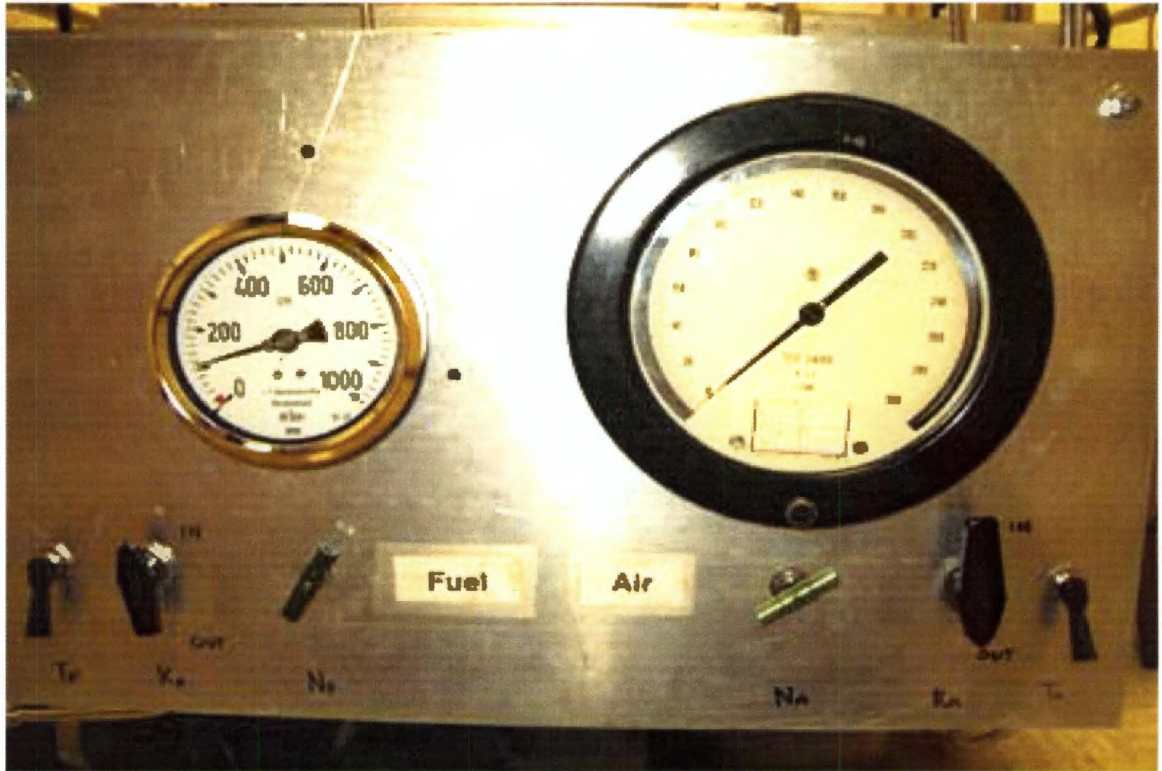
Figure 3.5 Photograph of the control panel used in the experiment

performed for a pressure range of 0.02 to 1.17 MPa, and the experiments for determining minimum ignition energies of methane-air mixtures were carried out for a pressure range of 0.1 to 1.04 MPa. At a given pressure the equivalence ratio was varied by varying the partial pressures of methane and air in the mixture in the minimum ignition energy experiments.

Prior to the experiment the combustion chamber was cleaned and dried thoroughly and then evacuated. For a given condition the partial pressures of both the gases were determined. For the range of the pressure investigated the partial pressure of methane was always below 0.1 MPa. Both the gases were introduced separately into the combustion chamber for a given condition. In the range of pressures investigated in the present investigation methane having a lower partial pressure was introduced first into the combustion chamber. To ensure proper mixing the mixture was allowed to mix for about 15-20 minutes prior to the experiment. A pressure relief valve was installed at the bottom of the combustion chamber and was set to activate when the pressure in the combustion chamber reached above 2 MPa.

After each test the burnt gases were exhausted out of the combustion chamber. As the ignition gases being hydrocarbons the products of combustion consisted of water. This water condensed and deposited on the glass windows and the walls of the combustion chamber. It was very important to clean off the water condensate from the fused silica windows; otherwise it would have lead to absorption of laser power. This would have lead to erroneous results in the values of minimum ignition energies. Consequently, after each experiment the flange of the combustion chamber was opened the chamber was thoroughly cleaned and dried.

The methane and air were introduced into the combustion chamber to form a mixture from the pressurized cylinders using the piping system shown in the sketch in Fig 3.6. Before introducing the gases into the combustion chamber, the system was evacuated using a vacuum pump. After each experiment the combustion chamber was depressurized by venting the burnt gases to the atmosphere. The proper concentration of gases for a given equivalence ratio was achieved by controlling the partial pressure of each gas. A low pressure gauge capable of measuring vacuum pressures was used to control the evacuation of the system. This gauge was also used for the pressurizing the chamber with methane up to a mixture pressure of 0.34 MPa. For experiments with higher mixture pressures, a pressure gauge with a larger range had to be used. The least count of the low pressure gauge was 20 mbar while the high pressure gauge has a least count of 2 psi (2 inches Hg in vacuum). The combination allowed the concentration of methane to be specified as X% ± Y% at a mixture pressure of 0.34 MPa, where X is the theoretical concentration of methane and Y is the error. As the pressure increases, the error in methane concentration decreases to a value of A% at 1.04 MPa. For experiments with mixture pressures of 0.1 MPa, the vacuum gauge with least count of 20 mbar was used to reduce the error in methane concentration to an acceptable level.

Before each experiment the laser was turned on for warming and was kept running for about 1 minute. Once the combustion chamber was charged and the gases were allowed to mix for 15-20 minutes, the laser beam was fired at a low energy. If the laser beam did not ignite the mixture, the laser energy was increased using a laser attenuator. The laser energy was increased till one could see ignition inside the combustion chamber. The ignition was said to occur when a flame propagating through

78
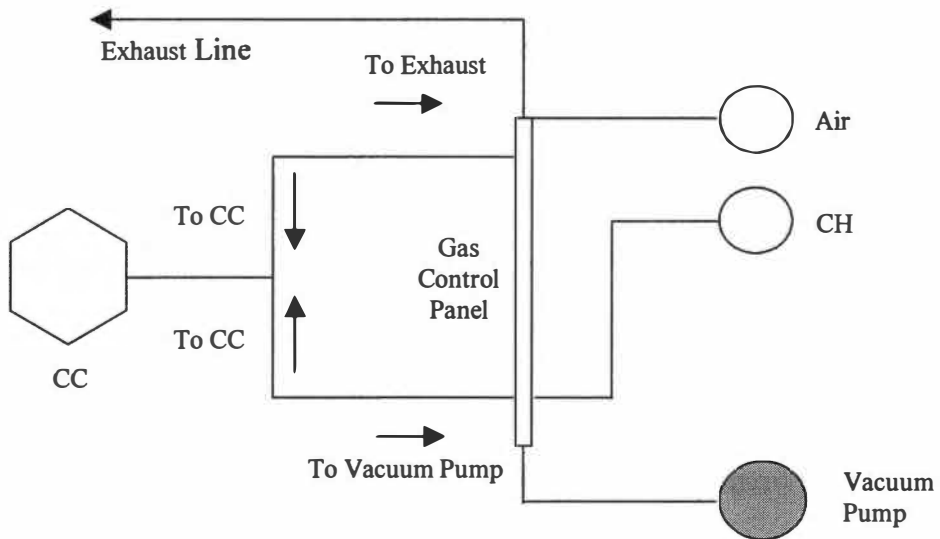
Figure 3.6 Schematic of piping system used in the experiment

the combustion chamber and water condensation on windows could be observed through the observation windows. Once the ignition had occurred the combustion chamber was evacuated, cleaned and recharged as described earlier. Using a laser attenuator the laser energy was reduced by a small fraction to ensure that the correct minimum ignition energy was delivered. If ignition was observed at this energy in the first shot the laser energy was still reduced by a small fraction and the experiment was repeated. This was carried out till only 50% of the laser shots resulted in ignition. This is because the minimum ignition energy of a methane-air mixture is defined as the laser energy absorbed at which 50% of laser shots would result in ignition.

Similarly for determining the breakdown threshold the combustion chamber was filled with the methane or air at a desired pressure and the laser beam was focused to the center of the combustion chamber. The breakdown was said to occur when a spark was seen inside the combustion chamber or a cracking sound of the gas breakdown was heard. If there was no breakdown observed the laser energy was increased and the process was repeated till the breakdown occurred. As done in determining the minimum ignition energy the laser energy was slightly reduced and the laser beam was fired again to see if breakdown occurred at a slightly lower energy. If the breakdown occurred the process was repeated reducing slightly the laser energy. This was carried out till only 50% of laser shots resulted in breakdown.

At least 8 experiments were performed at a given condition in determining minimum ignition energy or breakdown threshold energy. The average of these results was taken and an error range was calculated. In some experiments the laser power would

vary considerably or mixture would not mix properly which would result in no ignition even at the highest possible energy delivered by the laser. These data were eliminated during the analysis.

For determining the absorbed energy during the breakdown threshold and the minimum ignition energy experiments a calibration curve was plotted as shown in Fig 3.7. The calibration curve was plotted using the reflected energy measured by energy meter P2 on X-axis and the transmitted energy measured by energy meter P1 on Y-axis. As both the experiments involved absorption of energy, using the calibration curve it was possible to calculate the absorbed energy.

From the calibration curve at a given value of the reflected energy the actual energy that was delivered during the experiments could be known. The readings of reflected energy from P2 and transmitted energy from P1 measured during the breakdown threshold energy and minimum ignition energy experiments were superimposed on to the calibration curve. For a given reflected energy measured from the experiments an energy difference between the transmitted energies was calculated. This energy difference is the energy absorbed during the breakdown threshold energy and the minimum ignition energy experiments. This absorbed energy is the breakdown threshold energy for the breakdown threshold energy experiments or minimum ignition energy in the minimum ignition experiments. The calibration curve has an uncertainty of approximately ± 0.2 mJ.

The determination of the absorbed energy at a given pressure and equivalence ratio for minimum ignition energy experiments or at a given pressure for breakdown threshold energy experiments is illustrated by a simple example.

81
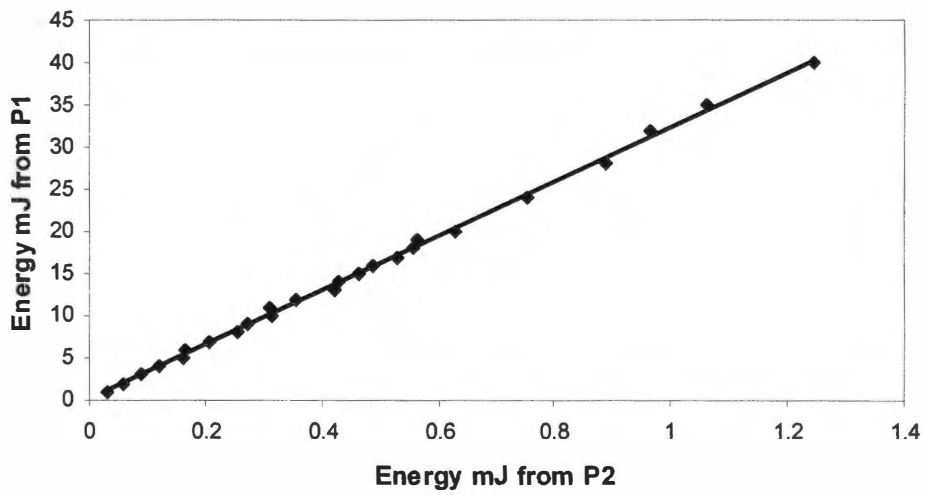
Figure 3.7 Calibration curve plotted for determining absorbed laser energy

Let the reflected energy from the experiment be denoted by Re and the transmitted energy from the experiment be Te. At a given reflected energy the actual transmitted energy can be determined using the calibration curve. So let at Re the actual transmitted energy without absorption from the calibration curve be Tc. Then the absorbed energy Ae for that experiment would be the difference between Tc and Te. The accuracy of the absorbed energy Ae calculated will be ± 0.2 mJ.

CHAPTER 4

RESULTS AND DISCUSSION

This chapter consists of a presentation and discussion of the results obtained from the present experimental study in which the effect of pressure on the breakdown threshold energies of methane and air and the effect of pressure and equivalence ratio on the minimum ignition energies of methane-air mixtures are investigated. The effect of pressure on breakdown threshold energies of methane and air is presented in Section 4.1. Section 4.2 describes the effect of equivalence ratio on the minimum ignition energies of methane-air mixture and its comparison with the results of the previous investigators. Section 4.3 discusses the effect of pressure on the minimum ignition energies of methane-air mixtures. Finally, the general observations from this investigation are presented in Section 4.4.

4.1 EFFECT OF PRESSURE ON BREAKDOWN THRESHOLD ENERGIES OF METHANE AND AIR

This section describes the results obtained from the current study on the effects of pressure on breakdown threshold energies of methane and air. Similar to the definition of minimum ignition energy, if 50% of the laser shots result in a breakdown of methane or air at a given pressure then the laser energy absorbed by the gas at that laser power is defined as the breakdown threshold energy of that gas at that pressure. For the breakdown threshold energy experiments the combustion chamber was charged with air

or methane alone at the desired pressure. For achieving the gas breakdown the laser shots were fired at increasing laser power each time the breakdown did not occur. When the breakdown occurred a spark was formed or a cracking sound was heard from the chamber. The energy readings on the energy meters were noted before and after the breakdown. These readings were used to determine the breakdown threshold energy of the gas. A calibration curve, which gave the actual laser energy deposited, was used to determine breakdown threshold energy.

Figs. 4.1 and 4.2 show the effect of pressure on the breakdown threshold energies of air and methane, respectively. The breakdown threshold energies and laser intensities for air and methane at different pressures are tabulated in Table 4.1. The results show that the breakdown threshold laser energy decreased rapidly as the pressure increased. For pressure increasing from 0.02 MPa to 1.17 MPa the breakdown threshold laser intensity for air decreased from 3.88×10^{12} to 3.64×10^{11} W/cm^2 and for methane the breakdown threshold laser intensity decreased from 3.12×10^{12} to 2.54×10^{11} W/cm^2 The breakdown threshold energies for air were found to be consistently higher than methane by about 2 to 3 mJ at a given pressure.

The present data show that breakdown threshold energy depends on pressure and can be expressed as $I_{thr} \alpha \ p^{-n}$, which is in agreement with the inverse bremsstrahlung absorption process for creating breakdown. The threshold dependence on pressure was found to be more for air than methane. The value of n was found to be 0.44 for air while n was found to be 0.378 for methane. These can be seen from the Figs 4.3 and 4.4
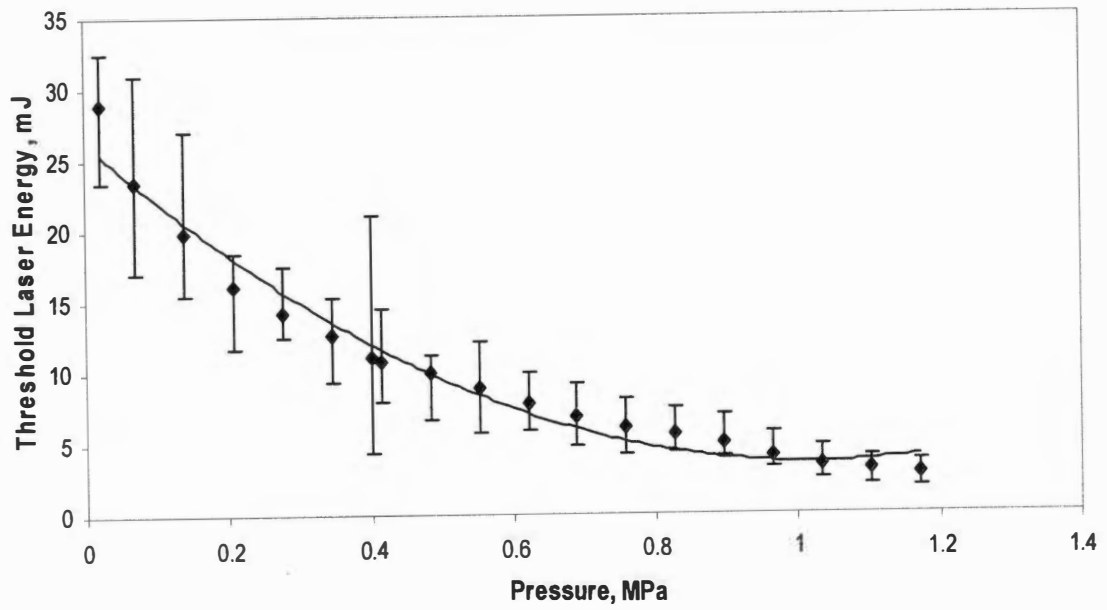
Fig 4.1 Effect of pressure on breakdown threshold energies of air
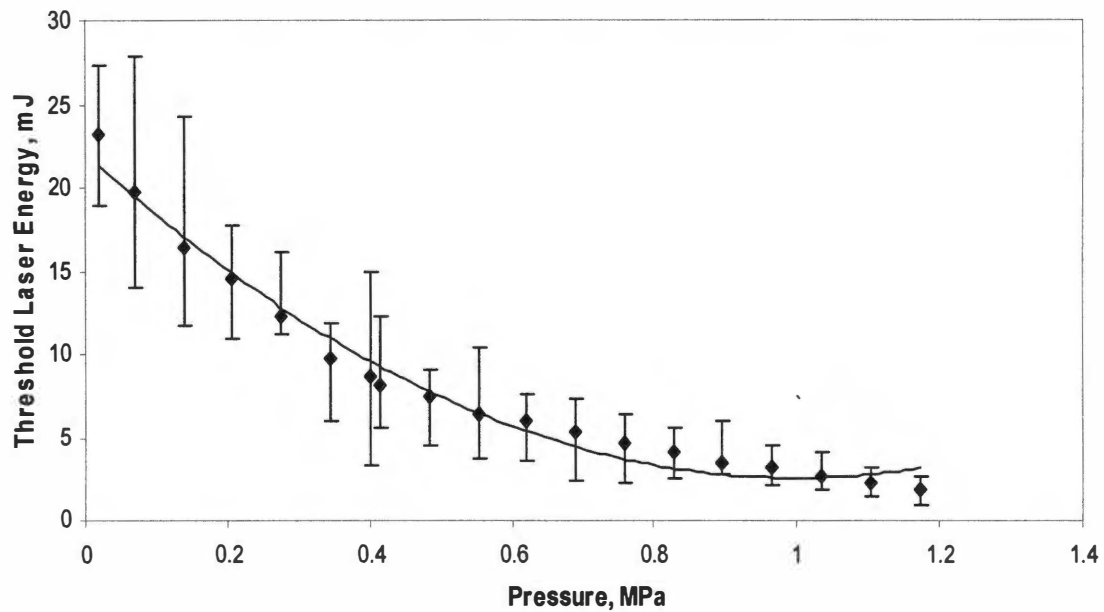
Fig 4.2 Effect of pressure on breakdown threshold energies of methane

Table 4.1 Breakdown threshold energies and laser irradiances for air and methane at various investigated pressures

Pressure	For Air		For Methane	
P, MPa	E_{thr}, mJ	I_{thr}, W/cm^2	E_{thr}, mJ	I_{thr}, W/cm^2
0.02	28.84	3.86×10^{12}	23.23	3.12×10^{12}
0.069	23.44	3.14×10^{12}	19.79	2.66×10^{12}
0.138	19.83	2.65×10^{12}	16.4	2.20×10^{12}
0.207	16.05	2.15×10^{12}	14.55	1.95×10^{12}
0.276	14.25	1.91×10^{12}	12.26	1.65×10^{12}
0.345	12.64	1.69×10^{12}	9.71	1.30×10^{12}
0.4	11.05	1.18×10^{12}	8.72	1.17×10^{12}
0.414	10.82	1.45×10^{12}	8.09	1.09×10^{12}
0.483	9.98	1.34×10^{12}	7.44	9.99×10^{11}
0.552	8.91	1.19×10^{12}	6.4	8.59×10^{11}
0.621	7.82	1.05×10^{12}	6	8.05×10^{11}
0.689	6.83	9.14×10^{11}	5.33	7.15×10^{11}
0.758	6.12	8.19×10^{11}	4.62	6.20×10^{11}
0.827	5.55	7.43×10^{11}	4.08	5.48×10^{11}
0.896	5.02	6.72×10^{11}	3.51	4.71×10^{11}
0.965	4.11	5.5×10^{11}	3.18	4.27×10^{11}
1.034	3.45	4.62×10^{11}	2.66	3.57×10^{11}
1.103	3.12	4.17×10^{11}	2.24	3.01×10^{11}
1.172	2.74	3.67×10^{11}	1.9	2.55×10^{11}

Figure 4.3 Laser irradiance plotted versus the methane pressure
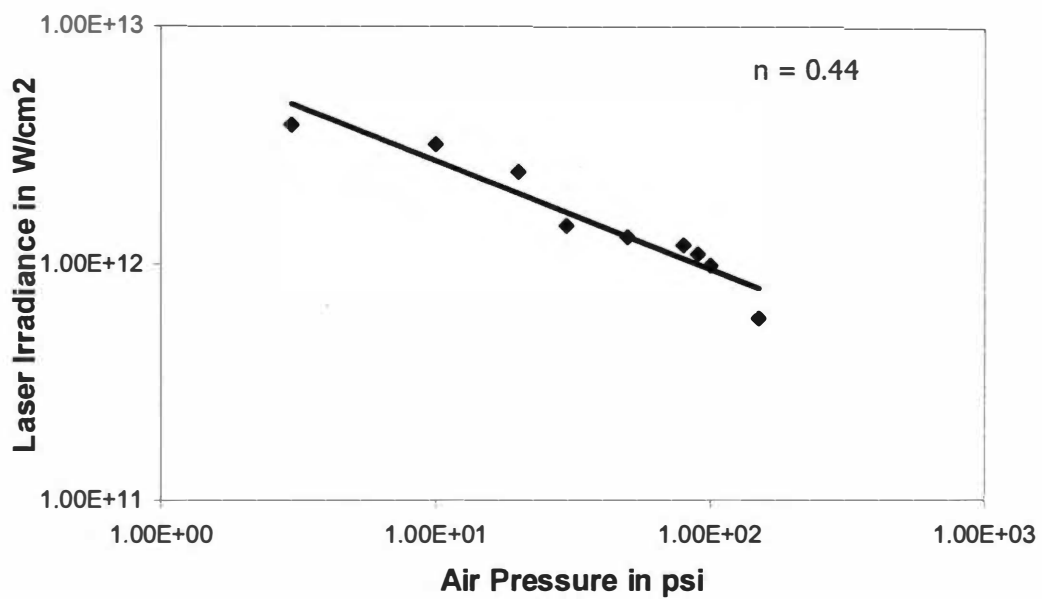
Figure 4.4 Laser irradiance plotted versus the air pressure

The effect of laser wavelength on threshold energy was also investigated using the second harmonics (532 nm) laser pulse. However, at that wavelength the laser energy kept on fluctuating and it was not possible to obtain a steady power output from the laser system hence the investigation for determining breakdown threshold energies at 532 nm wavelength was discontinued.

4.2   EFFECTS OF EQUIVALENCE RATIO ON MINIMUM IGNITION ENERGIES OF METHANE-AIR MIXTURES

This section discusses the results obtained from the present investigation on the effect of equivalence ratio on minimum ignition energies of methane-air mixtures at a given pressure. In the present study, if 50% of the laser shots result in ignition for a mixture of methane and air at a given pressure and equivalence ratio then the laser energy absorbed by the mixture at that laser power is defined as the minimum ignition energy of methane-air mixture at that pressure and equivalence ratio. For the minimum ignition energy experiments the combustion chamber was charged with air and methane in the amount determined previously to achieve the desired equivalence ratio at a given pressure. For igniting the mixture laser shots were fired with increasing laser power each time the ignition did not occur. When ignition occurred a flame front was formed which traveled through the combustion chamber. The energy readings on the energy meters were noted before and after combustion. These readings were used to determine the minimum ignition energy. A calibration curve, which gave the actual laser energy

deposition was used to determine the absorbed energy, which is the minimum ignition energy of methane-air mixtures at a given pressure.

Fig 4.5 shows the effect of equivalence ratio on the minimum ignition energy of methane-air mixtures at a pressure of 0.1 MPa. This plot was obtained because most of the previous experiments performed for determining minimum ignition energy of methane-air mixtures were done at this pressure. As there was no data for minimum ignition energy of methane-air mixtures available at high-pressures this plot was generated so that results could be compared with the available results. The equivalence ratio at this pressure was varied from 0.6 to 1.2.

As can be seen in Fig 4.5, the minimum ignition energy is lowest at stoichiometric conditions as expected for a typical hydrocarbon fuel. The minimum ignition energy increases as the mixture deviates from stoichiometric. It can be noted that the minimum ignition energy is influenced more by the lean composition of the mixture than the rich composition. The error bars in the plot show the range in which the minimum ignition energy was obtained for that condition. The values plotted are the average values of the minimum ignition energy obtained for that condition. The minimum ignition energy was measured to be 1.297 mJ at stoichiometric condition. It varied from 2.235 mJ to 1.487 mJ for an equivalence ratio of 0.6 and 1.2, respectively. Due to laser fluctuations and the randomness of the electrons colliding with the molecules there is a large variation in the obtained minimum ignition energy. Hence 6 to 8 experiments were performed at a given equivalence ratio and at a given pressure. The variation in the value of the minimum ignition energy reduces as the mixture pressure increases.
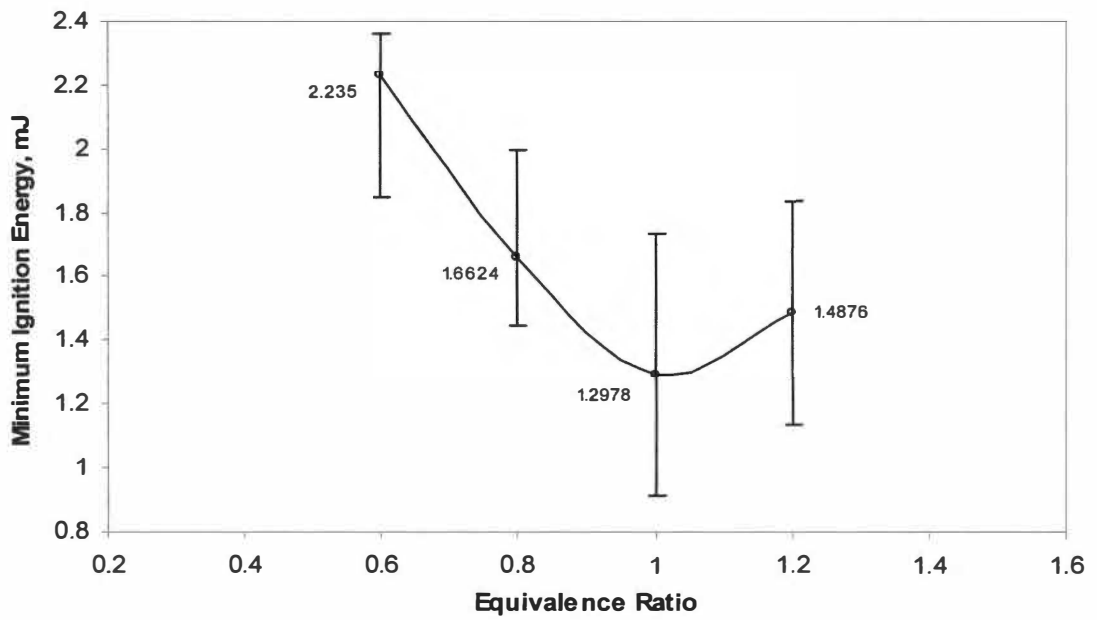
Fig 4.5 Effect of equivalence ratio on the minimum ignition energies of methane-air mixtures at 0.1 MPa

The trend observed for minimum ignition energies versus equivalences ratio at 0.1 MPa is similar to that at other pressures. This can be seen from Figs 4.6 to 4.9, which show the effect of equivalence ratio on minimum ignition energies at pressures of 0.2, 0.34, 0.68 and 1.04 MPa, respectively. Fig 4.10 shows the effect of equivalence ratio on the minimum ignition energies of methane-air mixture at different pressures.

Fig 4.11 shows the comparison between the minimum ignition energies of methane-air mixtures obtained in the present investigation at 1 atm and the minimum ignition energies of methane-air mixtures reported from previous investigations at 1 atm. The previous investigations include the electric spark ignition by Lewis and von Elbe [19], laser-induced ignition by Kingdon and Weinberg [28] and Lim et al. [29], a simple gas model by Syage et al. [32], and also the mathematical models used by Sloane and Ronney [21] and Ronney [1] for determining minimum ignition energies.

The minimum ignition energies measured in the present investigation are quite close to those measured by Lim et al using nanosecond pulses. This may be due to the fact that similar laser and optical systems were used in the respective studies. For example both used Q-switched Nd-YAG lasers at 1.064 μm wavelengths, however the pulse used by Lim et al was 10 ns while the pulse used in the present investigation was 5.5 ns. Also the beam was focused using a 100-mm focal length lens in the current study as compared to 38-mm focal length lens used by Lim et al. However, Phuoc and White [30] measured minimum ignition energies (not shown in the plot) much higher than those measured in the present investigation using a similar Nd-YAG laser. A 75-mm focal length lens and a 5.5 ns pulse were used for focusing the laser beam in their case. They reported minimum ignition energy for stoichiometric methane-air mixture at 1 atm to be

Fig 4.6 Effect of equivalence ratio on minimum ignition energies of methane-air mixtures at pressure of 0.2 MPa

Fig 4.7 Effect equivalence ratio on minimum ignition energies of methane-air mixtures at pressure of 0.34 MPa

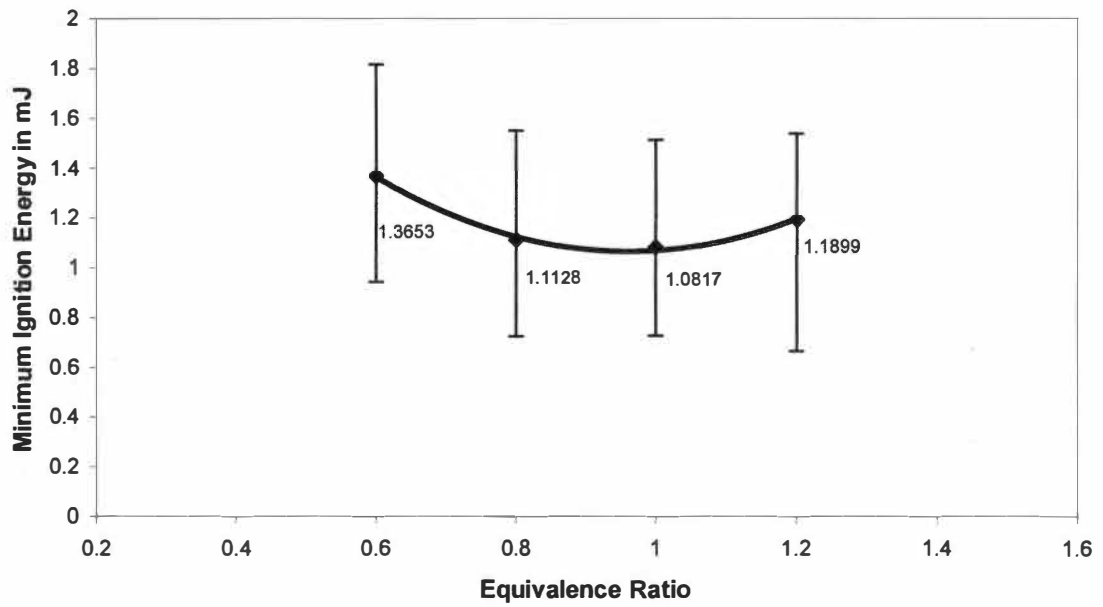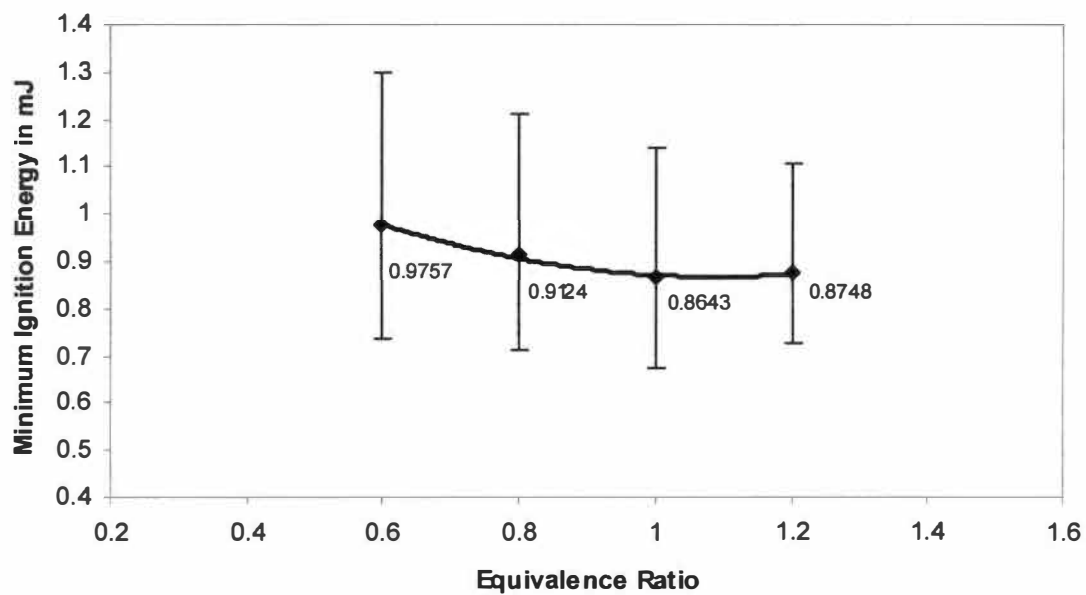**Fig 4.8** Effect of equivalence ratio on minimum ignition energies of methane-air mixtures at 0.68 MPa
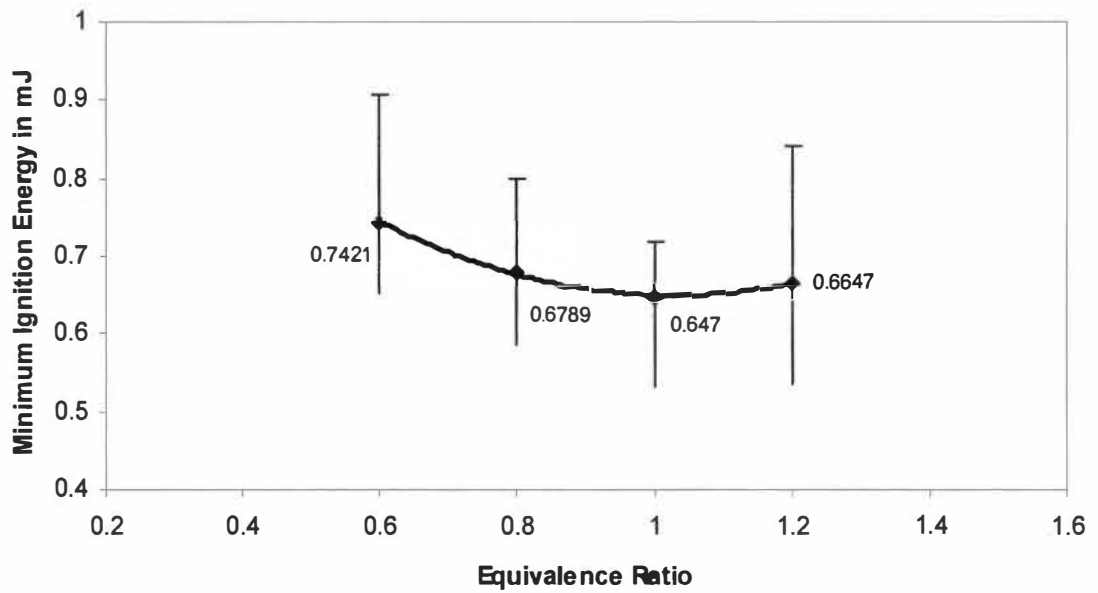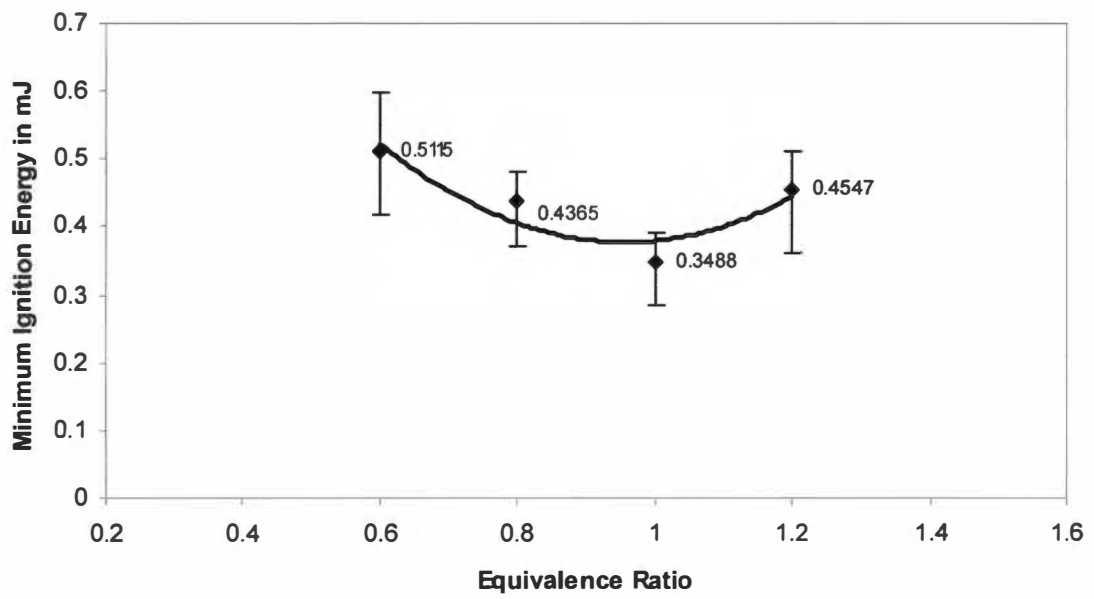
Fig 4.9 Effect of equivalence ratio on minimum ignition energies of methane-air mixtures at 1.04 MPa
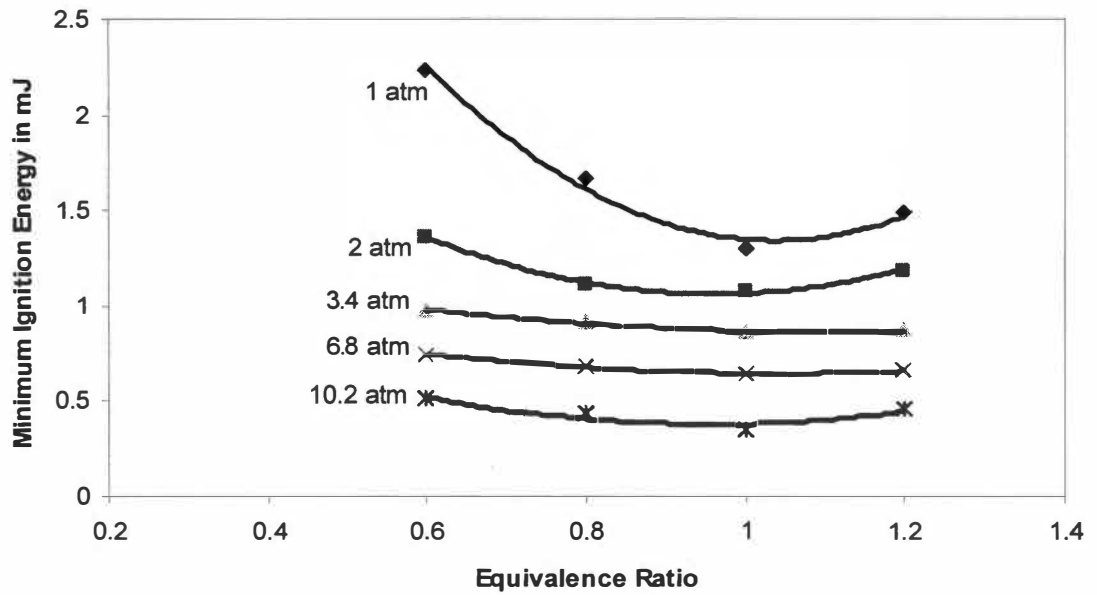
Fig 4.10 Effect of equivalence ratio of minimum ignition energies of methane-air mixtures at various pressures.
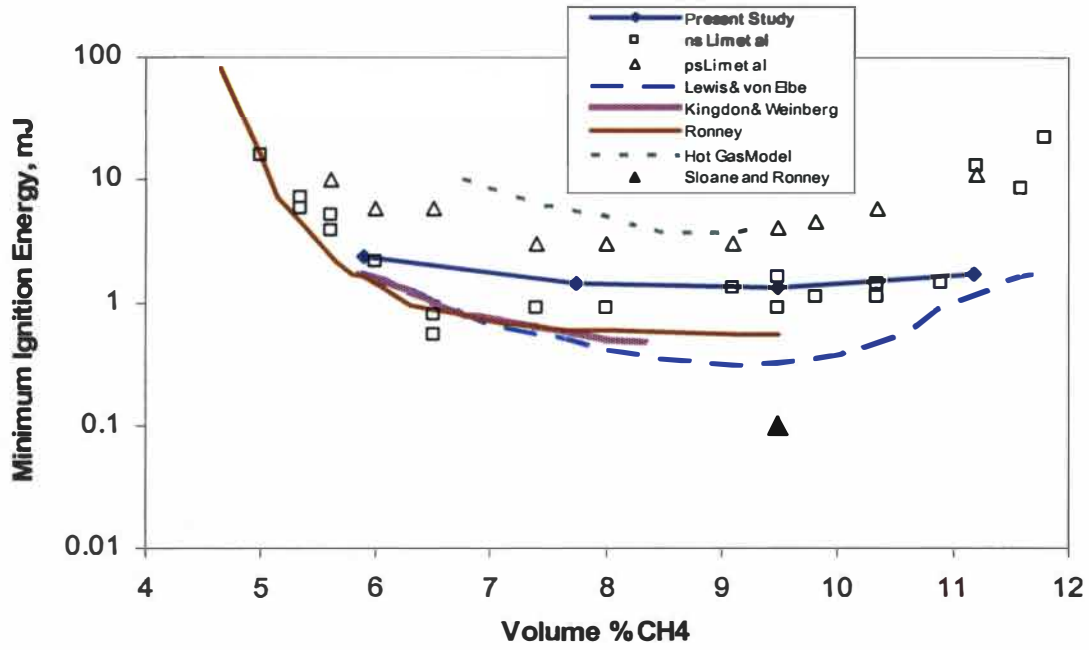
Fig 4.11 Comparison of minimum ignition energies with previous investigators at pressure of 0.1 MPa

3-4 mJ, which is approximately 3 times the minimum ignition energy measured in the present investigation. The discrepancy between the two measurements might be due to the shorter focal length arrangement employed in their investigation. This difference can be related to the thermal gradient mechanism as noted by Phuoc and White [18] that would associate higher ignition energy with shorter focal length arrangement. This theory if considered for the results obtained from Lim et al. gives completely opposite trend. But if one considers that Lim et al. [29] used a 10 ns pulse as compared to 5.5 ns pulse used in the present investigation as well as in Phuoc and White's study, then the minimum ignition energy is expected to be higher.

The minimum ignition energies obtained in the present investigation at 1 atm are higher than those reported by Lewis and von Elbe [19] using electric sparks. It is observed from the figure that the minimum ignition energies reported from laser-induced spark ignition are approximately three to four times larger than those reported from capacitance-discharge electric spark ignition. Lewis and von Elbe reported the minimum ignition energy to be 0.4 mJ at stoichiometric, whereas in the present investigation the minimum ignition energy was found to be 1.29 mJ at the same condition. Ronney [1] noted that, the minimum ignition energy measured from electric spark ignition is always less than that measured from laser spark ignition even though considering the heat losses through the electrodes are considerably more, which will result in requiring more energy for electrode ignition. The reason for this might be as the focal region where the energy is concentrated is so small, which results in increase in heat losses. Also the duration of the pulse being very small, flame kernel extinguishes before it ignites the mixtures. Hence more energy needs to be supplied, which increases the minimum ignition energy.

102

The results obtained by Sloane and Ronney [21] theoretically using detailed chemical, hydrodynamic and transport models are much less than those obtained in the present investigation (about 0.5 mJ for ER = 0.55, 0.10 mJ to 0.122 mJ for stoichiometric mixture, and 0.7 to 0.8 mJ for ER = 1.33). The simple hot gas model based on homogeneous heating of a minimum flame volume whose energy depends on the quenching distance for the mixture and a temperature specified through a chemical induction time, reported results that have the minimum ignition energies to be highest as compared to the other results. These results are like the upper limits for all the investigations at a given equivalence ratio.

4.3 EFFECT OF PRESSURE ON MINIMUM IGNITION ENERGIES OF METHANE-AIR MIXTURES

This section discusses the results obtained from the present study on effect of pressure on the minimum ignition energies of methane-air mixtures. All the previous investigations of minimum ignition energies of methane-air mixture were performed at atmospheric or sub-atmospheric pressures. Not much research was done at higher pressures. To determine the effect of pressure on minimum ignition energies of methane-air mixtures, the mixture pressure was varied from 0.1 MPa up to 1.04 MPa for a given equivalence ratio. The effect of pressure on minimum ignition energies was also investigated for different equivalence ratios.

Fig 4.12 shows the effect of pressure on minimum ignition energies of methane-air mixtures for different equivalence ratios investigated. As can be seen from the figure
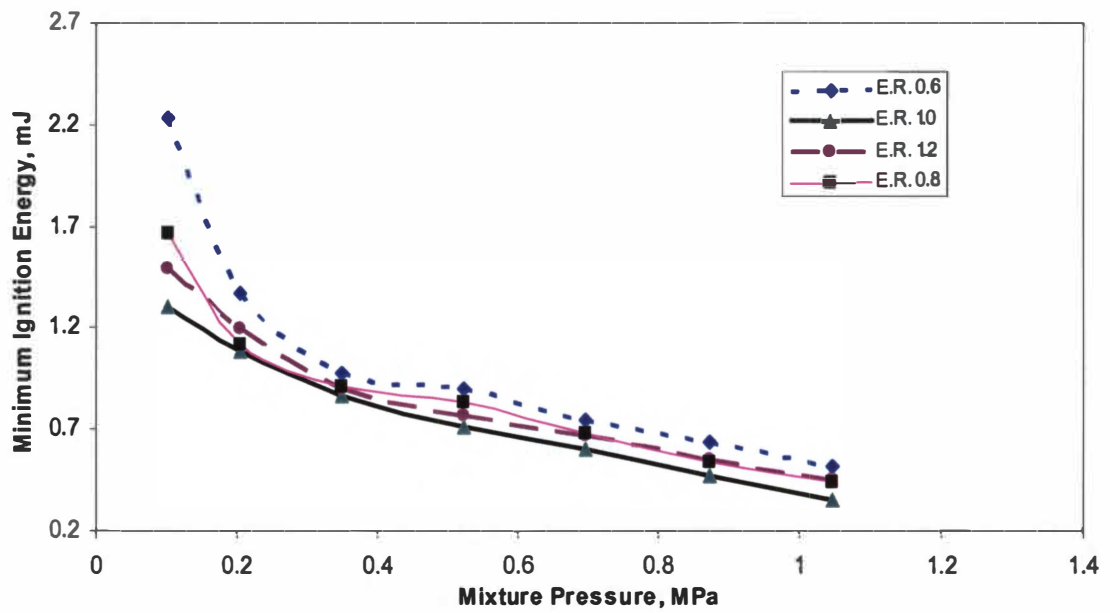
Fig 4.12 Effect of pressure on minimum ignition energies of methane-air mixtures for various equivalence ratios

the minimum ignition energy decreases with the increasing pressure. This trend is observed at all equivalence ratios investigated. In addition the minimum ignition energy is lowest at stoichiometric mixture and increases as the mixture deviates from stoichiometric. This is similar to the trend observed for methane-air mixtures at sub-atmospheric and atmospheric pressures.

As expected the minimum ignition energies decrease with increasing pressure. Due to the increase in collision frequency and number density of the molecules, less laser energy is required to ignite the methane-air mixture at high pressures. Even though the pressure is increased, the minimum ignition energy is measured to be lowest at stoichiometric conditions as observed by Lee et al. [31] for propane-air mixtures at low pressures. The minimum ignition energies of methane-air mixtures for different pressures at various equivalence ratios are listed in Table 4.2.

In this study at a given pressure the breakdown threshold energies for methane and air were much higher than the minimum ignition energies of methane-air mixtures at the same pressure. Hence there was no correlation between the breakdown threshold energies of methane and air and minimum ignition energies of methane-air mixtures.

4.4 GENERAL OBSERVATIONS FROM THIS STUDY

This section describes observations from and during the current investigation of determining the effect of pressure on breakdown threshold energies of methane and air and effect of pressure and equivalence ratio on minimum ignition energies of methane-air

Table 4.2 Minimum ignition energies of methane-air mixtures at different pressures and equivalence ratios

	Minimum Ignition Enery, mJ						
ER Φ	P = 1 atm	P = 2 atm	P = 3.4 atm	P = 5.1 atm	P = 6.8 atm	P = 8.5 atm	P = 10.2 atm
0.6	2.235	1.3653	0.9757	0.9006	0.7421	0.6322	0.5115
0.8	1.4002	1.1128	0.9124	0.8336	0.6789	0.5389	0.4365
1.0	1.2978	1.0817	0.8643	0.715	0.6002	0.4776	0.3488
1.2	1.4876	1.1899	0.8965	0.7498	0.6647	0.5497	0.4547

mixtures. The spark generated for breakdown of gases and for igniting the mixture had a shorter time scale compared to kinetic time scale or chemical induction time scale. The mixture during the minimum ignition energy experiments ignited before the spark was generated. In the focused region the temperature was of the order of 10^6 K and a pressure in the order of 10^3 atm [30]. This extreme condition ignited the mixture directly or created a rapidly expanding shock wave, which had sufficient strength to ignite the methane-air mixture.

During the experiments a lot of water was formed as a product of combustion. This water condensed while exhausting the burnt gases and accumulated on the walls and windows of the combustion chamber. Hence after each experiment the combustion chamber was opened to be cleaned and dried thoroughly. The condensation of water also caused a drop in the pressure in the airline of the system. The pressure drop was about 8 to 10 % of the air pressure inside the chamber.

For the minimum ignition energy experiments laser energy of the order of 20 to 40 mJ was found to be sufficient to ignite the mixture at all pressures and equivalence ratios investigated. As expected it was easier to ignite mixtures at higher pressure then at low pressures. For the mixtures on rich side a pinkish flame was observed while on the lean side the flame was bright yellow instead of being bluish in color.

For the breakdown threshold energy experiments lesser total laser energy of the order of 10 to 30 mJ was found to be sufficient for both methane and air at all pressures. The sparks created in air were very bright and white for some instances while sometimes gave a dull white color for the same pressure. On the other hand the sparks produced in

methane were dull and pinkish in color. This difference in colors observed for air and methane was due to the ionization of different species.

The total laser energy that is mentioned above consists of the reflected energy from the beam splitter, absorbed energy by the mixture or gas and transmitted energy through the combustion chamber. For determining the absorbed energy a calibration curve was plotted having the reflected energy on one axis and the transmitted energy on the other. This calibration curve was plotted by evacuating the chamber so that there will be no absorbed energy. The readings for reflected and transmitted energy recorded from the experiments were compared with the calibration curve and the absorbed energy was obtained.

During the minimum ignition energy experiments the mixtures up to equivalence ratio of 0.6 on lean side and 1.2 on the rich side could be ignited for all the pressure investigated. Outside these lean and rich limits the mixture did not ignite even though the laser energy was increased to maximum. It was assumed that this might be due to improper mixing of the gases. Hence the mixture was allowed to mix for up to 8 hours but still no ignition was observed. To ensure proper mixing a stainless steel pipe extension was installed inside the combustion chamber. This steel pipe extension was designed in such a way that it would provide a whirl to the gases while entering the chamber. The steel pipe was curved to the shape of the combustion chamber and the pipe was cut vertically up to 1 inch through the diameter. Still it was not possible to ignite the mixture below the limits mentioned before.

For the breakdown threshold experiments the breakdown was said to have occurred when a flash of the light from the spark was seen or a cracking sound from the

chamber was heard. The breakdown threshold energy was calculated in the same manner as the minimum ignition energy. It was decided to determine the breakdown threshold energies of methane and air up to a pressure of 14 atm but we were able to determine up to a pressure of 11.6 atm only. Above this pressure controlling of the laser energy became very difficult and hence it was impossible to determine the exact breakdown threshold energies. Also the low resolution of the energy meters restricted the measuring of laser power after certain extent. If an accurate laser varying devices and energy meters with higher resolution were available then it could have been possible to determine the breakdown threshold energies up to the desired pressures.

CHAPTER 5

CONCLUSIONS

The objective of this investigation was to investigate the effect of pressure on breakdown threshold energies of methane and air. In addition the effect of pressure and equivalence ratio on the minimum ignition energies of methane-air mixtures was also investigated. It was assumed that the formation of spark precedes the ignition process. Hence by determining the breakdown threshold energies and minimum ignition energies of methane-air mixtures a correlation could be determined between breakdown threshold energy and minimum ignition energy. And if a correlation existed then the minimum ignition energy of methane-air mixtures at a given pressure would be very close to the gas that has the lowest breakdown threshold energy at that pressure. But at a given pressure the breakdown threshold energies were found to be much higher than the minimum ignition energies. Hence there is no correlation between the breakdown threshold energies and minimum ignition energies. Also the methane-air mixture ignites before the spark is formed by the breakdown of individual gases.

The breakdown threshold energies were determined for air and methane separately with the pressures varying from 0.02 MPa to 1.17 MPa. The breakdown threshold energies for methane at 0.02 MPa and 1.17 MPa were 23.23 and 1.9 mJ and for air at 0.02 MPa and 1.17 MPa were 28.84 and 2.74 mJ, respectively. The breakdown threshold energies were found to decrease with the increasing pressure for both the gases. The breakdown threshold energies of air were found to be about 2 to 3 mJ higher than the breakdown threshold energies for methane at a given pressure. The breakdown threshold

111

energies of air and methane were found to be similar to those obtained by Phuoc [18] at lower pressures. The breakdown threshold energies showed p^{-n} pressure dependence, which is in good agreement with the electron cascade process for creating gas breakdown. The pressure dependence was found to be 0.444 for air and 0.378 for methane.

The minimum ignition energies were determined for pressures ranging from 0.1 MPa to 10.3 MPa with equivalence ratios varying from 0.6 to 1.2 using a 5.5 ns pulse from a Q-switched Nd-YAG laser at a wavelength of 1064 nm. At a given pressure the minimum ignition energy was found to be minimum for a stoichiometric mixture and it increased as the mixture deviated from stoichiometric. This trend was observed for all the pressures investigated.

The minimum ignition energies of methane-air mixtures at 1 atm were similar to those obtained by Lim et al. [29] for nanosecond pulses and were much lower than those of Phuoc and White [30]. Both of the above investigations were carried out using similar laser systems. The minimum ignition energies obtained in the present investigation were much higher than those obtained from electric spark ignition. The minimum ignition energies were found to decrease with increasing pressure at a given equivalence ratio.

For future studies a high-speed video camera can be installed and the combustion process can be captured and a better understanding of the combustion phenomena can be obtained. Using high-speed camera for breakdown process can give an insight on the formation of spark, which is very important for ignition. More accurate data can be obtained if an accurate laser power controller is available. The adjusting of laser power

near the ignition point can be well achieved by this controller, which in turn will assist in obtaining more accurate results.

REFERENCES

1   Ronney, P. D., (1994), "Laser Versus Conventional Ignition of Flames," *Optical Engineering*, Vol. 33, Number 2, pp. 510-521.

2   Chen, Y-L. A., (1998) "Laser-Induced Gas Breakdown and Ignition," Dissertation Presented for the Doctor of Philosophy Degree, The University of Tennessee, Knoxville.

3   Baravian, G., Godart, J. and Sultan, G., (1982) "Multiphoton Ionization of Molecular Nitrogen by a Neodymium-Glass Laser," *Physics Rev.*, A25, pp. 1483-1495.

4   Weyl, G. M., (1989) "Physics of Laser-Induced Breakdown: An Update," in Radziemski, L. J. and Cremers, D. A., editors, *Laser-Induced Plasma and Applications*, Marcel Dekker Inc., New York.

5   Keldysh, T., (1965) "Ionization in the Field of a Strong Electromagnetic Wave," *Soviet Physics, JETP*, vol. 20, pp. 1307-1314.

6   Dewhurst, R. J., (1977), "Breakdown in the Rare Gases Using Single Picosecond Ruby Laser Pulses," *Journal of Physics D: Applied Physics*, Vol. 10, pp. 283-289.

7   Dewhurst, R. J., (1978), "Comparative Data on Molecular Gas Breakdown Thresholds in High Laser-Radiation Fields," *Journal of Physics D: Applied Physics*, Vol. 11, pp. L191-L195.

8   Krasyuk, I. K. and Pashinin, P. P., (1972), *JETP*, Letter 15, pp. 333-334.

9   Bunkin, F. V. and Prokhorov, A. M., (1967), *Soviet Physics., JETP*, vol. 25, pp.1072-1075.

10   Voronov, G. S., Delone, G. A. and Delone, N. B., (1967), *Soviet Physics, JETP*, vol. 24, pp. 1122-1125.

11   Voronov, G. S. and Delone, N. B., (1966), *Soviet Physics, JETP*, vol. 23, pp. 54-58.

12   Bebb, H. B. and Gold, A., (1966), *Physics Review*, Letter 14, pp. 60-63.

13   Williams, W. E, Soileau, M. J. and Van Stryland, E. W., (1983), "Picosecond Air Breakdown Studies at 0.53 μm," *Applied Physics*, Letter 43, pp. 352-354.

14   Rosen, D. I. and Weyl, G., (1987), "Laser-Induced Breakdown in Nitrogen and the Rare Gases at 0.53 and 0.35 μm," *Journal of Physics D: Applied Physics*, Vol. 20, pp. 1264-1276.

15   Buscher, H. T., Tomlinson, R. G. and Damon E. K., (1965), "Frequency Dependence of Optically Induced Gas Breakdown," *Physics Review Letters*, Vol. 15, pp. 847-849.

16   Alcock, A. J., Kato, K. and Richardson, M. C., (1972), "New Features of Laser-Induced Gas Breakdown in the Ultraviolet," *Optics Communications*, Vol. 6, Issue 4, pp. 342-344.

17   Turcu, I. C. E., Gower, M. C. and Huntington, P., (1997), "Measurements of KrF Laser Breakdown Threshold in Gases," *Optics Communications*, Vol. 134, pp. 66-68.

18   Phuoc, T. X., (2000), "Laser Spark Ignition: Experimental Determination of Laser-Induced Breakdown Thresholds of Combustion Gases," *Optics Communications*, Vol. 175, Issue 4-6, pp. 419-423.Spiglanin, T. A., McIlroy, A., Fournier, E. W. and Cohen, R. B., (1995), "Time-Resolved Imaging of Flame Kernels: Laser Spark Ignition of $H_2/O_2/Ar$ Mixtures," *Combustion and Flame*, Vol. 102, pp. 310-325.

19   Lewis, B. and von Elbe, G., (1961) *"Combustion, Flames and Explosions of Gases,"* 2nd Ed., Academic Press, New York.

20   Frendi, A. and Sibulkin, M., (1990), "Dependence of Minimum Ignition Energy on Ignition Parameters," *Combustion Science and Technology*, Vol. 73, pp. 395-413.

21   Sloane, T. M. and Ronney, P. D., (1992), "A Comparison of Ignition Phenomena Modeled with Detailed and Simplified Kinetics," *Combustion Science and Technology*, Vol. 88, pp. 1-13.

22   Hill, R. A. and Laguna, G. A., (1980), "Laser Initiated Combustion of $CH_4 + O_2$ Mixtures," *Optics Communications*, Vol. 32, Issue 3, pp. 435-439.

23   Hill, R. A., (1981), "Ignition-Delay Times in Laser Initiated Combustion," *Applied Optics*, Vol. 20, Issue 13, pp. 2239-2242.

24   Chou, M.-S., Fendell, F. E., and Behrens, H. W., (1993), "Theoretical and Experimental Studies of Laser-Initiated Detonation Waves for Supersonic Combustion," *SPIE Proceedings Vol. 1862 – Laser Applications in Combustion and Combustion Dynamics*, (Liou, L. C. Ed.), SPIE, Los Angeles, pp. 45-58.

25   Root, R. G., (1989), "Modeling of Post-Breakdown Phenomena," *Laser-Induced Plasma and Applications*, (Radziemski, L. J. and Cremers, D. A. Eds.), Marcel Dekker Inc., New York, pp. 69-103.

26   Spiglanin, T. A., McIlroy, A., Fournier, E. W. and Cohen, R. B., (1995), "Time-Resolved Imaging of Flame Kernels: Laser Spark Ignition of $H_2/O_2/Ar$ Mixtures," *Combustion and Flame*, Vol. 102, pp. 310-325.

27   Schmieder, R. W., (1981), "Laser-Spark Ignition and Extinction of a Methane-Air Diffusion Flame," *Journal of Applied Physics*, Vol. 32, pp. 3000-3003.

28   Kingdon, R. G. and Weinberg, F. J., (1976), "The Effect of Plasma Constitution on Laser Ignition Energies," *16th Symposium (International) on Combustion*, The Combustion Institute, Pittsburgh, pp. 747-756.

29   Lim, E. H., McIlroy, A., Ronney, P. D. and Syage, J. A., (1998), "Detailed Characterization of Minimum Ignition Energies of Combustible Gases Using Laser Ignition Sources, *Transport Phenomena in Combustion* (Chan, S. H. Ed.), Taylor and Francis, London, UK, pp. 176-184.

30   Phuoc, T. X. and White, F. P., (1999), "Laser-Induced Spark Ignition of CH_4/Air Mixtures," *Combustion and Flame*, Vol. 119, pp. 203-216.

31   Lee, T. –W., Jain, V. and Kozola, S., (2001), "Measurements of Minimum Ignition Energy by Using Laser Sparks for Hydrocarbon Fuels in Air: Propane, Dodecane, and Jet-A Fuel," *Combustion and Flame*, Vol. 125, pp. 1320-1328.

32   Syage, J. A., Fournier, E. W., Rianda, R. and Cohen, R. B., (1988), "Dynamics of Flame Propagation Using Laser-Induced Spark Ignition: Ignition Energy Measurements," Journal of Applied Physics, Vol. 64, pp. 1499-1507.

VITA

Sameer Vidyadhar Bondre was born in Vadodara, Gujarat, India on June 4th, 1977. He graduated from Shreyas Vidyalaya, Vadodara in May 1992. The following fall he entered Polytechnic, Maharaja Sayajirao University, Vadodara, where he earned his diploma in Mechanical Engineering in September 1995. After working an year at FAG, Precision Bearing, Maneja, Gujarat, India he entered Faculty of Technology and Engineering, Maharaja Sayajirao University, Vadodara, where he earned his degree of Bachelor of Engineering with a major in Mechanical Engineering in August 2000. He then joined The University of Tennessee, Knoxville to continue his education, earning the degree of Master of Science in Mechanical Engineering in December 2004.